Refined Car-Following Model Incorporating the Behavior of the Vehicles from the Adjacent Lanes

A Thesis Submitted for obtaining
the Scientific Title of PhD in Engineering
from
Politehnica University Timișoara
in the Field of SYSTEMS ENGINEERING
by

Eng. Mădălin-Dorin Pop

PhD Committee Chair:
PhD Supervisor: prof.univ.dr.eng. Octavian Proștean
Scientific Reviewers:

Date of the PhD Thesis Defense: February 2022

BUPT

Foreword

This thesis has been elaborated during my activity in the Department of Automation and Applied Informatics of the Politehnica University Timişoara, Timişoara, Romania.

This thesis aims to develop new models for the road traffic modeling process at the microscopic level. The thesis is based on a reproduction of all achievements of the PhD candidate during his PhD research program.

I address my special thanks to the PhD supervisor, Prof.univ.dr.eng. Octavian Proștean, for his permanent support, trust, and encouragement during the period of the doctoral research program and thesis elaboration. Without a collaboration created between the PhD supervisor and PhD candidate, all the achievements from the PhD research program would not have been possible.

I also express my gratitude to the members of the guidance committee Conf. dr. eng. Florin Drăgan (Rector of Politehnica University Timişoara), Conf. dr. eng. Iosif Szeidert-Şubert (Department of Automation and Applied Informatics of the Politehnica University Timişoara) and Ş.l. dr. eng. Cristian Vaşar (Department of Automation and Applied Informatics of the Politehnica University Timişoara) whose advice and suggestions contributed to my personal and professional development.

I also want to express many thanks to Prof.univ.dr.eng. Gabriela Proștean (Department of Management, Politehnica University Timişoara), Jitendra Pandey (Department of Computing, Middle East College, Sultanate of Oman) and Velmani Ramasamy (Department of Electronics and Communication Engineering, Siddhartha Institute of Technology and Sciences, India) for their professional support and collaboration on scientific papers.

I also would like to express my special thanks to the management of the SC Joyson Safety Systems Arad SRL and especially to Eng. Bernard Schiess (Director of the Engineering Center Arad Steering Wheel) and Eng. Teodor Cocîrlă (Team Leader at the Software Development Center Timişoara) for their support and understanding of my both professional career paths as a PhD student and as a senior software engineer employed by the mentioned multinational company.

The validation of the proposed approaches from this thesis would not have been possible without the data received from Timişoara City Hall - General Directorate of Roads, Bridges, Parking and Utility Networks - Traffic Monitoring Office, Timişoara, Romania and I would like to thank all employees of this institution for their openness to support this research project with the necessary road traffic data.

At the same time, I would like to express my special thanks to my family for their encouragement and dedicated support, expressed during my doctoral studies.

Timişoara, February 2022   Mădălin-Dorin Pop

This PhD thesis is dedicated to my parents, Florica and Roman Pop, whose support and sacrifices provided me with the encouragement to pursue educational opportunities.

Abstract
This thesis approaches the road traffic modeling process at the microscopic level, focusing on the car-following models. A review of the recent trends in this field is provided by the state of the art chapter. This research emphasizes the disadvantage of the standard car-following model consisting of neglection of the behavior of vehicles moving on the adjacent traffic lanes. This study proposes a refinement process of this standard car-following model considering the behavior of the vehicles moving on the adjacent road traffic lanes in the follower vehicle acceleration control. Traffic lanes are modeled as nodes in a Markov chain, and the lane choice probabilities computation employ the Bayesian reasoning concept. A fault detection based on parity equations is performed to detect computational faults introduced by the refinement process. This research also brings novelties to the calibration process by proposing a hybrid online calibration method that combines the concept of Kalman filtering with the Takagi-Sugeno fuzzy inference system. This calibration method proved its utility for both standard and refined car-following models. All these new approaches have been validated through simulation experiments done in Simulink, part of MATLAB R2020a (MathWorks, Natick, MA, USA) based on real traffic data received from Timișoara City Hall - General Directorate of Roads, Bridges, Parking, and Utility Networks - Traffic Monitoring Office, Timișoara, Romania.

TABLE OF CONTENTS

NOTATIONS, ABBREVIATIONS AND ACRONYMS

ACC   – adaptive cruise control
ALV   – actions of LV

BPNN   – back-propagation neural networks

CAV   – Connected And autonomous Vehicle

DAVD   – density and acceleration velocity difference
DBM   – Driver Behavior Model/Modeling
DS   – distance between LV and FV

EV   – Electric Vehicle

FIS   – Fuzzy Inference System
FV   – Follower Vehicle
FVD   – Full Velocity Difference

GF   – Generalized Force
GHR   – Gazis-Herman-Rothery
GM   – General Motors
GMM   – Gaussian mixture model
GoF   – goodness-of-fit function

HDS   – Hybrid Dynamical System
HSIC   – human-simulated intelligent control

IDM   – Intelligent Driver Model
IoT   – Internet of Things
ITMS   – Intelligent Traffic Management System
ITS   – Intelligent Transportation Systems

LV   – Leader Vehicle

MAP   – Maximum-A-Posteriori
MIMO   – Multiple Input Multiple Output
MOP   – measure of performance
MPA   – Absorbing Markov Process
MPC   – model-predictive control
MPI   – Message Passing Interface
MSE   – Mean Square Error

NGSIM   – Next Generation Simulation Program

OD   – origin-destination
OEM   – original equipment manufacturers
OVD   – Optimal Velocity Difference
OVF   – Optimal Velocity Function

PMSM   – permanent magnet synchronous motor
PWARX   – piecewise auto-regressive exogenous

RCF   – reinforcement car-following
RDD   – Resilient Distributed Dataset
RM   – Roundabout Manager
RMSPE   – root mean square percentage error
RS   – relative speed

TraCI   – Traffic Control Interface
TRANSIMS   – TRansportation ANalysis and SIMulation System
TVD   – Two Velocity Difference

VR   – Virtual Reality

ε-SVR   – Epsilon-Support Vector Regression

LIST OF TABLES

LIST OF FIGURES

GLOSSARY OF TERMS

Calibration – The process of finding the proper values for the model parameters that provide a good description of the system behaviour as a result of the comparison between estimated values for the model parameters and the values retrieved from the measurements performed on the system.

Car-following – The fourth level of representation of the road network load model consisting of the behavioral study of vehicles that "follow" the front vehicle while moving on a lane. The vehicle that "follows" (FV - follower vehicle) the mode of travel of the front vehicle (LV - leader vehicle) must adapt its acceleration and thus velocity to ensure a safe distance from the LV.

Delay – Additional time experienced during the movement process beyond what would reasonably be desired for a given trip.

Density – The number of vehicles occupying a given length of lane averaged over time, usually expressed as vehicles per kilometer or vehicles per kilometer per lane.

Filtering – The process of removing the noise and perturbations from the modeling of a process.

Fault – An unacceptable deviation from the standard behavior of at least one feature of a system.

Flow – The number of vehicles that cross a given lane length in a previously set time interval, usually expressed as vehicles per second or vehicles per hour.

Green-interval – The period of time in a signal cycle during which the green signal indication remains constant at a signalized intersection.

Lane change – The action taken by a driver to change the current lane used for the movement process.

Macroscopic – Modeling technique approached from the perspective of continuous traffic flow theory, which provides a description in time and space of the evolution of macroscopic flow variables (flow and density).

Mesoscopic – Modeling technique approached from the perspective of studying the the behavior of the parameters corresponding to microscopic models under the influence of specific parameters of macroscopic models.

Microscopic – Modeling technique approached from the perspective of a detailed overview of each individual vehicle present in the road network, including acceleration behavior, traffic lights management, and car-following behavior.

Queue – A line of vehicles to be served by a system (e.g., an intersection, an entry/exit node of a road network in which the rate of flow from the front of the queue determines the average speed within the queue. The dynamics of the internal queue may involve a series of start and stop actions.

Offset – Adjustment value to be applied to the model parameters to improve the model.

Refinement – A process that aims to improve the characteristics of an existing model by incorporating additional parameters into the modeling process.

Velocity – A rate of motion expressed as a distance per unit of time.

Volume – The number of vehicles passing a point on a lane, crossroad, or road network during a specific time interval, often taken to be one hour, expressed in a number of vehicles.

1. INTRODUCTION

1.1. Problem Definition and Research Objectives

Driver behavior introduces uncertainties in road traffic modeling at the microscopic level. Various car-following models are single-lane oriented and cannot emphasize the influence of the vehicles moving on the adjacent traffic lanes. A lane change decision made by a vehicle from the current lane leads to a "leader change" in the modeling process and the FV shall adapt its acceleration control mechanism to respond to this stimulus. This control mechanism is mandatory for the assurance of collision avoidance.

Solutions for introducing in the modeling process the behavior of the vehicles moving, in the same direction, on adjacent lanes are mandatory. In this regard, the development of new car-following models shall provide control strategies for the FV movement by incorporating the interactions with the vehicles from adjacent traffic lanes. This plays an important role not only in better understanding the phenomenon of traffic, but also represents an important step for the development of autonomous driving systems.

The objectives of this thesis are as follows:
- providing an analysis of the intersections configuration methods;
- obtaining a more accurate prediction of the origin-destination traffic volumes, and implicitly creating a better overview of the driver behavior;
- developing new microscopic road traffic models capable of incorporating the lane choice behavior with high accuracy;
- developing new car-following models for multiple-lane roads;
- developing models for fault detection and analysis of car-following models that can highlight the faults introduced by the modeling process;
- developing new solutions for car-following model calibration that are easily adaptable to multiple-lane car-following models.

1.2. Research Approach and Layout

This thesis represents a synthesis of the author's achievements during his PhD research program. Besides his already published contributions as follows:
- 1 scientific article published in a journal indexed ISI Web of Science (WoS) with quartile Q1 and impact factor (IF) equal to 3.576;
- 1 scientific article published in a journal indexed ISI WoS without quartile IF;
- 11 scientific papers published in ISI WoS indexed proceedings of international conferences, one of these papers, [**Pop19_1**], being awarded with the *Best Paper Award "Honorable Mention"*;
- 1 scientific paper published in the proceedings of international conferences indexed BDI.

This thesis provides a deeper overview of the microscopic traffic modeling concept and describes the current research directions in this domain. All these information have been structured in 7 chapters on 133 pages, containing 60 figures,

10 tables, and having as a source of inspiration 130 bibliographic references, including the previously mentioned 14 papers as the author contributions.

Chapter 1 describes the motivation of the chosen research topic with a clear definition of the problem and a description of the research objectives. The presentation of the current drawbacks of the car-following models supports the understandability of the motivation of the author to find solutions to real road traffic issues.

Chapter 2 presents a complete analysis of the state of the art in road traffic modeling at the microscopic level. This analysis starts with an overview of the current developments in terms of road traffic simulators and continues with the recent trends in car-following control and modeling. Here, are discussed various car-following models proposed by scientific literature that aim to adapt this modeling method to the needs of some current research directions such as connected and autonomous vehicles (CAVs) or electric vehicles (EVs). This chapter also presents a critical overview of new developments in car-following calibration methods that are very important to obtain traffic models closer to reality.

Chapter 3 highlights the importance of road traffic modeling at the microscopic level. This chapter provides the author's contributions related to road traffic modeling. Simulations are performed using AnyLogic Simulation Software to analyse the impact of different crossroad configuration methods (uncontrolled intersections, signalized intersections, and roundabouts) on the velocities of the vehicles and the evolution in the number of vehicles passing through an intersection.

Car-following represents one of the "*four levels of representation of the microscopic road traffic network model together with crossroads configuration, links and lane choice* [Yin15]" [**Pop18_1**]. To better understand the factors of influence on the car-following modeling process, lane change behavior modeling has been described. Special attention was given to the incentive criteria definition that controls the acceleration behavior of the follower vehicle (FV) considering the behavior of the vehicle ahead, further referred as leader vehicle (LV). These incentive criteria play a crucial role in collision avoidance actions by proper control of the FV acceleration. Furthermore, this chapter presents various standard car-following models and highlights their advantages and disadvantages.

Chapter 4 illustrates the proposed methodology for the refinement of the standard discrete-time car-following model consisting of the extension of this single-lane oriented model to multiple-lane roads. Here, the driver behavior modeling (DBM) process and the Bayesian inference are described as the main research methodologies. This chapter defines traffic lanes as nodes in a Markov chain according to Pop and Proștean [**Pop19_2**]. Moreover, the origin-destination (OD) volumes estimation is discussed based on this modeling approach.

The refinement process uses the standard (single-lane) car-following model in discrete-time and permanently updates the acceleration value of the FV according to the lane change predictions based on Bayesian reasoning. Furthermore, the prediction of lane change harmonizes the incentive criteria equations with respect to the predicted driver decision. This chapter further conducts an experiment using MATLAB R2020a software (MathWorks, Natick, MA, USA) and real traffic data provided by "*Timișoara City Hall - General Directorate of Roads, Bridges, Parking and Utility Networks - Traffic Monitoring Office, Timișoara, Romania*" [**Pop20_2**], [**Pop20_3**]. The discussion of the experimental results for the refined model is the basis for the formulation of the advantages and disadvantages of this method.

Chapter 5 provides a fault analysis of the proposed refined model. The fault analysis assumes that the refined model introduces faults through internal calculations and is used both as an observed model and as a model with the defect. The nominal model consists of three standard car-following models, one for each traffic lane included in the experiment. The applied methodology consists of the usage of parity equations, as described by Kratz et al. [Kra98] and Isermann [Ise06], [Ise11]. According to this methodology, "*the identified residuals are the relative velocity residual and the dynamic running distance residual*" [**Pop20_3**]. Analysis of these residuals showed that "*the model is not suitable for a real-time switch from one lane to another to ensure lane change behavior monitoring for each lane*" [**Pop20_3**] but can still provide a good description of the behavior of the LV and FV from the target lane if a new vehicle joins this lane and becomes the new LV.

Chapter 6 focuses on the calibration process of the car-following models and proposes a new approach consisting of a hybrid online calibration solution that combines the concept of Kalman filtering with a Takagi-Sugeno fuzzy inference system (FIS). This method proves its efficiency through faster identification of the correct offsets to be applied to the model parameters compared to a simple Kalman filtering. In addition to the outcome of the research of Pop et al. [**Pop20_2**], this chapter adapts this calibration method and applies it to the refined car-following model.

Chapter 7 aims to present the conclusions and contributions of the author to the microscopic modeling of road traffic systems. Moreover, this chapter defines future research directions that can use these thesis contributions as fundamental.

2. STATE OF THE ART IN ROAD TRAFFIC MODELING AT THE MICROSCOPIC LEVEL

2.1. Preliminaries

Reduction of traffic congestion, finding environmentally friendly solutions for transportation, and assurance of traffic safety became our today priorities in the transportation domain. Some solutions to these things start with a proper understanding of the phenomenon of road traffic. Microscopic modeling represents the foundation of road traffic definition through its particularities of describing changes in vehicle parameters during their movement on a road network and the interactions with the other traffic participants (e.g., other vehicles, pedestrians, bicyclists, etc.).

In the last few years, many researchers brought their scientific contributions to different fields related to ITS such as autonomous driving, electric vehicles, driver behavior analysis and patterns recognition, etc. They used several technologies like Markov chains, fuzzy-based systems, neural networks, etc. This chapter concentrates on actual road traffic modeling approaches at the microscopic level by providing a critical analysis of the related works.

The chapter starts with a review among various microscopic road traffic simulators and shows how important are the following characteristics: scalability, workload partitioning, and partition organization. The next section provides a critical review of recent trends in car-following control and modeling. The concepts of CAVs and EVs are of great interest among researchers. Many of the standard car-following models that will be discussed in detail in **Chapter 3** have been adapted by researchers to respond to the needs of CAVs and EVs. Moreover, this thesis also discusses other improvements in standard car-following models that do not refer to CAVs and EVs.

Another section has been designed to pay special attention to the calibration process. This step plays a crucial role in the development of new models because it is responsible for providing a better approximation of the model parameters compared to the observed real road traffic parameters. This section will provide several approaches in this regard.

The last section will underline the current gaps in the car-following control and modeling process and also the implications of the continuous developments in the field of intelligent transportation systems (ITS).

2.2. Microscopic Road Traffic Simulators

The researchers analysed and proved the validity of their proposed models using various simulations. Simulations are appropriate for this because direct testing on the road infrastructure is difficult, from accessing the data collected by TMCs and the direct impact on the vehicles moving on the road. Furthermore, this chapter discusses some widely known simulation tools designed for microscopic road traffic.

Additionally, new developments in terms of microscopic traffic simulators will be discussed.

The TRansportation ANalysis and SIMulation System (TRANSIMS) contains the following modules for microscopic traffic simulation: population generation, activities generation, modal and route choice, and traffic micro-simulation [Nag01]. The last module ensures that the behavior of the travel plan of each individual in the simulation is executed on the basis of the plan set within the other modules. Being a simulator intended for distributed environments, TRANSIMS addresses the scalability topic through a non-spatial partitioning approach and uses graph cuts to partition the large road network (it cuts a geographical area into multiple similar size partitions) [Nag01], [Yu20]. Furthermore, this simulator applies the same partitions to the simulated vehicles. The parallelization of the simulation process represents the responsibility of the Message Passing Interface (MPI), TRANSIMS also implements mechanisms designed to minimize message passing costs and ensure an adaptive load balancing [Yu20].

The spatial-temporal databases used by TMCs require additional devices (e.g., GPS receivers installed in all vehicles) to ensure the acquisition of large-scale high-quality traffic data in urban environments. Simulators can generate this type of data but encounter weaknesses from the scalability and granularity viewpoints. Compared to macroscopic road traffic, microscopic traffic simulation is more difficult because it requires a detailed overview of each individual vehicle present in the road network, including acceleration behavior, traffic lights management, and car-following behavior. Fu et al. addressed these issues and proposed a simulator named GeoSparkSim [Fu19]. The purpose of this simulator was "*to generate large-scale road network traffic datasets to simulate the microscopic road traffic. It extends the Apache Spark and converts road networks to Spark graphs and simulated vehicles to vehicle resilient distributed datasets (RDDs)*" [Fu19]. In addition, it considers microscopic traffic characteristics and implements a simulation-aware vehicle partitioning method that provides a spatio-temporal overview of vehicle characteristics capable of dealing with dynamic spatial distribution. The biggest advantage of this simulator is its scalability, which is proved by a simulation involving the movement of 200 thousand vehicles on a road network composed of 250 thousand road junctions and 300 thousand road segments [Fu19].

Table 2.1 shows a comparison between GeoSparkSim [Fu19] and other microscopic traffic simulators [Yu20]. The strengths of GeoSparkSim are the distributed characteristic in terms of scalability, the quad-tree workload partitioning, and the partition organization as dynamic.

Table 2.1. "*Comparison among different microscopic traffic simulators*" [Yu20].

Simulation tool	Scalability	Workload partitioning	Partition organization	Distribution model
SUMO	Single node	-	-	-
TRANSIMS	Distributed	Graph cuts	Fixed	MPI
MATSim	Multi-thread	Uniform grids	Fixed	Thread sync.
ParamGrid	Distributed	Uniform grids	Fixed	CORBA
SMARTS	Distributed	Z-curve	Fixed	TCP sockets
GeoSparkSim	Distributed	Quad-Tree	Dynamic	RDD

Probably the biggest disadvantage of traffic simulators is the use of predefined algorithms to control vehicle movement behavior. Here, the low coverage of the uncertainties introduced by the decisions of real drivers and their reaction time arises. "*Most of the current traffic simulators have limited human-in-the-loop capabilities to capture the interactions between simulated vehicles (including simulation-controlled vehicles, human-controlled vehicles, or a mixture of these categories)*" [Has21]. Hasan et al. proposed a framework based on virtual reality (VR) to extend the standard simulator features by including distributed vehicles controlled by human-in-the-loop. The related paper discusses the mixture of human-controlled vehicles with autonomous vehicles and pedestrian behavior for signalized intersections (including traffic signs and traffic lights) in various scenarios of traffic conditions. The study does not cover the existence of roundabouts and unsignalized crossroads where the priority-to-the-right rule applies. In these situations, concerns arise regarding the capability of the virtual environment to synchronize with the real-time vehicle trajectory profiles and avoid the reproduction of wrong collisions in the simulation that have no corresponding collisions in real traffic. The proposed VR-based framework is advantageous because of its compatibility with all commercial and free microscopic simulation tools that provide an API for developers that are used as a core service.

Recent works focus not only on the development of new simulation tools but also on the improvements of existing ones, or the development of new frameworks to integrate different simulation platforms. In this regard, Acosta et al. proposed a framework (TraCI4Matlab) for the traffic control interface (TraCI) to integrate the SUMO road traffic simulator with Matlab through an adaptive software reengineering process [Aco15]. After employing object-oriented patterns, the existing TraCI for Python (TraCI-Python) and Java (TraCI4J) [***_1] has been used as a source of requirements for TraCI4Matlab during the reengineering process. The advantage of this TraCI implementation is the possibility of controlling the simulation objects from Matlab and also the acquisition and analysis of simulation data from SUMO using Matlab. A drawback of this development process was the neglect of performance analysis.

2.3. Recent Trends in Car-Following Control and Modeling

This section presents an overview of recent works in the field of car-following control and modeling. Researchers improved many of the existing car-following models by applying current development approaches based on neural networks [Col21], [Lu17]; genetic algorithms [Lu17], [Wan21]; machine learning [Yan19]; fuzzy systems [Li18], [Li19_2] or stochastic processes [Tia21], [Wu19], [Xu20], [Zak15].

Other works try to improve the accuracy of microscopic traffic models by employing some features from macroscopic models. Borsche and Meurer [Bor19] coupled these models to provide a better overview of the interaction between traffic flows and pedestrian dynamics. However, this approach has weaknesses in describing traffic in the case of studying vehicle movement when the density of pedestrians on the road is small. In reverse, Gkania and Dimitriou [Gka21] proposed the usage of microscopic traffic flow mechanics in combination with traffic information resulting from online traffic maps to overcome the drawbacks of estimation of macroscopic fundamental diagrams.

The interests of current researchers cover the improvements of car-following derivatives models such as Gipps [Jia20_2], [Mog17], [Yan19]; GHR [Bor19], [Col21], [Mog17]; OVD [Jia20_1], [Yu21]; FVD [Cao20], [Gou20], [Jia20_2], [Jia20_1], [Li19_1], [Yan19]; intelligent driver model (IDM) [Ech21], [Son18]. **Chapter 3** (**Section 3.4**) presents a detailed overview of these mentioned well-known derivatives of the car-following model. Moreover, special attention is given to the tailoring of the mentioned models to meet the needs of autonomous driving [Che21], [Ech21], [Gor20], [Has21], [Ker21], [Li19_1], [Yan19], connected vehicles [Che21], [Ech21], [Gor20], [Li19_1], [Jia20_1] and electric vehicles [Li18], [Li19_1], [Sch16], [Zha20]. Furthermore, in **Sections 2.3.1-2.3.3**, this thesis discusses in detail some of these approaches.

2.3.1. Connected and Autonomous Vehicles (CAVs)

Many OEMs (original equipment manufacturers) in the automotive industry invest in projects related to autonomous and connected vehicles that aim to provide a profound revolution in transportation systems [Gor20]. Not far from today's reality, these vehicles gained popularity through the expected comfort provided to passengers, collision avoidance and congestion management features [Ech21], [Has21], [Ker21], [Yan19]. Also, special attention is paid to electric CAVs [Li19_1], a topic covered in **Section 2.3.2**. However, there is a lack of standardization for this type of system even if a deeper analysis shows various modeling solutions regarding parameter description, dynamics representation, including the case of mixed traffic where both autonomous and manually driven vehicles are present, calibration methods [Gor20].

Chen et al. [Che21] proposed "*a human-machine cooperative scheme for car-following control to address the out-of-the-loop problem of autonomous traffic systems*". This approach consists of developing a $H\infty$ suboptimal control that ensures the optimization of controller parameters according to the desired performance index [Che21]. To improve the dynamic performance of velocity tracking, a fine-tuning has been applied considering the concept of human-simulated intelligent control (HSIC) [Che21]. In this case, the $H\infty$ control problem has been described by Equation (2.1):

$$\Sigma : \begin{cases} \dot{\varphi}(t) = A_1 \cdot \varphi(t) + B_1 \cdot v_{auto}(t) + E_1 \cdot \omega(t) \\ z(t) = C_1 \cdot \varphi(t) + D_1 \cdot v_{auto}(t) + D_2 \cdot \omega(t) \end{cases} \tag{2.1}$$

where $A_1 = \begin{bmatrix} 0 & -1 \\ 0 & -1/\mu \end{bmatrix}$, $B_1 = \begin{bmatrix} 0 \\ 1/\mu \end{bmatrix}$, $E_1 = \begin{bmatrix} 1 \\ 0 \end{bmatrix}$, ω is the disturbance of the system to be suppressed and $v_{auto}(t)$ represents the output of the velocity tracking controller computed as in Equation (2.2) [Che21]:

$$v_{auto}(t) = k_{fb} \cdot \varphi(t) + k_{ff} \cdot \omega(t) \tag{2.2}$$

where $k_{fb} = W \cdot Y^{-1}$, $k_{ff} = \beta$ are the gains of the full information feedback controller that provides the $H\infty$ optimal performance to the closed-loop system to Equation (2.1). The gains of the full information feedback controller computation start from

the premises that $D_1 \cdot k_{ff} + D_2 = 0$, and $H\infty$ has a disturbance level $\gamma = 1$ to find a solution for the matrices Y, W and the maximum deceleration β considering the Theorem 1 as taken from [Che21]:

"**Theorem 1.** *For any given constant* $\gamma > 0$, *if there exist asymmetric positive definite matrices* P *and* $Y = \gamma \cdot P^{-1}$, *matrix* W *and constant* β, *such that*

$$\begin{bmatrix} A_1 \cdot Y + B_1 \cdot W + (A_1 \cdot Y + B_1 \cdot W)^T & E_1 + B_1 \cdot \beta & (C_1 \cdot Y + D_1 \cdot W)^T \\ (E_1 + B_1 \cdot \beta)^T & -\gamma \cdot I & 0 \\ C_1 \cdot Y + D_1 \cdot W & 0 & -\gamma \cdot I \end{bmatrix} < 0 \qquad (2.3)$$

holds, the closed-loop system (2.1) *is asymptotically stable with an* $H\infty$ *disturbance attenuation level* γ " [Che21].

The obtained velocity profiles have been compared with those obtained with IDM and showed fast and non-overshoot velocity tracking performances, characterized by a good ability to maintain a fixed distance during movement over a road network. This contributes to the avoidance of "*rear-end collision caused by sudden or unpredictable deceleration of the preceding vehicle*" [Che21]. Among the disadvantages of this study is the neglection of the effects produced by unreliable communication, communication delays, and the incomplete evaluation of the "*relationship between driver's driving style and the distance tracking error*" [Che21].

Following this direction of human-in-the-loop simulations for car-following models, Hasan et al. [Has21] brought a solution involving VR technology to capture the reactions of the user (considered as a driver for a real situation) with high fidelity and accuracy. This brings benefits in creating driver behavior profiles that can be used as input by control algorithms designed for autonomous vehicles. Furthermore, this VR-based framework provides support for simulation of pedestrian-vehicle interactions, creating in this way a more accurate overview of the safety assurance directions to be covered by the control algorithm development process. This will also help in the future for a mixed traffic flow where we will not only have CAVs, but also manually driven vehicles where the anticipation of driver decisions by the autonomous vehicle algorithm is decisive in terms of safety assurance [Ker21].

Kerner and Klenov [Ker21] propose a methodology for mixed traffic modeling that guarantees collision avoidance and evaluates the movement of vehicles considering the adaptive cruise control (ACC) car-following model (for a better overview of the space representation of this model consisting of an LV – leader vehicle and ACC FV – follower vehicle, please see Figure 3.16, **Section 3.4**) from Equation (2.4), which is a Gipps-based model:

$$a^{(ACC)}(t) = K_1 \cdot \left(s(t) - v_{FV}(t) \cdot \tau_d^{(ACC)} \right) + K_2 \cdot \Delta v(t) \qquad (2.4)$$

where:

- $a^{(ACC)}$ is the acceleration of the ACC;
- K_1 and K_2 are coefficients of ACC adaptation;
- $s(t)$ is the dynamic distance value between FV and LV at time t;
- $v_{FV}(t)$ represents the value of the velocity of the FV at the moment t;
- $\Delta v(t) = v_{LV}(t) - v_{FV}(t)$ is the relative speed measured by the autonomous vehicle considering $v_{LV}(t)$ as the velocity of the LV vehicle;
- $\tau_d^{(ACC)}$ is the desired time headway of the autonomous vehicle to the LV [Ker21].

Yang et al. [Yan19] started from the Gipps model expressed in **Section 3.4.1** of this thesis by Relation (3.13) and proposed a model based on back-propagation neural networks (BPNN). This model addresses "*the weaknesses of the machine learning-based car-following models in controlling*" [Yan19] autonomous vehicles by providing a collision avoidance mechanism considering the specific kinematics of the Gipps model. The Gipps-BPNN model demonstrates the ability to imitate real driver behavior and provides an appropriate weight value *a* for the forecasting model described by "*the following objective function:*

$$min\ E = a \cdot E_{real} + (1-a) \cdot E_{safe}$$

$$= \sum_{t=1}^{N} \left[a \cdot \left(y_{t\_real} - \sum_{i}^{K} \omega_i \cdot y_{it} \right)^2 + (1-a) \cdot \left(y_{t\_safe} - \sum_{i}^{K} \omega_i \cdot y_{it} \right)^2 \right] \qquad (2.5)$$

$$s.t. \sum_{t=1}^{K} \omega_i = 1;\ \omega_i \geq 0;\ 0 \leq a \leq 1$$

where:
- *E represents the total error of all N samples;*
- *E_{real} and E_{safe} represent the total error for being close to a real driver, respectively to a safe driving state;*
- *y_{t_real} and y_{t_safe} are the real and safe value of the t-th sample;*
- *y_{it} denotes the predicted value of the i-th model;*
- *ω_i with $i = \{1,2,...,K\}$ denotes the optimal weight values for the K models used in the combination model*" [Yan19].

The efficiency of this combined Gipps-BCNN model has been proved by a comparison with a model obtained by combining Gipps kinematics with a random forest model.

Another car-following model adapted to the needs of CAVs is IDM. The Echeto et al. [Ech21] approach improves the standard IDM (please see a detailed overview of the standard IDM in **Section 3.4.6** of this thesis) by providing a longitudinal control in the traffic jam assistance function. This control method has been studied for various scenarios of a congested road, and the results showed potential improvements in traffic safety, including driver stress reduction by taking over driving off and acceleration [Ech21]. Equation (2.6) formulates this longitudinal

control for an improved desired spacing $s_d^*\left(v_i(t), \Delta v_i(t)\right)$ for the i-th vehicle moving in a chain on a road network [Ech21]:

$$s_d^*\left(v_i(t), \Delta v_i(t)\right) = s_0^{(i)} + max\left(0, s_1^{(i)} \cdot \sqrt{\frac{v_i(t)}{v_0^{(i)}}} + T^{(i)} \cdot v_i(t) + \frac{v_i(t) \cdot \Delta v_i(t)}{2 \cdot \sqrt{a^{(i)} \cdot b^{(i)}}}\right), \; i = \{1,2,...,n\} \; (2.6)$$

where $s_0^{(i)}$ is the desired spacing in the case of zero velocity of vehicle i; $v_0^{(i)}$ represents the desired velocity at time t; $a^{(i)}, b^{(i)}, \delta, T^{(i)}$ and $s_1^{(i)}$ are non-physical parameters of the i-th driver [Pun05], [Tre13_2].

   Referring to connected vehicles, many challenges arise from the influence of driver behavior "*on the dynamic characteristics of the car-following model under a vehicle-to-vehicle (V2V) communication environment*" [Jia20_1]. In a first step, Jiao et al. [Jia20_1] adapted the OVD (for more details please see **Section 3.4.4**, Equation (3.27)) by proposing a new optimal velocity function (OVF) $V\left(\Delta x_i(t)\right)$ according to Relation (2.7):

$$V\left(\Delta x_i(t)\right) = v_{max} \cdot \left[S\left(\Delta x_i(t)\right) - S\left(\Delta x_i^{safe}(t)\right)\right] + \left[1 - S\left(\Delta x_i(t)\right)\right] \cdot v_{i-1}(t), i = \{1,...,n\} \; (2.7)$$

where:
- v_{max} represents the maximal velocity of the vehicle;
- $v_{i-1}(t)$ is the velocity of the preceding vehicle at time t;
- $\Delta x_i^{safe}(t)$ denotes the safe space headway;
- $S\left(\Delta x_i(t)\right)$ represents the sensitivity of the optimal velocity to the space headway of the i-th vehicle computed as in (2.8) [Ban95], [Jia20_1]:

$$S\left(\Delta x_i(t)\right) = \frac{1}{1 + e^{\Delta x_i^{safe}(t) - \mu \cdot \Delta x_i(t)}}, \; S\left(\Delta x_i(t)\right) \in [0,1] \qquad (2.8)$$

where $\mu \in (0,1)$ is a parameter.

   This OVF shall comply with the following boundary conditions [Jia20_1]:
- if $\Delta x_i(t) = \Delta x_i^{safe}(t)$ then $V\left(\Delta x_i(t)\right) \in \left[0, v_{i-1}(t)\right]$, $i = \{1,...,n\}$;
- if $\Delta x_i(t) = \Delta x_i^{safe}(t)$ and $v_{i-1}(t) = 0$ then $V\left(\Delta x_i(t)\right) = 0$, $i = \{1,...,n\}$;
- if $\Delta x_i(t) \to +\infty$ then $V\left(\Delta x_i(t)\right) \to v_{max}$, $i = \{1,...,n\}$;

and further, combining it with a FVD-based model that incorporates the drivers' characteristics in the V2V communication environment, results in the reinforcement car-following (RCF) model characterized as follows:

$$\frac{\Delta v_i(t)}{dt} = k \cdot \left[V\left(\Delta x_i(t)\right) - v_i(t)\right] + \lambda \cdot \Delta v(t), \; i = \{1, 2, \ldots, n\} \tag{2.9}$$

where $\Delta v(t)$ is the relative velocity between LV and FV, k is a sensitivity constant and λ is a parameter.

2.3.2. Electric Vehicles (EVs)

EVs will ensure the sustainability of future transportation systems through the reduction of CO_2 emissions and the easier use of green energy sources. Nevertheless, this leads to changes in vehicle control systems by considering the specific characteristics of EVs. Therefore, an adaptation of current car-following models is mandatory to ensure safety movement on a road network where EVs are also present.

The dynamics of EVs play an important role in the movement process on a road network, especially when CAVs are involved. In this regard, the research of Li et al. [Li19_1] proposes a FVD-based model that incorporates these dynamics assuming that this information is shared between vehicles in a V2V communication environment. The most important parameter of EVs that influences the other movement characteristics at the microscopic level is the current magnitude of the permanent magnet synchronous motor (PMSM) of EV because it has a strong connection with the torque and acceleration of CAVs [Par14].

Li et al. consider that, in the case of electric CAVs, the FV perceives changes of current magnitude of PMSM of the LV and can provide a quick response to that stimulus as follows [Li19_1]:

$$a_i(t) = k \cdot \left[V\left(\Delta x_i(t)\right) - v_i(t)\right] + \lambda \cdot \Delta v_i(t) + \xi \cdot I_{i+1}(t), \; i = \{1, 2, \ldots, n\} \tag{2.10}$$

where $\xi > 0$, $\xi \in \mathbb{R}$ denotes the sensitivity coefficient; $I_{i+1}(t)$ represents the current magnitude of PMSM of the $(i+1)$-th EV at time t, and the significance of the other FVD-related notations is available in **Section 3.4.5** of this thesis. This approach proved its efficiency through a higher collision avoidance capability compared to the standard FVD.

EVs need efficient energy management during the movement process. Figure 2.1. highlights the design proposal of Schwickart et al. [Sch16] for a real-time predictive cruise control system. As stated above, a suitable approach to overcome the uncertainties in traffic and environment conditions is to apply a driving control strategy based on model-predictive control (MPC). This MPC aims to control the acceleration pedal that further influences the battery current using as input information like road curvature, altitude profile, velocity limits, and the running distance between FV and LV. Schwickart et al. integrated the charge consumption model from Equation (2.11) in their approach to obtain the optimal compromise between the velocity reference tracking and the energy consumption of the EV [Sch16]:

$$\frac{dC_{el}}{ds} = u_{cons} \tag{2.11}$$
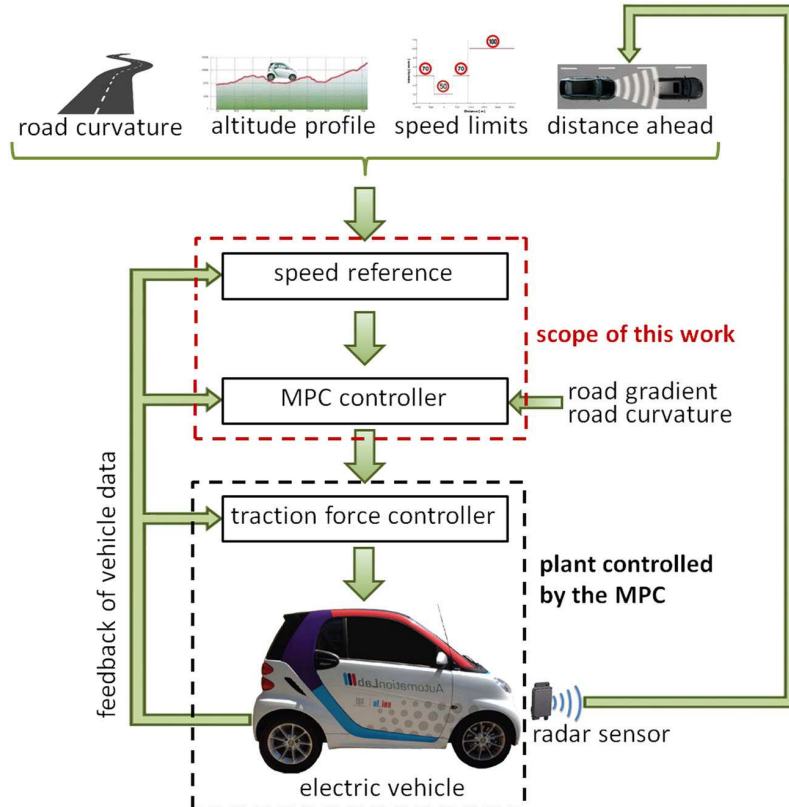
Figure 2.1. Predictive cruise control system for EV [Sch16] (fig.1).

where C_{el} is the charge consumption that the designed controller will try to minimise; s represents the vehicle position and u_{cons} denotes the charge consumption per meter of the EV as defined below:

$$u_{cons} = a_i \cdot e_{kin} + b_i \cdot F_{trac} + c_i \ \text{if} \ P_i \ \text{is active}$$
$$u_{cons} \geq a_j \cdot e_{kin} + b_j \cdot F_{trac} + c_i \ \text{if} \ j \neq i \tag{2.12}$$

where $e_{kin} \geq 0$ denotes the kinetic energy of the EV; F_{trac} is the traction force of the EV; a_k, b_k and c_k with $k = \{i, j\}$ are the coefficients of a P_k approximating linear function from a set of N functions $P_{fun} = \{P_1, \ldots, P_N\}$ defined as:

$$P_k = a_k \cdot e_{kin} + b_k \cdot F_{trac} + c_k \tag{2.13}$$

This approach proved its efficiency through a reduction in the charge consumption of EVs. Zhang and Zhuan [Zha20] proposed another approach to improve EV car-following models. Compared to the MPC previously discussed, this proposal considers safety and comfort as additional multiple objectives in addition to

energy consumption and tracking. The objective function of this MPC framework has the following definition [Zha20]:

$$
\begin{aligned}
J = &\sum_{i=1}^{p} \left[y_p\left(k+i \mid k\right) - y_r\left(k+i\right) \right]^{T} \cdot Q \cdot \left[y_p\left(k+i \mid k\right) - y_r\left(k+i\right) \right] + \\
&+ \sum_{i=0}^{m-1} u\left(k+i\right)^{T} \cdot R \cdot u\left(k+i\right)^{T}
\end{aligned}
\tag{2.14}
$$

where:
- p denotes the predicting horizon;
- m is the control horizon;
- $y_r\left(k+i\right)$ is a function that describes the response curves of a system that are smoothed as in Equation (2.15) considering the objective as $min\left[y\left(k\right)\right]$:

$$
y_r\left(k+i\right) = \begin{bmatrix} \rho_\delta^i & & & \\ & \rho_{\Delta v}^i & & \\ & & \rho_a^i & \\ & & & \rho_j^i \end{bmatrix} \cdot y\left(k\right), \; y\left(k\right) = \left[\delta\left(k\right), \Delta v\left(k\right), a\left(k\right), j\left(k\right)\right]^{T}
\tag{2.15}
$$

where ρ_δ^i, $\rho_{\Delta v}^i$, ρ_a^i and ρ_j^i represent the reference trajectory coefficients (values between 0 and 1) for the actual vehicle spacing error δ, relative velocity Δv, acceleration a and jerk j of the own vehicle;

- "*Q and R represent the weight coefficient in the objective function defined according to* Equation (2.16) *as follows:*

$$
Q = \begin{bmatrix} w_\delta\left(k\right) & & & \\ & w_{\Delta v}\left(k\right) & & \\ & & w_a\left(k\right) & \\ & & & w_j\left(k\right) \end{bmatrix}, \; R = \left[w_u\left(k\right)\right]
\tag{2.16}
$$

where, the $w_\delta\left(k\right)$, $w_{\Delta v}\left(k\right)$, $w_a\left(k\right)$ and $w_j\left(k\right)$ in Q matrix are the weights corresponding to the error of spacing, relative velocity, and acceleration and jerk of the own vehicle at moment k, $w_u\left(k\right)$ in the R matrix is the weight corresponding to the control command of the acceleration at moment k" [Zha20].

This optimization problem becomes an "*online constrained quadratic programming problem*" that combines the Equation (2.14) with the collision avoidance constraint (2.17) considering that the running distance $\Delta s\left(k\right)$ between

FV and LV shall be greater than the standard safety distance S at time k and the limitation (2.18) of velocity, "*acceleration, jerk and control variable of the own vehicle*" [Zha20]:

$$Constraint:\ \Delta s(k) \geq S \tag{2.17}$$

$$Constraints:\ \begin{cases} v_{min} \leq v(k) \leq v_{max} \\ a_{min} \leq a(k) \leq a_{max} \\ j_{min} \leq j(k) \leq j_{max} \\ u_{min} \leq u(k) \leq u_{max} \end{cases} \tag{2.18}$$

The uncertainties of a road traffic system involving EVs have also been addressed through adaptive fuzzy control methods. The robustness of the fuzzy-based sliding mode control method proposed by Li et al. [Li18] showed satisfactory results in terms of accuracy. This method involves the development of a switch logic with hysteresis boundary "*to ensure ride comfort, and the expected torque is calculated in real time based on the inverse dynamic model to track the desired acceleration planned by the upper control layer*" [Li18].

2.3.3. Improvements of Standard Car-Following Models

In addition to the models related to CAVs and EVs that have been discussed, there are still other approaches that improved the standard car-following models.

The Gipps model controls the acceleration/deceleration behavior of the FV based on the running distance to the vehicle ahead changes having as the main reason collision avoidance [Daa15], [Gip81]. Jia et al. [Jia20_2] starts with a big disadvantage of this model consisting of the neglection of lane change behavior. They proposed an extended model that prevents a lane change decision for the FV when the running distance between the FV and the LV has a large value. This model considers the scenario illustrated in Figure 2.2 and assumes that "*at the time t, vehicle n maintains a headway d_n with the vehicle $n-1$ and a headway h_n with the vehicle n_a on the adjacent lane*" [Jia20_2]. The other notations refer to vehicle positions (x) and velocities (v), the superscript a refers to the adjacent lane.
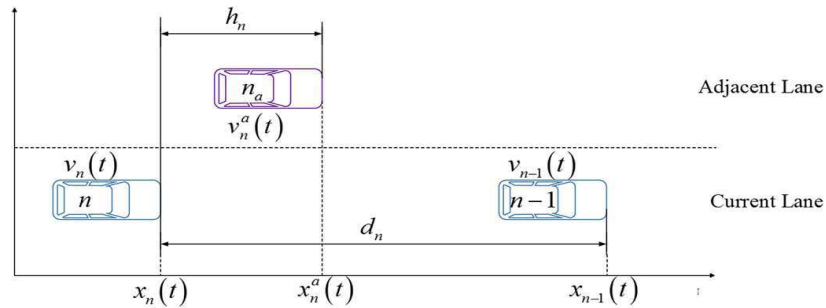
Figure 2.2. Car-following scenario considering the lane change prevention effect [Jia20_2] (fig.2).

Improvements have also been made to the FVD model [Jia01]. Cao et al. [Cao20] extended the FVD to a density and acceleration velocity difference (DAVD) model that incorporates traffic density and LV acceleration. This model showed satisfying results in V2V communication environments. Gounni et al. [Gou20] also paid special attention to the FVD model. They included the driver's anticipation effect and short-term driving of the previous vehicle in their proposal for an improved FVD. This approach demonstrated positive results in terms of safety, efficiency, and stability of the vehicle system by significantly influencing small perturbations.

Song et al. [Son18] integrated the IDM [Tre13_2] and MOBIL [Kes07] models into a microscopic traffic model-based tracking algorithm. This model defines motion estimators to predict "*the interactions among vehicles in longitudinal and lateral motions, respectively*" [Son18]. In addition to the good results with respect to the estimation of longitudinal and lateral states, this approach has a major drawback represented by a high computational cost.

The movement of the surrounding vehicles directly influences the driver's decisions. Yu et al. [Yu21] proposed an improved OVD model that incorporates the influence of heterogeneous velocity information in the honk environment. The results obtained based on the application of this approach were conducted to the following conclusions:

"*(1) Both the honk effect and the speed difference between the main lane and the adjacent lane have a significant impact on the stability of the traffic flow. The average speed of the adjacent lane also affects the stability of the traffic flow.*

(2) A timid driver is more beneficial to the stability of traffic flow than an aggressive driver. Moreover, the more skillful driver is more conductive to improving the stability of traffic flow under the same traffic environment.

(3) For timid drivers, more information about the speed of the preceding vehicle is more conductive to the stability of traffic flow, while for aggressive drivers, less information is better" [Yu21].

Standard car-following models have a large number of parameters that make the calibration process difficult [Mog17], [Pun21]. Moghadam et al. [Mog17] used the Epsilon-Support Vector Regression (ε-SVR) method to determine the acceleration of the FV and the Grid Search method for model parameters tuning. This approach proved higher robustness and reliability in the case of mild disturbances, and also a higher consistency with the field data compared to Gipps and GHR models.

2.4. Calibration of Microscopic Traffic Models

The development of new car-following calibration methods uses "*goodness-of-fit function (GoF) and measure of performance (MoP), or combination of MoPs*" to ensure a better approximation of the model parameters compared to the real observed road traffic parameters [Pun21]. The most used MoPs are velocity, acceleration, and inter-vehicle spacing. Punzo et al. [Pun21] provide a complete overview of the car-following calibration methods, including guidelines on calibration settings. They consider inappropriate settings the usage of percentage-based GoFs "*if two or more MoPs are adopted in the objective function*" [Pun21] and recommend the use of inter-vehicle spacing in the objective function if only MoP is adopted. A VR-based human-in-the-loop microscopic traffic simulation can simplify the calibration process by allowing a more convenient acquisition of driving behavior parameters [Has21].

Fang et al. [Fan20] proposed an online calibration method based on a genetic algorithm for microscopic traffic simulators (Figure 2.3). The selection strategy chosen by these researchers was the tournament selection algorithm, due to efficiency and easier implementation reasons. This approach has been tested under a SUMO simulation environment and the results showed values of mean absolute percentage errors lower than 11%, which proved that it is a satisfying method for online calibration.
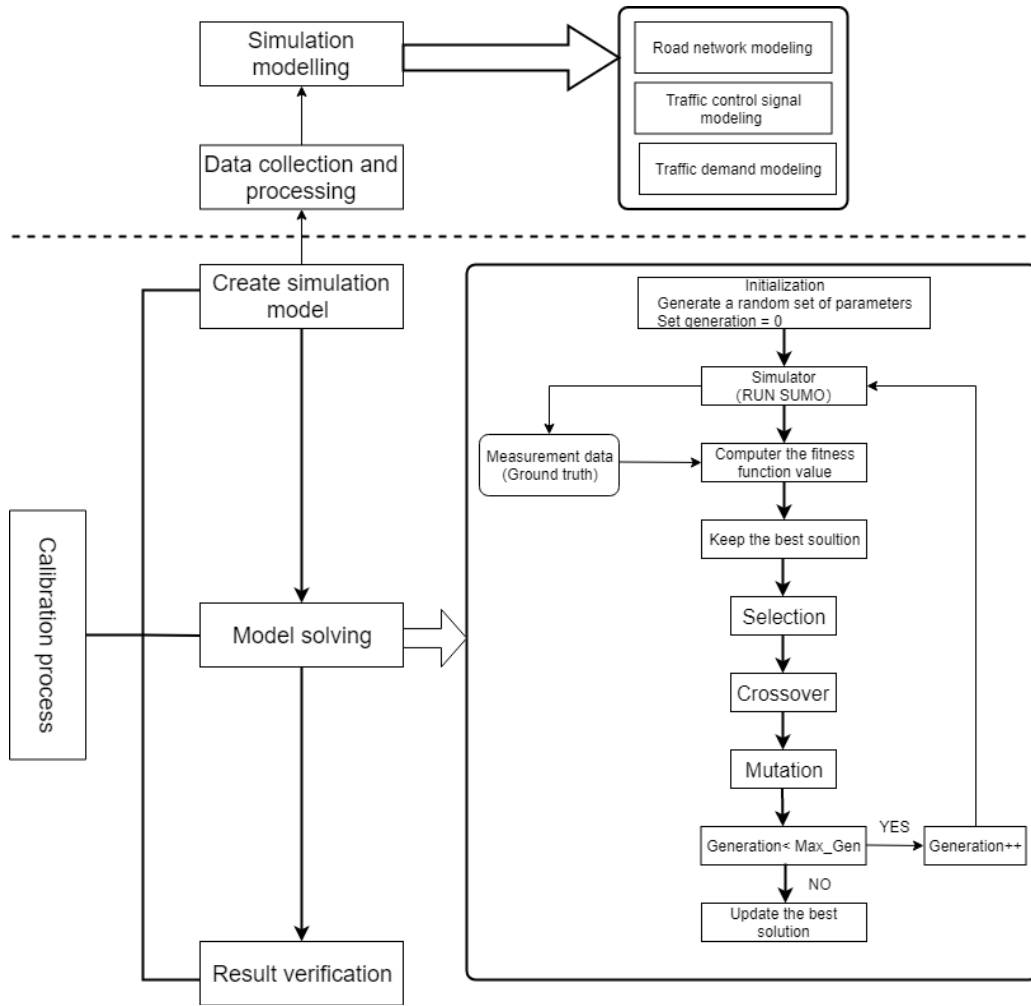
Figure 2.3. Online calibration framework based on genetic algorithm [Fan20] (fig.1).

This calibration problem considers traffic volume as a performance measure according to Equation (2.19):

$$min_{Q(k)} \sum_{i=1}^{n} \left\| \frac{\bar{F}_i^{measured}(k) - \bar{F}_i^{simulated}(Q(k))}{\bar{F}_i^{measured}(k)} \right\|_{\infty} \qquad (2.19)$$

where " $\bar{F}_i^{measured}(k)$ *is the average traffic volume of edge* i *from the ground truth at step* k ; $\bar{F}_i^{simulated}(Q(k))$ *represents the average traffic volume of edge* i *produced by the calibrated simulator in the previous simulation time window* k ; $Q(k)$ *represents the applied calibration parameter*" [Fan20].

Zaky et al. [Zak15] propose another calibration method based on genetic algorithms for IDMs. Furthermore, this approach includes a method based on the Markov switching model to detect various car-following regimes and calibrate the system accordingly. To minimize the gap between the simulated model and the observed driving behavior, this method uses an objective function represented by the root mean square percentage error (RMSPE). This objective function F considers both the FV velocity v_{FV} and the running distance s between FV and LV for a number of n observations moments as follows [Zak15]:

$$F = \sqrt{\frac{\sum\limits_{t=1}^{n}\left(v_{FV}^{obs}(t) - v_{FV}^{sim}(t)\right)^2}{\sum\limits_{t=1}^{n}\left(v_{FV}^{obs}(t)\right)^2}} + \sqrt{\frac{\sum\limits_{t=1}^{n}\left(s^{obs}(t) - s^{sim}(t)\right)^2}{\sum\limits_{t=1}^{n}\left(s^{obs}(t)\right)^2}} \qquad (2.20)$$

where with *obs* and *sim* have been marked the observed and simulated values, respectively. This calibration based on driving behavior showed satisfactory results, and further works will imply the usage of different objective functions for each regime. A simplified similar approach has been proposed by Zhu et al. [Zhu19] where only two driving styles have been considered, aggressive and conservative. The corresponding objective function (2.21) applies RMSPE only to the inter-vehicle spacing s and neglects the velocity changes compared to [Zak15]. This approach achieved good performance in the calibration of car-following and confirmed the existence of heterogeneous car-following behaviors, as also argued by Wang et al. [Wan21].

$$F = \sqrt{\frac{\sum\limits_{t=1}^{n}\left(s^{obs}(t) - s^{sim}(t)\right)^2}{\sum\limits_{t=1}^{n}\left(s^{obs}(t)\right)^2}} \qquad (2.21)$$

Genetic algorithms have also been used by Wang et al. [Wan21]. They proposed using the mean square error (MSE) as an objective function according to Equation (2.22) only considering the running distance s between the vehicles because this "*reveals the overall trend of driving and has a higher detection accuracy*" [Pun21], [Wan21]. This research identified seven classes of driving conditions using the Next Generation Simulation Program (NGSIM) and after applying the calibration process discussed the heterogeneity property using a Kolmogorov-Smirnov test.

$$MSE = \frac{1}{n} \cdot \sum_{t=1}^{n} \left(s^{sim}(t) - s^{obs}(t) \right)^2 \tag{2.22}$$

Pourabdollah et al. [Pou17] proposed the GoF-based method from Relation (2.23) where three MoPs have been used:

$$F = \frac{\in (P) + \in (v_{FV}) + \in (s)}{3} \tag{2.23}$$

where $\in (\cdot)$ denotes the normalized MSE for power demand P, FV velocity v_{FV}, and inter-vehicle spacing s according to the definitions from (2.24), (2.25) and (2.26):

$$\in (P) = \left\| \frac{P^{obs}(t) - P^{sim}(t)}{P^{obs}(t) - mean\left(P^{obs}(t)\right)} \right\|^2 \; , \; P = \frac{C_d \cdot A_f \cdot \rho \cdot v_{FV}^2}{2} + m \cdot g \cdot R_c + m \cdot a_{FV} \tag{2.24}$$

where "m, A_f, C_d, ρ, g, and R_c are the vehicle mass, frontal area, air drag coefficient, air density, gravitational acceleration, and rolling resistance coefficient, respectively" [Pou17].

$$\in (v_{FV}) = \left\| \frac{v_{FV}^{obs}(t) - v_{FV}^{sim}(t)}{v_{FV}^{obs}(t) - mean\left(v_{FV}^{obs}(t)\right)} \right\|^2 \tag{2.25}$$

$$\in (s) = \left\| \frac{s^{obs}(t) - s^{sim}(t)}{s^{obs}(t) - mean\left(s^{obs}(t)\right)} \right\|^2 \tag{2.26}$$

This calibration approach has been applied for three car-following models: IDM (**Section 3.4.6**), Krauss (Equation (3.14), **Section 3.4.1**), and Wiedemann [Wie92]. The results showed improvements for IDM and "*Krauss and Wiedemann car-following models improve significantly, but still they have higher errors than IDM*" [Pou17].

The use of Kalman filters proved their efficiency as a calibration method for CAV-related car-following models [Ema19]. This research direction has previously been addressed by Zhu and Ukkusuri [Zhu17], who developed "*a modified expectation maximization algorithm based on the Kalman smoother [...] to solve the optimal estimation problem*" [Zhu17]. This last study underlined that the greatest limitation in the case of mixed road traffic involving CAVs is "*the exchange of short range and real time traffic information, based on which connected vehicles can alter routes or departure time*" [Zhu17].

2.5. Discussions and Conclusions

This chapter presented an overview of microscopic traffic control and modeling starting with the evaluation of different road traffic simulators, the analysis of new approaches based on standard car-following models, and the analysis of calibration methods related to microscopic traffic models. The newest modeling approaches cover the needs that arise from the developments based on CAVs and EVs.

Sensor networks and the Internet of Things (IoT) play an important role in microscopic traffic control. Currently, IoT services meet the following limitations with respect to their integration with ITS:

- network infrastructure efficiency and scalability;
- "*lack of flexibility in the interaction between the vehicles and other applications based on the IoT*" **[Pop20_5]**;
- "*limited power sources that cannot ensure highly intensive full functionalities*" **[Pop20_5]**;
- "*limitation in self-recovery mechanisms to handle the transition from an error state to the normal operational mode for ITS systems*" **[Pop20_5]**.

Future networks 2030 aim to provide solutions to these limitations through "*a common platform that allows the deployment of a wide variety of technologies and architectures*" **[Pop20_5]**, [Pur18]*, "cost reduction by using low-cost sensors, deployment services and reducing energy consumption*" [Che20], **[Pop20_5]**, "*self-recovering mechanisms from failure states*" **[Pop20_5]***,* [Tse19], "*appropriate policies and regulations systems*" [Mis12], **[Pop20_5]** or "*systems designed for the storage and management of large volumes of road traffic data*" [Mas16], **[Pop20_5]**, [Pur18], [Sal13].

The review of recent works showed a lack of solutions related to the fitting of the car-following models to multiple-lane roads. Multiple uncertainties have also been identified in the calibration process. This thesis aims to provide solutions for these drawbacks in the following chapters. Moreover, research in this field has a gap regarding fault diagnosis and analysis, and part of this topic is considered by the calibration process through correct parameter setting. Fault detection means not only finding a solution by permanently applying an offset to the models' parameters, but finding the root cause of the defect and providing a solution for it.

3. ROAD TRAFFIC MODELING AT THE MICROSCOPIC LEVEL

3.1. Introduction

Road traffic modeling is a very important step in understanding the concept of road transportation. Modeling processes offer, in many cases, possible sources of improvement for today's problems. Road traffic is one of these issues that should be addressed due to its impact in many urban areas through crowded intersections. These agglomerations harm the citizens quality of life through higher travel times, increased CO_2 emissions, and higher exposure to traffic injuries.

3.1.1. Objectives and Layout of the Chapter

This chapter aims to present an overview of the modeling process of road traffic at the microscopic level and the personal contributions of the author of this thesis in this direction. The path to obtaining new contributions needs a general presentation of a theoretical basis related to the road traffic modeling process. This will lead to a better understanding of the results of this research.

Analysis of the levels of representation for the microscopic road network loading model consists of the first step in understanding the microscopic model of road traffic. In this direction, a critical analysis of the intersection configuration modes and simulation is performed. In the design phase of a crossroad, the travel times and the number of vehicles crossing the road network represent key parameters in the decision-making process to establish the best configuration mode for that crossroad [**Pop20_1**]. A simulation was conducted for a specific crossroad from Timișoara using the AnyLogic Simulation Software. The results analysis shows the advantages of choosing the roundabout as a traffic coordination method, but also highlights its drawback in case of crowded traffic that leads to gridlocks after the capacity of the roundabout has been exceeded.

After the analysis of the representation levels of the microscopic road network loading model, this chapter details the concept of lane change behavior. Furthermore, the author of this thesis synthesizes the possible behavior of lane change actions in a single figure (see Figure 3.15) to provide a better overview of the lane change maneuvers. The definitions for the incentive criteria responsible for the safety assurance of the participants in traffic during a lane change action can also be found there.

The last two subchapters provide a critical overview of the car-following models. Some well-known models are presented such as Gipps, Pipes, Gazis-Herman-Rothery (GHR), Optimal Velocity Difference (OVD), Full Velocity Difference (FVD), Intelligent Driver Model (IDM), fuzzy-based model, and other variations of these models. Considering the theoretical foundation of the car-following modeling process, this study identifies the main advantages and disadvantages of this modeling approach.

In addition to all the mentioned contributions, this chapter creates the necessary framework for the building process of a refined car-following model. The new car-following model shall be adapted to multiple lane roads by considering the lane change behavior of the drivers during the movement on a road network. The next chapter will treat this subject.

3.1.2. Overview of the Road Traffic Modeling Process

"*Traffic dynamics can be defined by mathematical traffic flows obtained through the interaction between drivers, vehicles, and infrastructure. Thus, in these mathematical models, large amounts of information are taken into account: the behavior of drivers in terms of the degree of acceleration of the car, the agglomeration of the streets, the speed at which they travel, the pedestrian flow, the positioning of the road signs, etc. By processing these data, it is desirable to get the best possible time to cross the intersections, in order to reduce road jams*" [**Pop18_1**].

Simulation models are developed considering as input the data retrieved from various traffic monitoring sensor networks such as inductive loops, infrared sensors, video camera sensors, or radars. "*By running a simulation model, predictions of traffic evolution can be made and intersections with the highest risk of blockage can be seen*" [**Pop18_1**]. The determination of the root cause of these blocking areas is mandatory to ensure the proposal of a sustainable solution to improve traffic flow.

"*It is noteworthy that the values for the model parameters are chosen so that the simulation will match the data obtained from the traffic. This operation is called model calibration, and its endpoint consists of a calibrated model that can be used to predict traffic flow. A schematic representation of all these considerations is presented in* Figure 3.1" [**Pop18_1**].
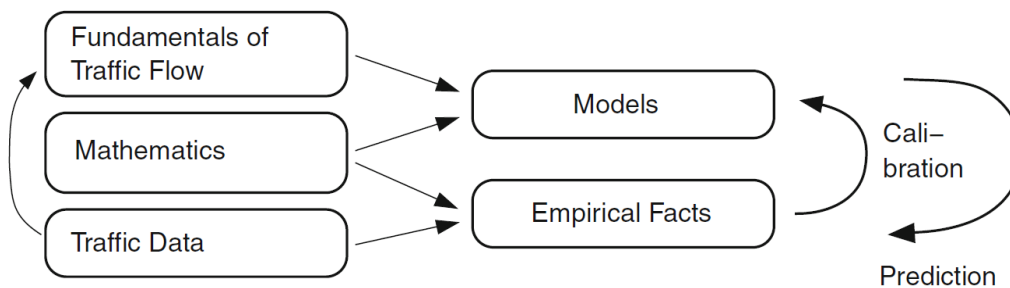
Traffic Flow Modeling

Figure 3.1. Traffic modeling process [Tre13_1] (pp.2, fig.1.1).

Figure 3.2 shows "*a clearer relationship between simulated and real-time traffic systems. To validate a simulated traffic system, it must reproduce the real system in a realistic manner. The simulated system receives as input the values from the real system. Besides, there are also entries that cannot be directly observed, requiring the use of estimated values*" [**Pop18_1**]. The dynamics of origin-destination matrices are part of the category of inputs to be estimated.
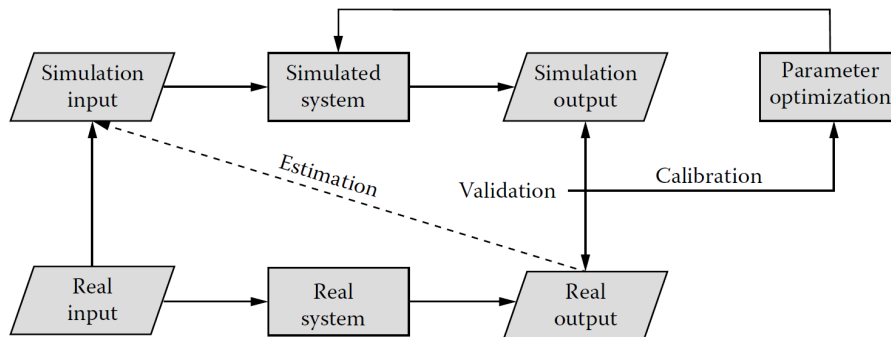
Figure 3.2. "*Relationship between simulated and real systems and locations of calibration and validation processes*" [**Pop18_1**], [Daa15] (pp.3, fig.1.1).

"*It can be noticed that in the proposed architecture, in the calibration, the simulation output values are compared with the data corresponding to the real system. Following this comparison, an adjustment of the simulated system parameters will be made so that the differences between the two outputs are minimal or reach a minimum specified by the requirements*" [**Pop18_1**].

3.2. Levels of Representation of the Microscopic Road Network Model

"*Microscopic traffic models* [Fer18] *pay more attention to the details of the traffic flow and are vital for traffic analysis, especially in the presence of ITS. Initial model calibration is necessary to identify the parameter values. It requires the activities of all participants in traffic in order to have feedback of the traffic with parameters such as vehicle position, accelerations/decelerations, and vehicle speed*" [**Pop20_2**].

In addition to microscopic models, there are two types of models in traffic modeling theory, macroscopic and mesoscopic models. "*Macroscopic models are approached from the perspective of continuous traffic flow theory. The objective of these models is to provide a description in time and space of the evolution of macroscopic flow variables. To achieve this description, the concepts of flow and density are used. Flow means the number of vehicles that cross a part of the road network (x) in a previously set time (Δt)*" [**Pop17**]. "*Mesoscopic models can be seen as a combination of microscopic and macroscopic models. In most cases, in these models, the behavior of the parameters corresponding to microscopic models is studied under the influence of specific parameters of macroscopic models. The classic example of this approach is to model the behavior of a vehicle with respect to others in traffic, taking into account aspects related to its dynamics*" [**Pop17**].

The microscopic representation of traffic "*is characterized by the emphasis on studying the individual behavior of each vehicle on the road network or on the length of queues in a discrete-time system. Microscopic models contain four levels of representation for the road network load model*" [**Pop18_1**], [Yin15]:

- crossroads configuration;
- links;
- lane choice;
- vehicle-following.

"*The interaction between the vehicles involved in the movement process needs special attention and is very important in analysing the movement process*" [Bar10], [**Pop20_2**]. Usually, this interaction is visible through lane change maneuvers. "*A lane change can be defined as the decision taken by a driver to change his/her current lane. This action can be observed as a process that usually occurs in two main cases. The first case is when the LV has low velocity and the FV changes lane only for a while, before returning to its previous lane. In this case, the only reason for the change is the driver's desire to move at a higher speed without changing his/her planned destination. The second case arises from issues like leaving the road network using an exit lane or possible future restrictions of lane changes that can influence the planned destination*" [**Pop20_3**]. The following subsections will describe these concepts in detail.

Obtaining a sustainable smart mobility system is not enough to develop new traffic control algorithms, but also to identify relevant metrics and indicators of smart mobility that can indirectly improve urban traffic. As shown by Pop and Proștean [**Pop19_3**], having a standardized set of metrics and indicators will make it possible to make a more objective assessment of a smart city, strictly in terms of smart mobility, without taking into account its geographical area or other indicators specific only to the evaluated city. In this direction, Pop et al. [**Pop18_4**] proposed a common legal framework of policies and rules on the implementation of the concept of smart mobility applicable anywhere in the world. It should be mentioned that this legal framework contains several stages between various levels of management, national, regional, and local, defining the relations and the way of communication between the institutions corresponding to the mentioned levels [**Pop18_4**]. According to Pop and Proștean [**Pop18_2**], Romania implemented several approaches that improved the smart city score for some Romanian cities and implicitly the traffic flow. Table 3.1 shows a comparison between the actions taken by local administrations from Romania to improve the quality of the urban mobility system.

Table 3.1. Actions taken by Romanian smart cities [**Pop18_2**].

Actions	Cluj-Napoca	Craiova	Sibiu	Timișoara
Charging stations for electric vehicles	✓	-	✓	✓
Bike-sharing programs	✓	-	-	✓
Additional local transportation systems	✓	-	-	✓
Mobile applications for mobility	✓	✓	✓	✓
Intelligent traffic lights systems	✓	✓	-	✓
Intelligent parking systems	✓	✓	-	✓

3.2.1. Crossroads Configuration

The configuration of crossroads (or intersections) is the first level of representation of the network loading model [Yin15]. Modeling at this level involves many challenges, such as collision avoidance assurance and maintenance of a simple model that will bring positive effects from the computational effort perspective [Bun14_1]. In addition, the chosen configuration mode can partially

solve traffic congestion problems that became more common in medium-sized and big cities around the world. Depending on the characteristics of the existing road infrastructure and its adaptability to different configuration modes can be used as input for various studies on the reduction of travel time values. "*Another parameter that describes the efficiency of a chosen intersection coordination method consists of the number of vehicles that can cross a road network containing multiple intersections, in a specific time interval*" [**Pop20_1**].

The configuration modes that can apply to a crossroad are the following:

- uncontrolled intersections;
- signalized intersections;
- roundabouts;

and further details will be provided. Furthermore, a critical analysis of the implementation of these configuration modes for intersection will be done based on a crossroad from Timișoara (Romania) as presented in [**Pop20_1**]. This study presents the decision-making process for establishing the best crossroad configuration mode for the Circumvalațiunii intersection. The modeling process uses the AnyLogic Simulation Software, which has a dedicated Road Traffic Library that simplifies the road network design. For a better understanding of the simulation model that will be further illustrated, it is necessary to describe the main blocks included in the AnyLogic Road Traffic Library (Table 3.2).

Table 3.2. Simulation blocks included in the Road Traffic Library (AnyLogic Simulation Software) [Gri16], [**Pop20_1**], [***_2].

Symbol	Name	Significance
	CarSource	"*Creates the cars and attaches the coordinates according to a specified location. Car arrivals can be defined using the arrival rate, interarrival rate, etc.*" [**Pop20_1**].
	CarMoveTo	"*Is used for managing car movements. The destination can be a stop line, a road, a parking place etc. If movement to a specified destination is not possible, the car can be routed to a destination specified using port onWayNotFound*" [**Pop20_1**].
	CarDispose	"*Eliminates a car from the road network*" [**Pop20_1**].
	TrafficLight	"*Controls vehicle movement using stop lines or lane connectors by associating the timing for each color signal. This block ensures the simulation of traffic light behavior*" [**Pop20_1**].

For the chosen case study, the following nodes were identified as main connection points, according to Figure 3.3: Iulius Town, Cetății Boulevard, Jiul Passage and Gheorghe Dima Street. These nodes consist of street names or important landmarks of the city located in the neighborhood of the target crossroad.

Figure 3.3. Circumvalațiunii crossroad from Timișoara (Romania) – OpenStreet Maps View

Figure 3.4 shows the simulation model from AnyLogic that considers Iulius Town as the source node for the experiments developed in the following paragraphs. The model will look similar when considering another node as the origin. "*Destination nodes are chosen using the selectOutput5 block, based on the probabilities obtained from real traffic data*" [**Pop20_1**]. "*The probabilities used in the current simulation, for all cases, are presented*" [**Pop20_1**] in the paragraph that analyses the simulation results.
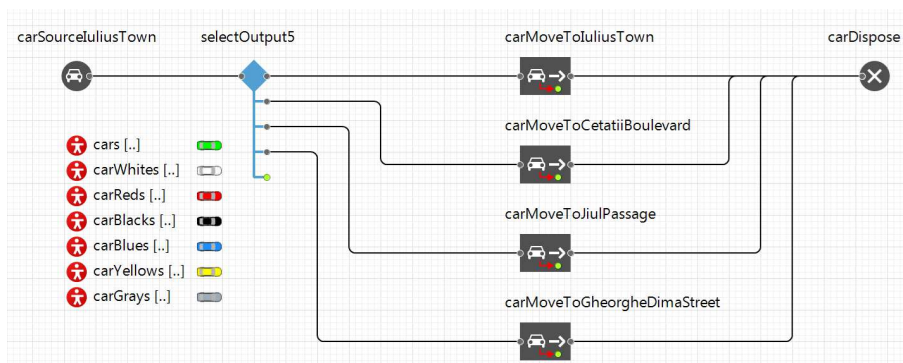
Figure 3.4. Traffic model for vehicles starting from Iulius Town [**Pop20_1**].

Uncontrolled Crossroads Configuration

The main characteristic of uncontrolled intersections is the "*lack of traffic signals or signs for traffic flow control. The vehicles flow through these crossroads is done by applying the priority-to-the-right rule. In this case, if a driver wants to turn left and a vehicle comes from the right side on the perpendicular road with direction straight, the driver shall apply the priority-to-the-right rule. If the vehicle on the perpendicular road turns left or right, the driver of the target vehicle can turn left in the meantime*" [**Pop20_1**].

"*This type of configuration method can lead to gridlock if the road network becomes overloaded. In this situation, traffic congestion appears because many cars try to give priority-to-the-right to other cars entering the intersection from distinct directions*" [**Pop20_1**]. For these reasons, this configuration mode increases the level of congestion in crowded cities.

Bungartz et al. present in [Bun14_1] the four-phase model (Figure 3.5) for a crossroad that ensures collision avoidance through a set of rules that apply based on each driver's own turning preferences. This brings advantages especially during the simulation phase of a road network where each turning option of a driver from a specific road can be analysed separately or in conjunction with the vehicles movement patterns of the other roads entering the intersection. Moreover, this model does not involve the other traffic participants and successfully eliminates the gridlocks. Besides the mentioned benefits, it brings as a disadvantage the fact that it "*is not so close to reality as the priority-to-the-right rule*" [Bun14_1].
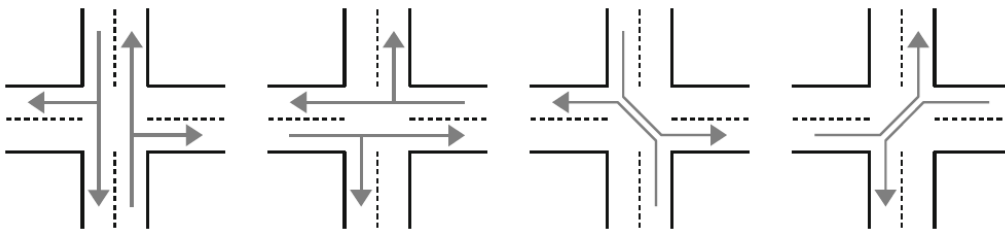
Figure 3.5. The four-phase model for a crossroad [Bun14_1] (pp.190, fig.8.10).

The four-phase model is also suitable for a traffic light system that has a separate phase for left-turning traffic. Also, it applies to controlling the "*right-of-way for uncritical, not too frequently used crossroads like those from residential areas*" [Bun14_1].

Figure 3.6 presents the simulation for the case where the intersection of the chosen case study "*has no crossing method defined. In this case, the vehicles will apply the priority-to-the-right rule. The policy of giving priority to the right is embedded in the simulation tool and does not need to be configured separately*" [**Pop20_1**]. The simulation tool ensures that collisions are avoided for vehicles crossing the simulated road network.
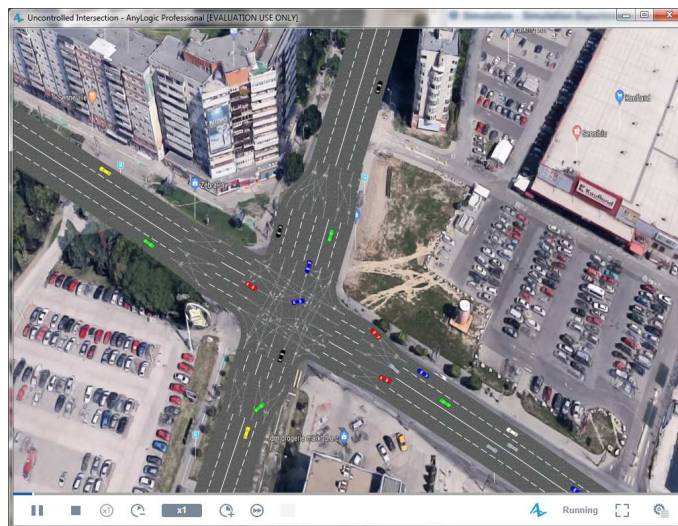
Figure 3.6. Simulation of the uncontrolled crossroad configuration for the Circumvalațiunii intersection [**Pop20_1**].

Signalized Crossroads Configuration

"*The problem of gridlock, as previously mentioned, can be solved by installing traffic lights that use three colors to control traffic flow*" [**Pop20_1**]. The appearance of the first three-colored traffic light system in 1914 (Ohio) represents the historical starting point of the ITS [Ash16], [**Pop17**].

The "*setting of green intervals, which allows vehicles to enter the intersection, plays a crucial role in reducing traffic congestion. The timing of these intervals and phases is usually chosen using previous traffic data and estimating the possible future load for each crossroad* [Bun14_1]*. The entry of the vehicle into the intersection can be configured in two modes: based on stop lines or based on lane connectors*" [**Pop20_1**]. For a better understanding of these traffic lights configuration modes, it is necessary to present the four-way intersection model of the crossroad used as a case study (Figure 3.7).
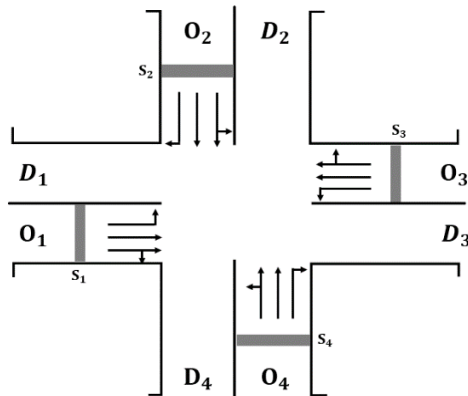
Figure 3.7. The four-way model for the Circumvalațiunii intersection [**Pop20_1**].

Figure 3.8 shows the AnyLogic simulation model for the Circumvalațiunii intersection in the case of placing traffic lights as a signalized traffic coordination method.
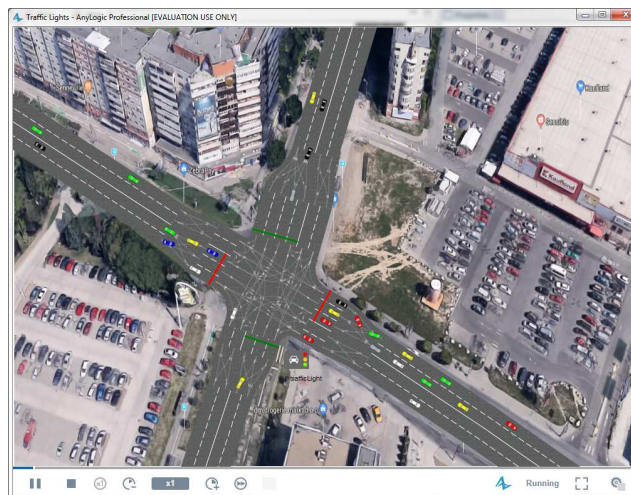
Figure 3.8. Traffic lights configuration for Circumvalațiunii intersection [**Pop20_1**].

The traffic lights configuration based on stop lines gives "*a green traffic signal for one of the stop lines s_i, i=$\overline{1,4}$ during a traffic signal cycle that ensures the crossing of the intersection from each origin node. To reduce the time spent at the intersection, the green signal can be given at the same time for vehicles coming from opposite directions (e.g. vehicles from O_1 and O_3), while considering that those vehicles changing their direction of movement shall give priority to vehicles moving straight. All vehicles from the lanes affected by the red traffic light shall wait for the green light, independent of the direction chosen after leaving the intersection (see* Figure 3.9*). For the simulated case study, it was considered that by having green time for two traffic lights at the same time, the vehicles that are moving to the left, in both cases, shall give priority to the right to vehicles crossing the perpendicular road that are moving ahead*" [**Pop20_1**].
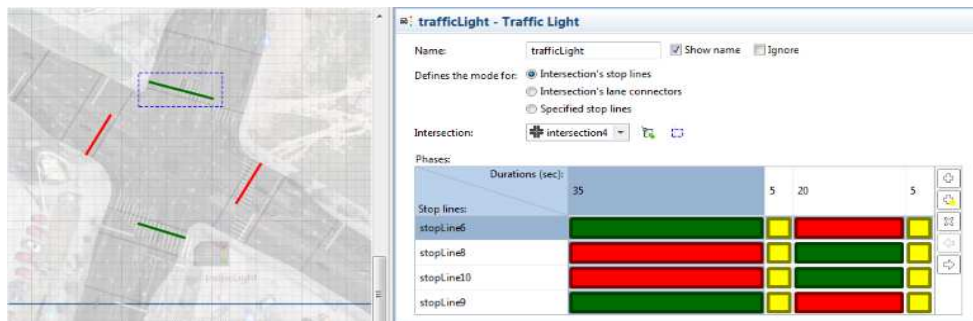
Figure 3.9. Traffic lights – configuration based on stop lines for the Circumvalațiunii intersection [**Pop20_1**].

"*The second method of traffic lights configuration is based on lane connectors in a manner that ensures avoidance of traffic jams. This case highlights the possible directions that can be reached, taking into account the current lane of the target vehicle. The advantage of this crossroad configuration mode is the additional green time that can be given to vehicles that are turning right. In this case, the restriction of giving priority to vehicles arises from the perpendicular road that has a green signal to go straight*" [**Pop20_1**]. Figure 3.10 illustrates the mapping of this traffic lights configuration mode to the chosen case study.
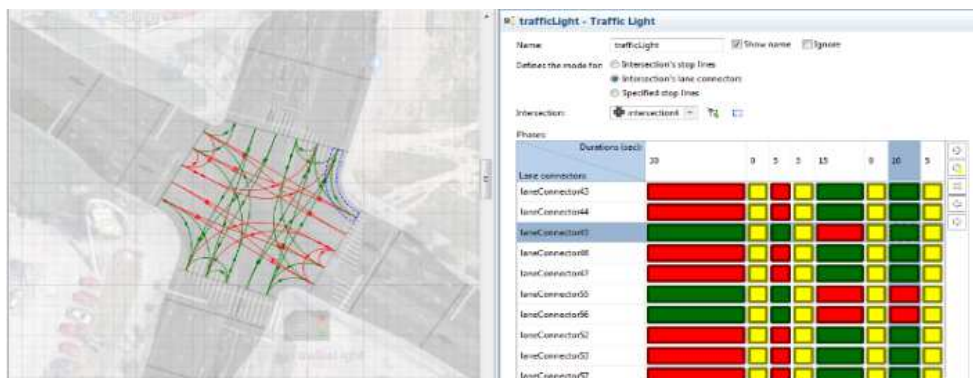
Figure 3.10. Traffic lights – configuration based on lane connectors for the Circumvalațiunii intersection [**Pop20_1**].

In addition to traffic lights configuration based on infrastructure characteristics (stop lanes or lane connectors), the development of new algorithms ensures improvements in the allocation of traffic lights phases that lead to a reduction of traffic congestion in intersections. In this regard, Pop [**Pop19_4**] proposed a planning algorithm based on the concept of rate-monotonic scheduling. "*The traffic signal controller was developed in the MATLAB R2012a version using Simulink with the Simevents library as in* Figure 3.11" [**Pop19_4**], considering as a starting point the approach proposed by Aljaafreh and Al Oudat [Alj14].
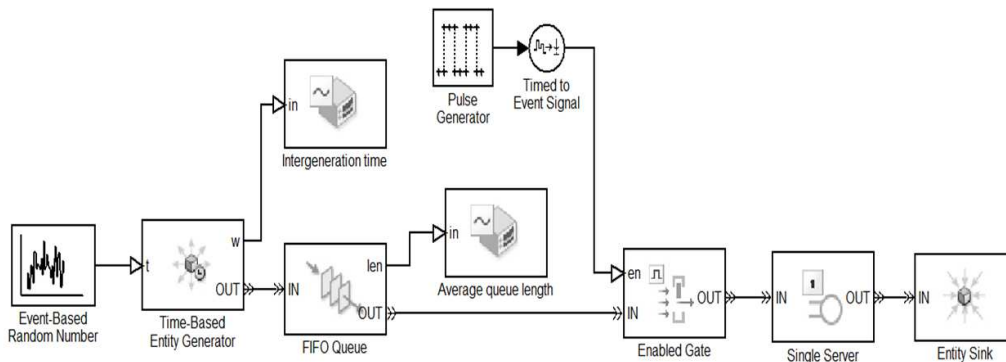
Figure 3.11. Simulation model of the signal processing unit for traffic lights [**Pop19_4**].

Crossroads Configuration using Roundabouts

"*Roundabouts, also known as traffic circles, proved their efficiency as a traffic coordination method in many cases*" [**Pop20_1**] through their self-organizing capacity. Roundabouts "*are one-way circular lanes that have entry points for vehicles coming from several directions. The movement of vehicles entering a roundabout is conditioned by the priority of those vehicles already present at the roundabout*" [**Pop20_1**]. A new vehicle enters the roundabout only after checking on the left side of the entry point if one of the fields can be reached with the maximum allowable velocity [Bun14_1]. Wrong approximations of the vehicles speed from the left of the entry point can lead to gridlocks by forcing those vehicles to reduce their speed or, in the worst-case scenario, to traffic collisions. Moreover, small roundabouts are prone to gridlocks based on previous assumptions [Bun14_1] and due to this, the design phase of a roundabout shall apply a complex analysis of roundabout capacity. This analysis monitors the existing road structure and uses standard formulas that, unfortunately, do not consider the influence of pedestrians or bicycles [Ber00].

"*In the case of a four-way intersection, where there are four incoming and outcoming roads, the intersection can be modeled itself with four fields*" [Bun14_1], [**Pop20_1**]. Each field has its specific behavior for the vehicles. According to [Ber00], the modeling process of a roundabout with multiple lanes is complex due to the need to cover the driver lane change behavior inside the roundabout lanes.

The AnyLogic simulation model of the roundabout was designed as a one-way road with two traffic lanes, "*and the four existing entrances were modeled as intersections that give priority to the vehicles that are already in the roundabout*" [**Pop20_1**]. The simulation software controls the movement inside the roundabout to avoid collisions. The studied intersection with roundabout looks as in Figure 3.12.
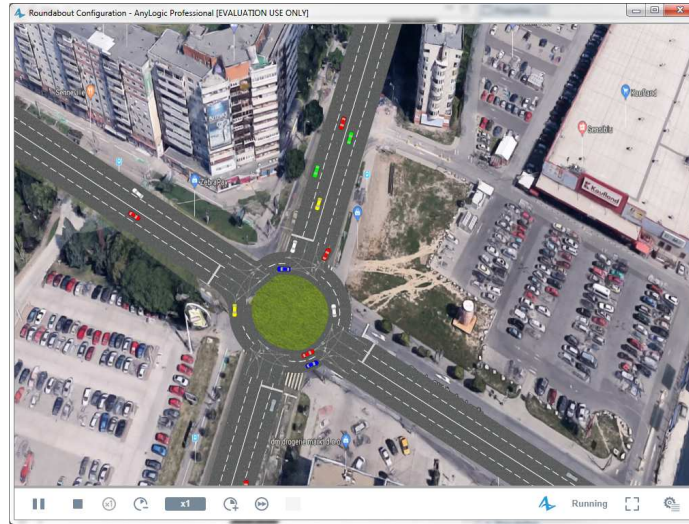
Figure 3.12. Roundabout configuration for the Circumvalațiunii intersection [**Pop20_1**].

Roundabouts need special attention in terms of safety for CAVs. In this case, the need arises for "*a central controller that manages conflicts within a roundabout named Roundabout Manager (RM) or Intelligent Traffic Management System (ITMS). This controller prioritizes the incoming vehicles based on different strategies and adjusts their trajectories, considering the type of roundabout. All strategies, algorithms, paradigms, results, environment, scenarios, scenes related to this kind of controller are simulated on a computer from the TMC*" [**Pop21**]. Some perturbative factors like large volumes of traffic data, weather conditions, and vehicular communication protocols influence the functionality of RM systems [**Pop21**].

Simulation Results and Discussion for the Chosen Case Study
The probabilities computation was performed based on real road traffic data "*received from Timișoara City Hall-General Directorate of Roads, Bridges, Parking and Utility Networks—Traffic Monitoring Office, Timișoara, Romania (Romanian official institution name: Primăria Municipiului Timișoara—Direcţia Generală Drumuri, Poduri, Parcaje și Reţele Utilitare–Birou Monitorizare Trafic, Timișoara, Romania)* based on the approved request *RE2019-002611/18.12.2019*" [**Pop20_2**], [**Pop20_3**]. The data collection process used inductive loops placed on the road infrastructure. Table 3.3 shows the calculated route choice probabilities for the case study discussed that were used as inputs for the simulation of all presented crossroad configuration methods.

Table 3.3. Route choice probabilities for the chosen case study [**Pop20_1**].

Origin nodes	Destination nodes			
	Iulius Town	Cetății Boulevard	Jiul Passage	Gheorghe Dima Street
Iulius Town	0.050	0.150	0.650	0.150
Cetății Boulevard	0.550	0.050	0.200	0.200
Jiul Passage	0.700	0.050	0.050	0.200

Origin nodes	Destination nodes			
	Iulius Town	Cetății Boulevard	Jiul Passage	Gheorghe Dima Street
Gheorghe Dima Street	0.600	0.050	0.250	0.100

"*The simulation was run for 15 minutes and the results are shown in* Table 3.4*. Parameters of interest include the number of vehicles and their necessary time to cross the road network. We can see that all intersection configuration methods have a positive impact on reducing traffic congestion compared to the case of an uncontrolled intersection. These results highlight that the roundabout configuration is the best for this case. Only for 15 minutes of traffic simulation can be observed an increase of 16 in the number of vehicles that are crossing the intersection. This configuration mode can lead to a long-term improvement in traffic flow through the intersection*" [**Pop20_1**].

Table 3.4. "*Travel time and number of vehicles based on different crossroad configuration methods*" [**Pop20_1**].

Crossroad configuration method	Travel time			Number of vehicles
	Min (s)	Max (s)	Mean (s)	
Uncontrolled intersection	14.074	793.007	251.933	174
Traffic lights – stop lines	14.060	445.112	93.050	453
Traffic lights – lane connectors	19.240	339.611	89.113	460
Roundabout	14.017	298.157	82.078	476

3.2.2. Links

Links are the second level of a network representation of the microscopic road traffic model. To better understand this concept, it is necessary to start with an example of a road network containing five crossroads (see Figure 3.13), as depicted in [Yin15]. This figure also includes the crossroads configuration modes. Within each intersection, there are eight mobility possibilities. Notations S1, S2, etc. represent the traffic requests for each lane inside of a link during the simulation process. "*The random traffic input data satisfy the Bernoulli 0-1 distribution in a discrete-time procedure*" [Yin15]. Within the presented road network are three types of links, called entrance links, inside links, and exit links [**Pop17**], [Yin15].
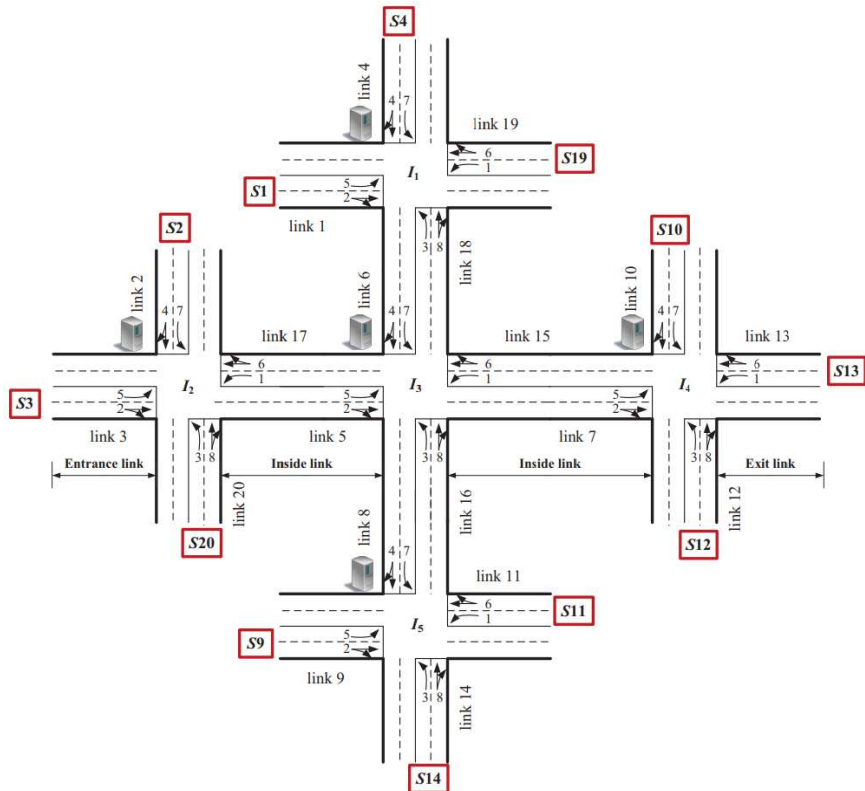
Figure 3.13. Road network containing five intersections [Yin15] (fig.1).

The entrance and exit links allow vehicles to enter and exit the road network. In the case of a road traffic simulation using AnyLogic Simulation Software, the *CarSource* blocks are positioned at the entrance links and the *CarDispose* blocks are connected to the exit links. The inside links allow the vehicle to move within the road network, directed using the *CarMoveTo* simulation block, from an entrance link to an exit link. According to Figure 3.13, each inside link contains two lanes. The driver uses one of these two lanes to go forward or to turn right and the other lane to make only a left turn. The next section will provide more details about the representation of traffic lanes.

3.2.3. Lane Choice

Lane choice is the third level of representation of the road network model. Within an internal link (see Figure 3.14), two traffic lanes are associated with one direction of travel. From the beginning of a link, until its end, equal discretized parts of the road can be considered. Each of these cells corresponds to a vehicle waiting in the queue. The cell size includes the lengths of the vehicles and the safety distance between vehicles. These sections of road will be numbered from 1 to L, where L is the maximum number of vehicles that can be at that time on that internal link. The entrance area of the vehicles moving from node A to node B was numbered with 0 [**Pop17**], [Yin15].
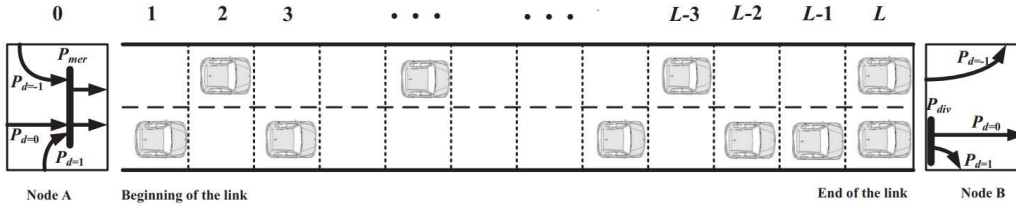
Figure 3.14. Inside link - lanes configuration [Yin15] (fig.2).

Both nodes A and B contain three directions of movement. The values $P_{d=-1}$, $P_{d=0}$ and $P_{d=1}$ associated with node A define the probabilities for the left-turn, straightforward and right-turn decisions of a target vehicle. In node B the following probabilities computation apply [**Pop17**], [Yin15]:

$$P_{d=-1} = P_{mer}^1$$
$$P_{d=0} = P_{mer}^2 \cdot P_{div}^1$$
$$P_{d=1} = P_{mer}^2 \cdot P_{div}^2$$

(3.1)

where $P_{mer} = [P_{mer}^1, P_{mer}^2]$ represent the merged probabilities consisting of two random distributions for the lane destined to left-turn and for the lane intended to straight movement (or the right-turn) after leaving node A. The previous equation uses $P_{div} = [P_{div}^1, P_{div}^2]$ to define divergent probabilities which are random distributions associated with straightforward movement and for making a right-turn before reaching node B.

The lane choice representation needs a dynamic update during the movement process inside a link. Lane change behavior is a complex activity that involves both traffic conditions and drivers' behaviors. All these aspects will be treated in more detail in **Section 3.3**.

3.2.4. Car-Following Level

The last level intends to highlight the representation of vehicles in the road network, from which its name as car-(vehicle-)following level arises. Each vehicle in the road network can be characterized by the following parameters: vehicle speed (also mentioned as velocity), vehicle position within the traffic network, and direction of movement [**Pop17**]. In a "*discrete-time procedure, all vehicles present in the network move in parallel according to the current positions and velocities*" [Yin15]. This action involves the movement of individual vehicles in the discrete places of the lane (see the cells in Figure 3.14). The degree of acceleration or deceleration of vehicles may also be taken into account, as well as the safety distance between vehicles.

This subchapter gave only a short presentation about the specific characteristics of the car-following representation level. **Section 3.4** will offer a detailed overview of the car-following modeling process where some well-known models will be discussed.

3.3. Lane Change Behavior Modeling

"*Lane change can be defined as the concept that describes the decision taken by a driver to change its current lane for movement. This action can be observed as a process that usually occurs in two main cases. The first case is when the LV has low velocity and the FV will change the lane only just for a while, with a return to its previous lane. In this case, the only reason is the driver desire to move at a higher speed, without changing its planned destination. The second case arises as a result of a reason like leaving the road network using an exit lane or possible ahead restrictions of lane changes that can influence the planned destination*" [**Pop19_1**].

"*Based on situations explained previously, in car-following modeling they have the leader change concept as correspondent. In all circumstances of the lane change, the LV will be changed, even if we talk about switching roles between the current LV and the FV, or the introduction of a new LV from the new joined traffic lane*" [**Pop19_1**].

"*For a better understanding of the behavior of lane changes, in* Figure 3.15 *are represented all possible situations that can appear during this action for a road that has three lanes for a direction of movement. Moreover, the relation with the terms specific for car-following models is illustrated*" [**Pop19_1**].

Figure 3.15 shows a "*possible lane change action during a road network crossing. We assume that we have one LV associated with each lane, and the positions of the lanes are as follows: : L_{i-1}- right lane, L_i - middle lane, L_{i+1} - left lane. The purpose is to study the behavior of the FV from lane L_i. This car has two options to change its lane. If the choice is lane L_{i+1}, the FV_{L_i} becomes the follower of the $FV_{L_{i+1}}$ (Figure 3.15a). At this point, the driver can then choose to return to his/her previous lane or to leave the road network if lane L_{i+1} is a left exit lane. In the other case, by moving to lane L_{i-1}, the FV_{L_i} becomes the follower of the $FV_{L_{i-1}}$ (Figure 3.15b)*" [**Pop19_1**], [**Pop20_3**].

"*Similar to the previous situation, the driver can further choose to return to his/her previous lane or leave the road network if lane L_{i-1} is a right exit. We can see that in all presented situations, the new role of a vehicle is highlighted with an asterisk, notation further used also in the case of parameters to identify the parameter value after a role change. In addition to the classic lane change based on a possible decision made by the driver to modify his/her initial itinerary, a lane change action taken only based on the low velocity of the LV is also possible*" [**Pop20_3**].
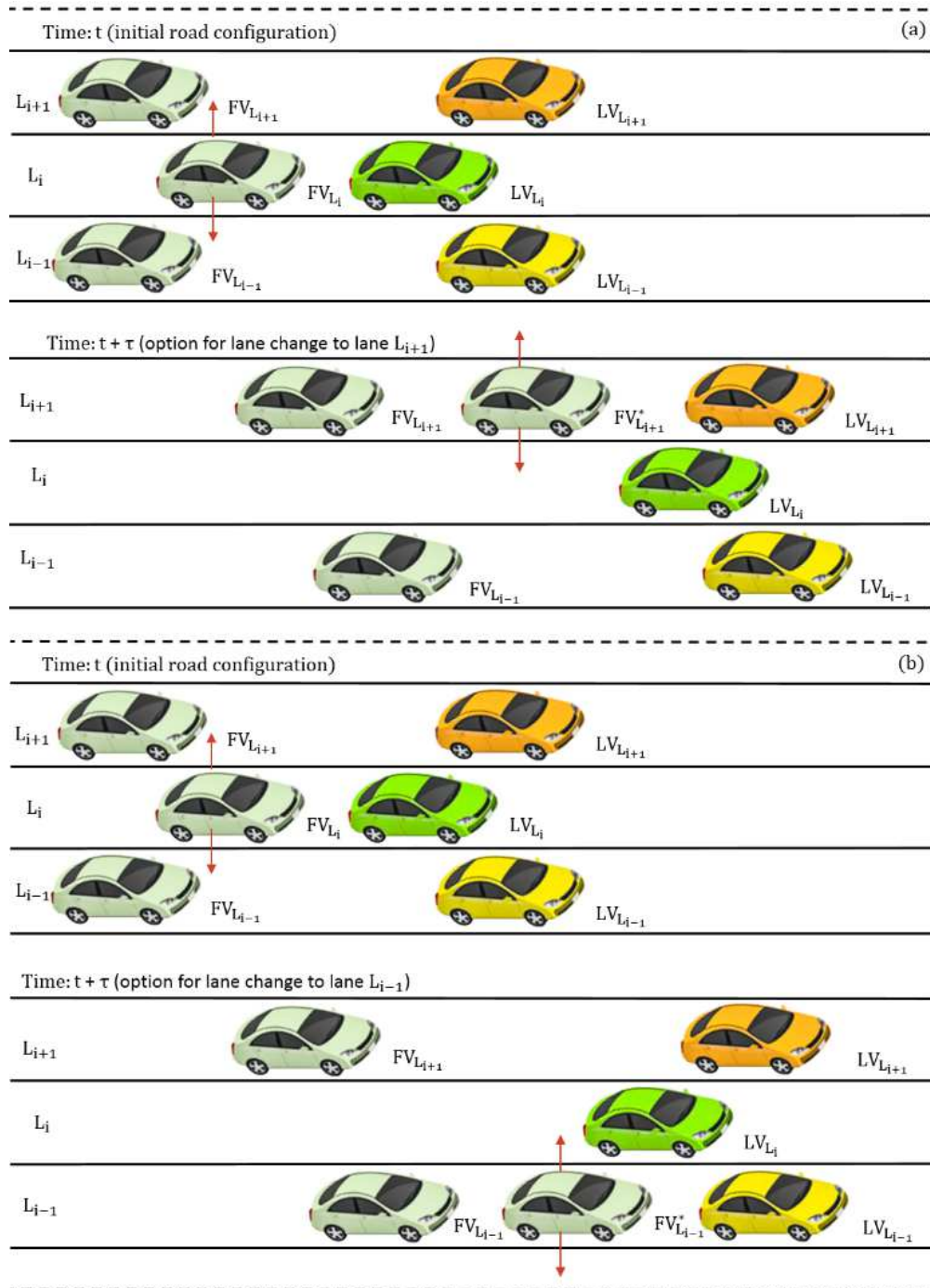
Figure 3.15. "*Lane change behavior: (a) movement of FV_{L_i} from lane L_i to lane L_{i+1} at time $t+\tau$; (b) movement of FV_{L_i} from lane L_i to lane L_{i-1} at time $t+\tau$* " [**Pop20_3**] (fig.2).

"*As shown before, the vehicle that initiates the lane change maneuver influences the behavior of the two vehicles from the current and the target lanes* [Kes07]*. To see that a lane change can lead to improvements in the individual local traffic situation of a driver, the incentive criterion was defined*" [**Pop20_3**].

"*Considering the following notations for the accelerations of the vehicles involved in the FV_{L_i} lane change action*:

$$
\begin{cases}
a_{driver} = a_{FV_{L_i}^*}(t + \tau) - a_{FV_{L_i}}(t) \\
a_{newfollower} = a_{FV_{L_{i+1}}}(t + \tau) - a_{FV_{L_{i+1}}}(t) \\
a_{driver} = a_{FV_{L_i}^2}(t + \tau) - a_{FV_{L_i}^2}(t)
\end{cases}
\tag{3.2}
$$

where $a_{FV_{L_i}^2}$ represents the acceleration of the FV_{L_i} successor and assuming that we

have symmetric lane change rules, the incentive criterion is represented by Relation (3.3) [Kes07]:

$$
a_{driver} + p \cdot (a_{newfollower} + a_{oldfollower}) > \Delta a_{th}
\tag{3.3}
$$

where p is the politeness factor that denotes the total advantage of the two immediately affected neighboring vehicles, and Δa_{th} is the switching threshold" [**Pop19_1**], [**Pop20_3**].

"*According to the driving rules established by law, some lane changes are forbidden. Here, we can reformulate the incentive criterion based on asymmetric passing rules defined according to the majority of European countries' traffic legislation* [Kes07]" [**Pop20_3**].

"*For asymmetric passing rules, two forms of incentive criterion can be defined:*

- *lane change from left to right* [Kes07]:

$$
a_{FV_{L_i}^*}^{eur}(t + \tau) - a_{FV_{L_i}}(t) + p \cdot a_{oldfollower} > \Delta a_{th} - \Delta a_{bias}
\tag{3.4}
$$

- lane change from right to left [Kes07]:

$$
a_{FV_{L_i}^*}(t + \tau) - a_{FV_{L_i}}^{eur}(t) + p \cdot a_{newfollower} > \Delta a_{th} + \Delta a_{bias}
\tag{3.5}
$$

where $a_k^{eur}, k = \left\{ FV_{L_i}^*, FV_{L_i} \right\}$ are the accelerations adapted by the driver to the majority of European countries' traffic legislation and Δa_{bias} is a constant that represents the keep-right directive of the lane change rule" [**Pop20_3**].

"Another important criterion specific to this action is the safety criterion: the deceleration of the successor vehicle from the target lane ($FV_{L_{i+1}}$ or $FV_{L_{i-1}}$) shall not exceed a given safe acceleration limit, as defined by Equation (3.6) [Kes07]" [**Pop20_3**].

$$a_{FV_{L_j}} (t + \tau) \geq -a_{safe}, j = \left\{ i-1, i+1 \right\}$$
(3.6)

"Lane change behavior can be measured by calculating the lane changing rate using the relation below [Kes07]:

$$r(\rho) = \frac{n}{\Delta x \cdot \Delta t}$$
(3.7)

where n is the number of lane changes during a Δt interval of time on a section of road with a length of Δx kilometers" [**Pop20_3**].

3.4. Car-Following Model and its Derivatives

Car-following is the most well-known microscopic modeling procedure of road traffic and has various variations depending on the influence of a certain parameter of the model. This type of modeling consists of the behavioral study of vehicles that "follow" the front vehicle while moving on a lane [Bar10], [Ger75]. In this way, the vehicle that "follows" (FV - *follower vehicle*) the mode of travel of the front vehicle (LV - *leader vehicle*) must adapt its acceleration and thus speed to ensure a safe distance from the LV.

A car-following model can be represented as a stimulus-response equation according to the Relation (3.8). The response of FV to the actions of LV translates into the tendency to accelerate/decelerate with a time delay τ from the moment of receiving the stimulus (LV action) [Ger75]. The stimulus function is represented by a combination of several factors: acceleration, speed, the relative speed of FV compared to LV, the threshold value for speed, the dynamic distance between vehicles, vehicle performance, etc. [Rot01]. Sensitivity consists of a proportionality factor with a role in equating the stimulus function with the response or control function [Rot01].

$$Response(t + \tau) = Sensitivity \times Stimulus(t) \qquad (3.8)$$

Starting from the previous relationship, variations of the model may occur based on the "*answers to the following questions:*

• *What is the nature of the response given by FV?*

• *What are the stimuli to which FV responds and how can its sensitivity be measured?"* [Bar10], [Ger75].

To provide the response to the stimulus function, it is necessary for the FV driver to complete the following steps, as described in [Rot01]:

• perception - the FV driver collects information from his field of vision regarding LV behavior (degree of acceleration, speed, evolution of running distance from LV);

• decision making - the interpretation of the perception on the driving behavior of the LV and its correlation with landmarks of previous travel experiences lead to the development of a FV control strategy from which the driver's driving skills evolve;

• control - represents the implementation of the decision taken by the driver through the coordinated and dexterous execution of the necessary maneuvers and their constant evaluation until the final goal is achieved.

"*The main parameters of interest considered in this concept are vehicle position, velocity, acceleration/deceleration and direction of movement. In addition to the aforementioned parameters, other parameters that influence the movement behavior of a vehicle, some of which depend on the vehicle characteristics, are presented in* Figure 3.16a" [**Pop19_1**], [**Pop20_3**]:

• L_{FV} - length of FV;

• L_{LV} - length of LV;

• S - standard safety distance between FV and LV calculated according to Relation (3.9) [Kho10], [**Pop20_2**], [**Pop20_3**]:

$$S = L \cdot \left(1 + \frac{x_{FV}}{16.10}\right) \qquad (3.9)$$

where L is the average length of a vehicle and is approximately $L = 4.50\,m$ in the case of passenger vehicles (cars);

• "m_i - *mass of the vehicle* i *where* $i = \{FV, LV\}$;

• $g \simeq 10\ m/s^2$ - *acceleration of gravity used to represent the weight of a vehicle according to mechanics theory (product between mass and acceleration of gravity);*

• a_i - *acceleration/deceleration value of the vehicle* i *where* $i = \{FV, LV\}$;

- F_i - inertial force of the vehicle i where $i = \{FV, LV\}$ that can be computed according to Relation (3.10), after applying Newton's second law of motion $t - \tau$ " [**Pop19_1**], [**Pop20_3**]:

$$\vec{F_i} = m_i \cdot \vec{a_i} \qquad (3.10)$$
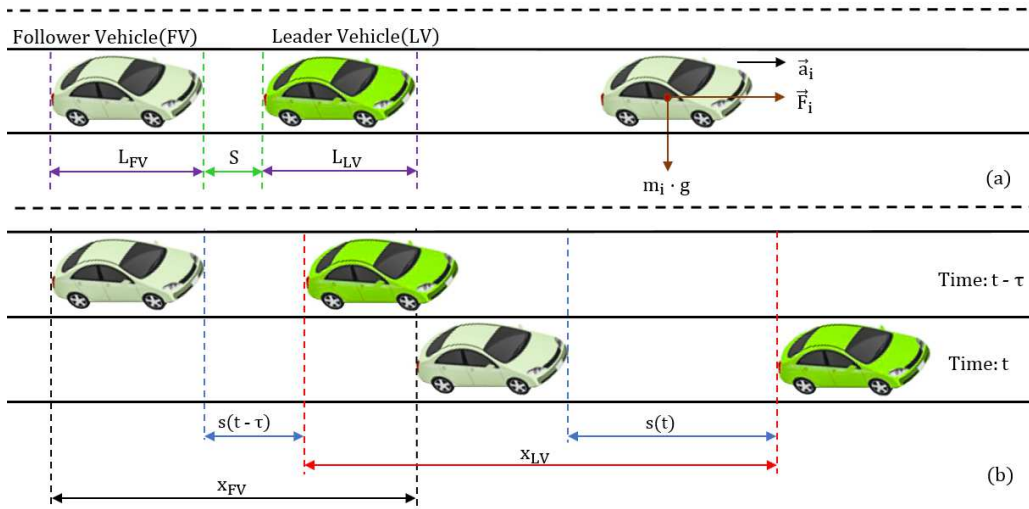
Figure 3.16. "*Car-following concept: (a) vehicle characteristics; (b) parameters of interest and vehicles behavior (the listed parameters will be used further in the car-following model definition)*" [**Pop20_3**] (fig.1).

"*To better understand the influence of the car-following model parameters,* Figure 3.16b *illustrates the interaction of a LV and FV at time* $t - \tau$ *and* t. *The parameters of interest for the vehicle's movement behavior are:*

- x_{FV} - running distance of FV during a τ interval of time;
- x_{LV} - running distance of LV during a τ interval of time;
- $s(t)$ - dynamic distance value between FV and LV at time t ;
- $s(t - \tau)$ - dynamic distance value between FV and LV at time $t - \tau$ "

    [**Pop19_1**], [**Pop20_3**].

3.4.1. Gipps

The Gipps model is the most known *car-following* model. It is part of the class of traffic models based on maintaining the safety distance between vehicles and avoiding their collisions. The main purpose of the model is to control the acceleration/deceleration behavior of the driver by ensuring the compliance of the restriction with a safe distance to the vehicle in front [Daa15].

The original form of the Gipps model, as proposed in [Gip81] and taking into account the rewritings in [Daa15], [Pun05] to simplify the understanding of the concept, is presented by Relation (3.11):

$$v_{FV}(t+\tau) = min\{v_{a,FV}(t+\tau), v_{b,FV}(t+\tau)\} \qquad (3.11)$$

where $v_{a,FV}(t+\tau)$ represents the value of the velocity of the FV at the moment $t+\tau$, if there is no LV in front of it. This velocity is defined using (3.12) based on a free-flow acceleration profile that facilitates the attainment of maximum speed by the vehicle:

$$v_{a,FV}(t+\tau) = v_{FV}(t) + 2.5 \cdot a_{FV}^{max} \cdot \tau \cdot \left(1 - \frac{v_{FV}(t)}{V_{FV}}\right) \cdot \sqrt{0.025 + \frac{v_{FV}(t)}{V_{FV}}} \qquad (3.12)$$

noting that the following notations have been used:

- a_{FV}^{max} – the maximum acceleration rate desired by the FV;
- V_{FV} – the value of the velocity at which the FV wants to move;
- τ – reaction time of the FV.

The second case, represented by the calculation of $v_{b,FV}(t+\tau)$, corresponds to the situation in which this velocity is chosen by the driver to respect the specific safety distance to rest at any braking of the LV at the maximum deceleration rate:

$$v_{b,FV}(t+\tau) = b_{FV} \cdot \tau + \sqrt{b_{FV}^2 \cdot \tau^2 - b_{FV} \cdot \left[2 \cdot (x_{LV}(t) - x_{FV}(t) - S) - v_{FV}(t) \cdot \tau - \frac{v_{LV}(t)^2}{\hat{b}_{LV}}\right]} \quad (3.13)$$

where b_{FV} represents the maximum deceleration rate of FV, and $\hat{b}_{LV}$ is the maximum value estimated by FV of the deceleration that LV intends to achieve.

The Gipps model has various variations, among which it is necessary to mention the "*Krauss model which is a stochastic version of the original model*" [Kra97], [Tre13_2]. This model directly calculates the desired velocity value v_d [Kra97], [Pou17], [Son14]:

$$v_d(t) = min\{v_{max}, v_{FV}(t) + a_{max} \cdot \Delta t, v_{safe}(t)\} \qquad (3.14)$$

considering the safety velocity v_{safe} defined as:

$$v_{safe}(t) = v_{LV}(t) + \frac{s(t) - v_{FV}(t) \cdot \tau_k}{\frac{v_{LV}(t) + v_{FV}(t)}{2 \cdot b_{max}} + \tau_k} \qquad (3.15)$$

and the fact that a random disturbance $\eta > 0$ can affect the current speed of the FV (v_{FV}) while driving:

$$v_{FV}\left(t + \Delta t\right) = max\left\{0, v_d\left(t\right) - \eta\right\} \tag{3.16}$$

The significance of the notations used in Equations (3.14), (3.15) and (3.16) are:

- "b_{max} - *maximum deceleration that a driver is willing to use in non-emergency situations;*
- τ_k - *reaction time of the driver (about 1 s);*
- v_{max} - *maximum vehicle speed;*
- a_{max} - *maximum acceleration a driver is willing to use;*
- Δt - *step duration of the simulation*" [Pou17], [Son14].

According to [Pou17], a_{max}, b_{max} and τ_k are optimization variables, which must be calibrated for each trip.

3.4.2. Pipes

This model introduces the dynamic of a chain of traffic (see Figure 3.17) as it results from the assumption "*that the drivers of the various vehicles on the line at all times obey a postulated traffic regulation*" [Pip53], [Rot01]. This regulation suggests how the FV shall handle the maintenance of a safe distance to LV based on velocity control: "*A good rule for following another vehicle at a safe distance is to allow yourself the length of a car (about fifteen feet) for every ten miles per hour you are traveling*" [Pip53]. "*According to Pipes car-following model, the minimum safe distance headway increases linearly with speed. A disadvantage of this model is that at low speeds, the minimum headways proposed by the theory are considerably less than the corresponding field measurements*" [Mat14].
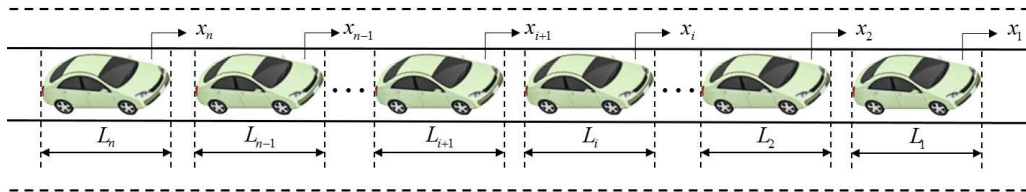
Figure 3.17. A line of traffic with n vehicles.

The following dynamical equations describe the interaction between the vehicles moving in a row on a traffic lane considering their separation based on the postulated "*legal distance*" [Pip53] mandatory:

$$x_i = x_{i+1} + \left(S + T \cdot v_{i+1}\right) + L_i, \ i = \left\{1, 2, \ldots, n-1\right\} \tag{3.17}$$

where $T = 1.02\ s$ is the constant time prescribed by the postulated "*traffic law*" and is also used in the definition of velocities:

$$T \cdot \dot{v}_{i+1} + v_{i+1} = v_i, \ i = \{1,2,...,n-1\} \tag{3.18}$$

By applying a p multiplied Laplace transform of the velocity, Pipes introduces the following relation [Pip53]:

$$Lv_i(t) = V_i(p), \ i = \{1,2,...,n-1\} \tag{3.19}$$

to transform the differential Equation (3.18) into the following algebraic relation:

$$(T \cdot p + 1)V_{i+1} = V_i + T \cdot p \cdot v_{i+1}(0), \ i = \{1,2,...,n-1\} \tag{3.20}$$

which considers $v_i(0)$ as the initial velocities at time $t = 0$.

3.4.3. Gazis-Herman-Rothery

Classified as a stimulus-response model, this model originates from General Motors (GM) research from 1958. This GM model [Cha58] "*specifies the stimulus as the relative speeds of vehicles, that is, each vehicle tended to move at the same speed of its front vehicle*" [Li12]. The Relation (3.21) considers Figure 3.16 notations and describes this mentioned approach:

$$a_i(t + \tau) = k \cdot \Delta v_i(t), \ i = \{1,2,...,n\} \tag{3.21}$$

where $a_i(t + \tau)$ represents the acceleration of the i-th vehicle at time $t + \tau$, with $\tau \in \mathbb{R}$ as the driver reaction time, $k \in \mathbb{R}, k > 0$ - the sensitivity coefficient describing the responsive intensity of the driver to the unit stimulus and the $\Delta v_i(t)$ is the difference between the velocities of the leading i-th vehicle and the following $i+1$-th vehicle as presented below:

$$\Delta v_i(t) = v_i(t) - v_{i+1}(t), \ i = \{1,2,...,n\} \tag{3.22}$$

A series of changes of the original GM model led to obtaining the GHR model in 1959. The GHR model starts from the drawback of the GM model that "*could not describe the road traffic process in higher density since the behavior of the driver had nothing to do with running distances in* (3.21)" [Gaz59], [Li12]. The new proposed model from (3.23) also facilitates the adaptation of (3.21) to a macroscopic description of the road traffic:

$$a_i(t + \tau) = k \cdot \frac{\Delta v_i(t)}{\Delta x_i(t)}, \ i = \{1,2,...,n\} \tag{3.23}$$

where $\Delta x_i(t)$ is the dynamic distance value between the leading i-th vehicle and the following $i+1$-th vehicle at time t:

$$\Delta x_i(t) = x_i(t) - x_{i+1}(t), \; i = \{1,2,\dots,n\} \qquad (3.24)$$

Further developments conducted by Edie [Edi61] succeeded in a new model that considers that the velocity of the vehicle itself has the capacity to influence the driver behavior. The modified GHR model can be generalized as follows to relate the "*acceleration to the velocity of the LV, relative velocity and spacing between FV and LV, and driver reaction time*" [Edi61], [Li12], [Pan05]:

$$a_i(t + \tau) = k \cdot v_i^m(t) \cdot \frac{\Delta v_i(t)}{\Delta x_i^l(t)}, \; i = \{1,2,\dots,n\} \qquad (3.25)$$

where $m, l \in \mathbb{R}^+$ are constants during the calibration process of the model for a particular road network. According to [Gaz61], the most favorable values determined for these parameters respect the following constraints $m \in [0,2]$ and $l \in [1,2]$.

This model opens the path to new developments regarding the optimization of the calibration parameters m and l. It must be mentioned that the main outcome of this model is to establish a mathematical relationship between various stimuli and the acceleration and offers a good starting point for determining the factors that influence the behavior of the FV [Oss05].

3.4.4. Optimal Velocity Difference

The OVD model is another stimulus-response approach that takes into account the driver behavior. Proposed by Bando et al. [Ban95], OVM consists of a dynamic model oriented to traffic congestion that considers the running distances between vehicles moving in a row and the velocity difference between the vehicles [Mat14]. These parameters represent the inputs for the calculation of the optimal velocity that each vehicle should achieve. In this case, the dynamical equation of the traffic system from (3.26) "*assumes that the driver seeks a safe velocity based on the distance to LV*" [Li12]:

$$a_i(t) = k \cdot \left[V(\Delta x_i(t)) - v_i(t) \right], \; i = \{1,2,\dots,n\} \qquad (3.26)$$

where $k \in \mathbb{R}, k > 0$ - is the sensitivity coefficient (assumed to be independent of i) describing the responsive intensity of driver to unit stimulus and $V(\Delta x_i(t))$ represents the optimal velocity function defined as in (3.27):

$$V(\Delta x_i(t)) = \frac{1}{2} \cdot v_{max} \cdot \left[tanh(\Delta x_i(t) - s(t)) + tanh(s(t)) \right], \; i = \{1,2,\dots,n\} \qquad (3.27)$$

where v_{max} represents the maximal velocity of the vehicle, $s(t)$ - the dynamic safety distance between the vehicles and $tanh(\cdot)$ is the hyperbolic tangent function.

The optimal velocity function from (3.27) "*is a monotonically increasing function with* $\Delta x_i(t)$ *and it has an upper bound, while it has a turning point defined as*" [Li12]:

$$\Delta x_i(t) = s(t) : V''(s(t)) = 0, \ i = \{1,2,\ldots,n\} \tag{3.28}$$

Further studies showed that the OVD model could not describe the "*nonlinear characteristics of traffic flow (e.g., traffic jam information, stop and go waves, non-equilibrium traffic flow etc.)*" [Ban98], [Li12]. For this reason, Bando et al. introduced a time delay $\tau \in \mathbb{R}$ in the initial OVD model as follows [Ban98]:

$$a_i(t + \tau) = k \cdot \left[V(\Delta x_i(t)) - v_i(t) \right], \ i = \{1,2,\ldots,n\} \tag{3.29}$$

In addition to this improvement related to inclusion of nonlinear characteristics, this model produces excessive accelerations and decelerations [Hel98]. Helbing and Tilch [Hel98] tried to solve this problem by applying a calibration based on the follow-the-leader concept [Li12]. These researchers argued the necessity of considering the relative velocity of successive vehicles, so they developed the Generalized Force (GF) model [Hel98], [Li12]:

$$a_i(t) = k \cdot \left[V(\Delta x_i(t)) - v_i(t) \right] + \lambda \cdot \Delta x_i(t) \cdot H(-\Delta x_i(t)), \ i = \{1,2,\ldots,n\} \tag{3.30}$$

where $\lambda \in \mathbb{R}, \lambda > 0$ is the sensitivity coefficient describing the relative velocity response intensity [Cao20] and $H(\cdot)$ represents the Heaviside function defined as:

$$\begin{cases} H(x) = 0, \ \forall x \leq 0 \\ H(x) = 1, \ \forall x > 0 \end{cases} \tag{3.31}$$

3.4.5. Full Velocity Difference

This concept emerges as a future development of the OVD and GF models. The main benefit of the FVD model is to cover the effect of the positive velocity difference ignored by the GF model, which misleads the calculation of the vehicle moving delay [Cao20]. Taking into account both positive and negative velocity differences, the FVD model has the following definition as proposed by Jiang et al. [Li12], [Jia01]:

$$a_i(t) = k \cdot \left[V(\Delta x_i(t)) - v_i(t) \right] + \lambda \cdot \Delta v_i(t), \ i = \{1,2,\ldots,n\} \tag{3.32}$$

Another advantage of using this model is that it could describe the phase transition of traffic flow and provide good predictions regarding the evolution of traffic congestion levels. Furthermore, numerical simulations proved that the FVD model can describe vehicle start delays and disturbance propagations [Cao20].

A major drawback of the FVD model consists of the unrealistic modeling procedure due to the fact that it models the velocity differences symmetrically

[Li12]. Furthermore, other numerical simulations showed that this approach has too high deceleration. A solution involving the ITS for the obtaining of real-time traffic data comes from the Ge et al. proposal from [Ge08]. The researchers proposed the Two Velocity Difference (TVD) model which considers both $\Delta v_i(t)$ and $\Delta v_{i+1}(t)$ velocity differences as follows:

$$a_i(t) = k \cdot \left[V\left(\Delta x_i(t) \right) - v_i(t) \right] + \lambda \cdot G\left(\Delta v_i(t), \Delta v_{i+1}(t) \right), \; i = \{1,2,\ldots,n\} \qquad (3.33)$$

where $G(\cdot)$ is a generic, monotonically increasing function defined as:

$$G\left(\Delta v_i(t), \Delta v_{i+1}(t) \right) = p \cdot \Delta v_i(t) + (1-p) \cdot \Delta v_{i+1}(t), \; i = \{1,2,\ldots,n\} \qquad (3.34)$$

where $p \in \mathbb{R}, p > 0$ represents the weighting value.

The simulation results based on the application of TVD and its comparison with FVD showed the disappearance of unrealistic high decelerations corresponding to the FVD approach.

3.4.6. Intelligent Driver Model

"*IDM is a continuous response model that does not consider a reaction time and assumes that the acceleration of FV is a continuous function of the FV velocity, the running distance between FV and LV and the relative velocity of FV to the LV velocity*" [Pun05]. According to Treiber and Kesting, IDM "*is probably the simplest complete and accident-free model producing realistic acceleration profiles and a plausible behavior in essentially all single-lane traffic situations*" [Tre13_2].

Equation (3.35) defines the IDM acceleration a_i of the i-th vehicle as following [Pun05], [Tre13_2]:

$$a_i(t) = a^{(i)} \cdot \left\{ 1 - \left(\frac{v_i(t)}{v_0^{(i)}} \right)^{\delta} - \left[\frac{s_d\left(v_i(t), \Delta v_i(t) \right)}{s(t)} \right]^2 \right\}, \; i = \{1,2,\ldots,n\} \qquad (3.35)$$

which mediates the tendency to accelerate in order to reach the desired velocity $v_0^{(i)}$, and the deceleration tendency when the running distance between FV and LV is less than the desired spacing $s_d\left(v_i(t), \Delta v_i(t) \right)$ defined as:

$$s_d\left(v_i(t), \Delta v_i(t) \right) = s_0^{(i)} + s_1^{(i)} \cdot \sqrt{\frac{v_i(t)}{v_0^{(i)}}} + T^{(i)} \cdot v_i(t) + \frac{v_i(t) \cdot \Delta v_i(t)}{2 \cdot \sqrt{a^{(i)} \cdot b^{(i)}}}, \; i = \{1,2,\ldots,n\} \qquad (3.36)$$

where:

- $s_0^{(i)}$ - represents the desired spacing in the case of zero velocity of vehicle i ;

- $V_0^{(i)}$ - is the desired velocity at time t ;

- $a^{(i)}, b^{(i)}, \delta, T^{(i)}$ and $s_1^{(i)}$ are nonphysical parameters of the i -th driver.

  According to [Tre13_2], the dynamical term $\dfrac{v_i(t) \cdot \Delta v_i(t)}{2 \cdot \sqrt{a^{(i)} \cdot b^{(i)}}}$ is responsible for

the implementation of the intelligent breaking strategy.

In the case of the extension of the IDM to two-lane roads, the nonphysical parameter δ will be equal to 4 and the Relation (3.35) becomes [Kes05]:

$$a_i(t) = a^{(i)} \cdot \left\{ 1 - \left(\frac{v_i(t)}{V_0^{(i)}} \right)^4 - \left[\frac{s_d(v_i(t), \Delta v_i(t))}{s(t)} \right]^2 \right\}, \ i = \{1,2,\ldots,n\} \qquad (3.37)$$

3.4.7. Fuzzy-Based Model

As the driver behavior is an important source of uncertainties in the modeling process of the interaction between the vehicles moving on a lane, the fuzzy approach can be employed as a solution. In fuzzy modeling, driver behavior "*is abstracted as a fuzzy controller, whose inputs are the status information of the preceding vehicles and the output consists of the decision taken as a result of a series of thinking*" [Li12].

Kikuchi and Chakroborty were the first researchers who tried to fuzzify the GHR model [Kik92], [Li12]. The proposed model "*divides the selected inputs into some fuzzy sets and applies further logical operators to produce fuzzy output sets or rule-based car-following behavior*" [Pan05]. The structure of the Fuzzy Inference System (FIS) is defined as follows [Kik92]:

Input : $s(t), \Delta v_i(t), r$

Rule i: *IF* $s(t) = DS_i$ *AND* $\Delta v_i(t) = RS_i$ *AND* $r = ALV_i$

        THEN $y = AFV_i$

… … … … … … … … … … … … … … … …   , $i = \{1,2,\ldots,n\}$ (3.38)

Rule n: *IF* $s(t) = DS_i$ *AND* $\Delta v_i(t) = RS_i$ *AND* $r = ALV_i$

        THEN $y = AFV_i$

Conclusion : $y = AFV'$

where:
- "*r - the rate of change of velocity of LV (in specific number);*
- DS_i *- the perceived distance (in fuzzy number);*
- RS_i *- the perceived relative speed (in fuzzy number);*
- ALV_i *- the perceived rate of change of LV speed (in fuzzy number);*
- AFV_i *- the perceived rate of change of FV speed (in fuzzy number);*
- AFV' *- the predicted reaction of FV in acceleration/deceleration rate (in fuzzy number)*" [Kik92].

Table 3.5 presents the categories of premise variables as they were used in the car-following approach from [Kik92].

Table 3.5. Fuzzy sets of premise variables [Kik92].

Fuzzy sets	Distance between LV and FV (DS)	Relative speed (RS)	Actions of LV (ALV)	
			Acceleration	Deceleration
(1)	very small	FV slower	strong	strong
(2)	small	FV slightly slower	somewhat strong	somewhat strong
(3)	adequate	near zero	normal	normal
(4)	more than adequate	FV slightly faster	mild	mild
(5)	large	FV quite faster	very mild	very mild
(6)	very large	FV faster	none	none

3.5. Advantages and Disadvantages of the Car-Following Modeling Approach

The biggest disadvantage of car-following models is their orientation towards the examination of road traffic on a single lane. In this way, problems arise in the case of the integration of a new vehicle as a result of the driver's decision to change its current traffic lane. In this case, there is a need for an adaptive model that is able to manage LV / FV role changes in cases such as:
- entry of a new vehicle on the modeled traffic lane;
- leaving the lane by one of the vehicles;
- the departure by the FV of the current lane with return as a reason for the initial movement of the LV at low speed, in which case we are talking about the change of roles of the two vehicles (the FV becomes the new LV).

Another problem specific to this type of modeling is the integration of heavy vehicles. A study in this regard is presented in [Che16] and aims to demonstrate the low capability of car-following in terms of removing disturbances in traffic parameters in the case of mixed travel, having both cars and heavy vehicles. A delayed response of the heavy vehicle driver was observed in the case of deceleration, in response to the LV deceleration represented by a vehicle, but also to the timely takeover of the previous velocity level during and after the execution of an acceleration operation. If a car follows a heavy vehicle, a higher deceleration trend was observed than LV continued with gradual acceleration, following the perception of a deceleration action of the heavy vehicle.

3.6. Summary and Conclusions

This chapter discussed the concept of road traffic modeling at the microscopic level. The first step was to familiarize with the levels of representation of the road traffic modeling process such as crossroads configuration, links, lane choice, and car-following level. A critical analysis was provided on the configuration modes of th crossroads sustained by the simulation results for an intersection from

Timișoara (Romania), taken as a case study. One more time, the efficiency of the roundabout configuration was proven but also its disadvantage was highlighted in case of crowded traffic. In these situations, the usage of roundabouts leads to gridlocks when the capacity of the roundabout has been exceeded.

Due to its high influence on the real-time interaction of vehicles during the movement process, the lane choice concept was expanded in a separate subchapter. The incentive criteria that are the basis of the safe coordination of lane change maneuvers were defined in this thesis.

Based on the same considerations regarding the impact on the interaction between vehicles during movement, a special subchapter was assigned to a critical analysis of the most well-known car-following models. Furthermore, many derivatives of these classical car-following models were presented. This critical analysis aimed to identify the advantages and the disadvantages of the traditional car-following, which is single-lane oriented.

This chapter serves as a foundation for building a refined car-following model that easily addresses the multiple-lane roads that are widely found nowadays. The next chapter will present in detail this new approach that incorporates the lane change behavior of the vehicles moving on the adjacent road traffic lanes in the description of the driving strategy of the FV and LV from a target lane.

4. REFINEMENT OF THE CAR-FOLLOWING MODEL

4.1. Preliminaries

The purpose of this chapter is to provide a solution to refine the car-following model. Based on transportation theory, the car-following model is single-lane oriented. Here, an approach to extend the standard model to multiple-lane roads by considering the lane change behavior of the vehicles moving on the adjacent traffic lanes.

The chapter starts with an analysis of the driver behavior modeling (DBM) concept and its main implementation approaches. The most used DBM implementation techniques are the "*Gaussian mixture model (GMM) and the piecewise auto-regressive exogenous (PWARX) model*" [Ang11] which are presented in detail in this thesis. Both approaches are studied concerning the concept of car-following and underline the influence of the observed LV parameters on the changes in FV driver behavior during the movement process. Further, the thesis presents how traffic modeling can be modeled using Markov chains. The application of this modeling approach proves its benefits, especially in the simplification process of the origin-destination (OD) volumes estimation. The accuracy of these estimations brings improvements in traffic lights management through real-time control of green-interval settings.

This thesis further concentrates on the application of "*a DBM at the maneuvering level based on tactical route execution, more explicitly based on lane change behavior*" [**Pop20_4**]. The proposed procedure for the refinement of the car-following model consists of the application of the "*decisions taken to fulfill small and coordinated portions of a trip* [Ham12]" [**Pop20_4**]. Here, arises one of the main contributions of this thesis consisting of the modeling of the road traffic lanes as Markov nodes, and the transitions between several nodes of the modeled road network represent the lane change maneuvers. The probabilities associated with each node of the Markov chain consist of the probability of changing the movement by joining a specific traffic lane. The probabilities computation uses the traffic data from time t-1 and updates these values in real-time by permanently retrieving the traffic parameters from the inductive loops placed on the road network.

Because of the uncertainties introduced by drivers behavior, the lane change action is modeled further as a Bayesian specific problem. The use of the Bayesian probabilistic concept at this level of traffic modeling represents another important contribution to this thesis. This Bayesian-based computation considers the movement parameters for the FV from the current traffic lane and also some specific probabilities related to the target lane. These target lane related probabilities arise from the driver decision to leave the road network through an exit that is accessible only from an adjacent lane. Another case that leads to a lane change decision of the FV relates to the LV velocity changes (acceleration/deceleration behavior), and the FV changes its current traffic lane just for passing the LV with a return to its initial lane after the maneuvering execution.

The proposal of the multiple-lane car-following model considers the traffic lanes as Markov nodes of a road network modeled as a Markov chain, and the lane

change predictions are included as part of the car-following model. The modeling approach starts from the state space representation of the single-lane oriented car-following model, referred in this thesis also as the standard car-following model. After the presentation of the refinement proposal of the standard car-following model, a simulation has been done in Simulink, part of MATLAB R2020a (MathWorks, Natick, MA, USA) to prove that it is implementable. The results show good results in the estimation of the target vehicle movement behavior. Also, the proposed approach brings some drawbacks that can be addressed in future works. The main disadvantage consists of the neglection of the FV vehicle from the new joined traffic lane of the FV from the current lane. This situation, recognized as "leader change", allows the FV from a lane i to become LV for the vehicle moving behind on the lane j.

The last section of this chapter highlights the contributions made by the employed approach in the refinement process of the car-following model. This part also provides an overview of the benefits and drawbacks of the proposed multiple-lane car-following model and defines possible future directions of improvements. In addition, a subchapter contains the conclusions of this work.

4.2. Driver Behavior Modeling

"*DBM has high complexity due to many parameters of influence such as planned destination, level of overload of the road network, changes in the initial driver decision, the influence of the other participants in traffic, etc.* Table 4.1 *shows the specific DBM for each driver's decision level. Each DBM has specific decisions and time horizons* [Ham12]" [**Pop20_4**].

Table 4.1. "*DBM classification based on time horizons* [Ham12]" [**Pop20_4**].

DBM	Decision	Time horizon
Pre-trip	departure time, destination	> 1 h
Strategic en-route	route choice and switching	30/60 s – 1 h
Tactical route execution	lane change, overtaking	5s – 30/60 s
Operational driving	acceleration, gap acceptance	instantaneous – 5 s
Vehicle control	human-machine interaction needs	mechanical/electric specifications related

"*Probably the most known model in DBM is the hierarchical control model. Proposed by Michon, this model illustrated in* Figure 4.1 *consists of three levels of modeling with specific internal and external outputs* [Mic85]*. The control level is the lowest level of this model and is responsible for sudden braking and turning decisions to ensure traffic safety or comply with traffic regulations. The next level, named maneuvering or tactical level, consists of decisions to achieve short-term goals, such as lane changes, turns, and stops, also considering the criteria derived from the strategical level* [Abu16]*. This level enables us to address the necessity of early prediction of the driver intention before the execution of a tactical maneuver. The strategical level, the highest level in this model, contains the long-term driver goals from travel planning, route, and modal choice to cost and risk assessment* [Abu16], [Mic85]" [**Pop20_4**].
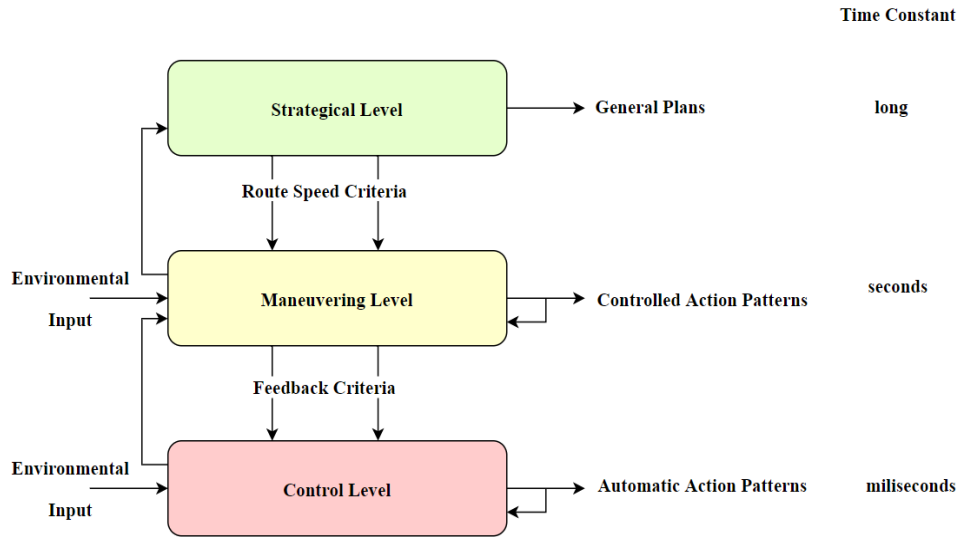
Figure 4.1. Hierarchical driver model [Bek03], [Mic85], [**Pop20_4**].

According to Figure 4.2, DBM is part of the car-following modeling process. The output of the driver model represents the decision control of the intensity that the driver applies to the acceleration or brake pedals [Ang11]. The main decisions taken in this case are at the maneuvering level and are the result of direct dependency on the LV behavior. Considering the maintenance of the safety distance, the FV decides the intensity of pressing the acceleration or brake pedal to adapt for short-term the running distance to the car in front. The pressing of the chosen pedal further influences the acceleration/deceleration rate of the FV, and the driver of the FV will check again the movement status of the LV. Based on this new evaluation, the driver model will forward a new decision, in terms of a chosen pedal and the intensity applied on that pedal, to the vehicle dynamics system. These steps apply cyclically during the movement process, and they are replicated for each FV in the case of several cars moving in a chain.
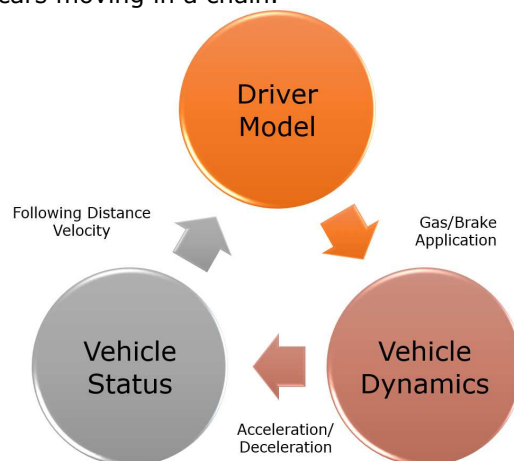
Figure 4.2. DBM as part of the car-following modeling process [Ang11].

Boer et al. improved Michon's hierarchical driver model by including in the modeling process also the dynamic aspects previously described [Boe98], [Kug00]. As shown in Figure 4.3, this model focuses on the attention management concept and covers the switches between intra- or interprocess levels, providing a detailed overview of the selected maneuvers in the case of manual driving, and the transitions between the operating modes in the case of driver-assisted systems [Kug00]. The attention manager is responsible for the process of understanding the driver's intentions related to lane change actions and acceleration/deceleration behavior.
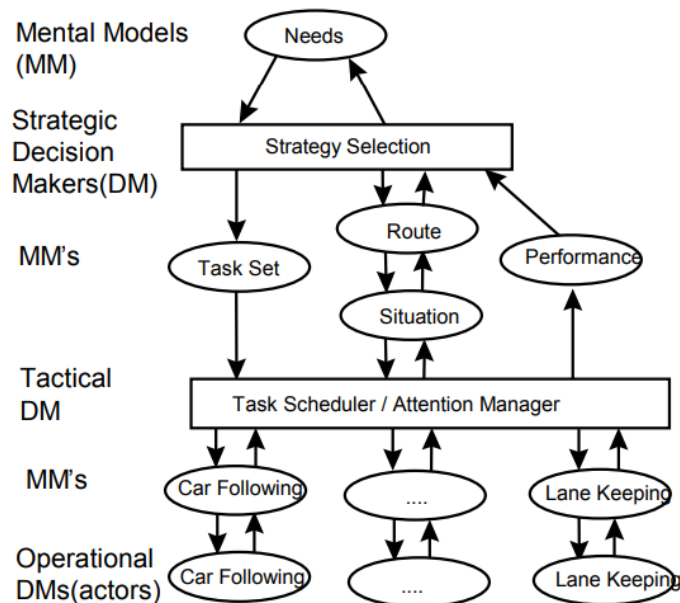
Figure 4.3. Integrated driver model [Boe98], [Kug00].

The application of the integrated driver behavior model facilitates the process of extracting road traffic data and evaluating driver actions (Figure 4.4). Traffic data extraction during a lane change action is carried out in the period between command presentation and the first peak of the steering wheel angle, and for lane keeping, data should be extracted during a five-second interval from the original data measured with the driving simulator [Kug00].
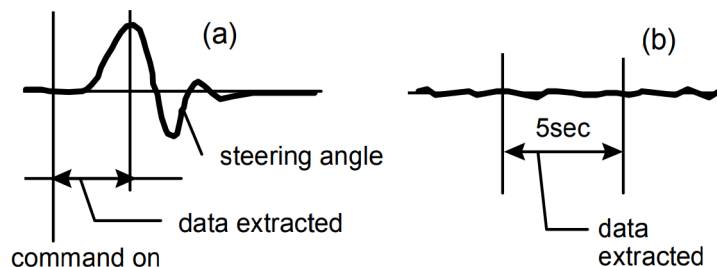
Figure 4.4. Data extraction method: a) lane change; b) lane keeping [Kug00].

Stochastic processes are usually applied in the DBM. Further, a short overview of two DBM techniques that analyses the relationship between the observed and predicted parameters is presented. These modeling techniques are the GMM [Nis07] and the PWARX model [Ang11]. According to the research results of Angkititrakul et al., the GMM-based technique shows good performance in short-term predictions, while the PWARX model is more appropriate for long-term predictions due to its characteristic of capturing a more generalized overview of the driver behavior [Ang11]. The capture process of dynamical characteristics is performed differently by these techniques. The GMM-based approach incorporates "*dynamical characteristics in terms of Δ and Δ^2 components of the feature vector and the PWARX-based model transforms the neighboring information around the data point of interest into a suitable feature space*" [Ang11]. In both cases, an unsupervised clustering applies to address the uncertainty of parameter relationship within each state. The PWARX model uses a discrete switch "*among the driving modes to identify an appropriate formulation (i.e., linear prediction) at each time instant with mode classification to describe the relationship between the input and output parameters*" [Ang11]. On the other hand, "*GMM employs soft prediction made by all mixture components with higher weights applied to the more likely mixture components and then expresses the input-output parameter relationship by non-linear maximum a posteriori prediction of the joint distribution among parameters*" [Ang11].

4.2.1. GMM-based Model

The scope of this model is the generation of driver behavior patterns for individual drivers involved in a modeled movement process based on the concept of car-following. In strong relation to Figure 4.2, the patterns that bring interest relate to the application of the gas/brake pedal that influences the observed velocity and running distance of the LV.

Angkititrakul et al. [Ang11] started from the Nishiwaki et al. [Nis07] approach and adapted the model by including a Bayesian-based mechanism to estimate the FV driver behavior in terms of pedal control actions in response to the observed LV behavior. This modeling proposal follows the following three steps:

- feature extraction and model representation;
- pedal pattern prediction;
- Bayes adaptation.

Feature Extraction and Model Representation

The process of modeling the gas pedal pattern needs "*an observed feature vector at time t, x_t. This vector contains vehicle velocity, following distance, and gas pedal pattern (G_t) with their first- (Δ) and second-order (Δ^2) derivatives as described by the following equation*" [Ang11]:

$$x_t = \left[v_t^f, \Delta v_t^f, \Delta^2 v_t^f, F_t, \Delta F_t, \Delta^2 F_t, G_t, \Delta G_t, \Delta^2 G_t \right]^T \tag{4.1}$$

having the $\Delta(\cdot)$ operator computed as:

$$\Delta x_t = x_t - \frac{\sum_{t=1}^{Q} \tau \cdot x_{t-\tau}}{\sum_{t=1}^{Q} \tau} \tag{4.2}$$

where Q is a window length (e.g., $0.8\,s$). Equation (4.3) defines a set of augmented feature vectors y_t as follows:

$$y_t = \begin{bmatrix} x_t^T & G_{t+1} \end{bmatrix}^T \tag{4.3}$$

Consequently, the joint density between the "*values of the observed feature vector x_t and the next pedal operation G_{t+1} can be modeled by a GMM Φ as:*"

$$p(y \mid \Phi) = \sum_{k=1}^{K} a_k \cdot \varphi(y) = \sum_{k=1}^{K} a_k \cdot N\left(y, u_k^y, \Sigma_k^{yy}\right) \tag{4.4}$$

where a_k represents the prior probability of the k-th mixture component which reflects the significance of such localized joint density, K is the total number of Gaussian components, and $\varphi(\cdot)$ is the unimodal Gaussian distribution with a mean vector $u_k^y = \begin{bmatrix} u_k^x \\ u_k^G \end{bmatrix}$ *and a covariance matrix* $\Sigma_k^{yy} = \begin{bmatrix} \Sigma_k^{xx} & \Sigma_k^{xG} \\ \Sigma_k^{Gx} & \Sigma_k^{GG} \end{bmatrix}$ *"* [Ang11].

"*That is, the mean vector u_k^y is a concatenation of a mean vector of the present observed driving signals u_k^x and a mean of the subsequent pedal pressure u_k^G (the subscripts t and $t+1$ were omitted for the notation simplicity. Similarly, the covariance matrix Σ_k^{yy} contains the auto-covariance (Σ_k^{xx} and Σ_k^{GG}) and cross-covariance (Σ_k^{xG} and Σ_k^{Gx}) matrixes of these two parameter sets*" [Ang11].

Pedal Prediction

The calculation algorithm for the predicted gas pedal pattern $\hat{G}_{t+1}$ uses weighted predictions resulting from all mixture components of the GMM [Dar06], according to Relation (4.5):

$$\hat{G}_{t+1} = \sum_{k=1}^{K} h_k(x_t) \cdot \hat{G}_{t+1}^{(k)}(x_t) \tag{4.5}$$

where $\hat{G}_{t+1}^{(k)}(x_t)$ represents the Maximum-A-Posteriori (MAP) prediction of the observed parameters x_t given the k-th mixture component [Raj04] as shown below:

$$\hat{G}_{t+1}^{(k)}(x_t) = arg \ \ max\left\{p\left(G_{t+1} \mid x_t, \varphi_k\right)\right\} = u_k^G + \Sigma_k^{Gx}\left(\Sigma_k^{xx}\right)^{-1}\left(x_t - u_k^x\right) \tag{4.6}$$

"*The posterior probability of the observed parameter x_t belonging to the k-th mixture component uses as notation $h_k(x_t)$ and its computation is done as defined by* Equation (4.7)*:*

$$h_k(x_t) = \frac{a_k p\left(x_t \mid \varphi_k^x\right)}{\sum_{i=1}^{K} a_i p\left(x_t \mid \varphi_i^x\right)}, k \in \left[1; K\right] \tag{4.7}$$

where $p\left(x_t \mid \varphi_i^x\right)$ *represents the marginal probability of the observed parameter x_t generated by the i-th Gaussian component*" [Ang11].

The same approach applies in the brake pedal prediction process. In this case, the formulas adaptation consists of replacing the gas pedal signal (G_t) with the brake pedal signal (B_t).

Bayesian Adaptation

Used in the literature also as MAP adaptation, Bayesian adaptation performs a re-estimation of "*the model parameters individually by shifting the original statistic towards the new adaptation data*" [Ang11]. The obtainment of an adapted GMM starting from a data set $\left\{y_n\right\}, n = 1, ..., N$, and an initialized GMM (i.e., driver model), the computation of the mean vector is done as in Equation (4.8)

$$\hat{u}_k^y = \frac{\eta_k}{\eta_k + r}E_k + \frac{r}{\eta_k + r}u_k^y \tag{4.8}$$

where, r is a constant relevant factor (e.g., 16), η_k can be computed according to (4.9), and E_k calculation is done as in (4.10).

$$\eta_k = \sum_{n=1}^{N} h_k(y_n) \tag{4.9}$$

$$E_k = \frac{1}{\eta_k}\sum_{n=1}^{N} h_k(y_n) \cdot y_n \tag{4.10}$$

The adapted GMM-based model allows the mixture components with high data counts from a specific characteristic/correlation to rely more on the statistic estimation of the final parameters.

4.2.2. PWARX-based Model

This modeling approach is used as a mathematical model for identifying hybrid systems, in the current situation concentrating on the relationship between observed sensory information and driver. The "*driver behavior is appropriately switched between the simple control laws*" [Ang11]; therefore, it can be modeled as a hybrid dynamical system (HDS).

Implementations of piecewise linear models describe several modes of driver behavior in car-following [Aki07], [Oku10]. The approaching index (*KdB*) represents the observed input feature of the driver behavior model. It is a "*time derivative of rearward area of LV* [Wat07]*, following distance and its first derivative, and vehicle velocity. The output driver behavior consists of a combined pedal operation signal (i.e., gas pressure subtracted by brake pressure)*" [Ang11].

In the parameter identification process of the PWARX model, the clustering and categorization of input and output parameters into different driving modes is applied. "*These distinct driving modes are defined by a clustering procedure in a transformed feature space, where several seconds of driving data around the feature of interest are considered during transformation. Subsequently, back to the original feature space, the PWARX parameters (i.e., ARX coefficients) can be obtained by applying the least square estimation within each defined cluster or driving mode. The classifiers, obtained by using the defined mode class and feature vectors, identify the switching between driving modes*" [Ang11].

For computation efficiency reasons, Angkititrakul et al. [Ang11] chose the tree-based classifier [Bre84] and defined the prediction equation as follows:

$$\begin{aligned}
\hat{G}_{t+1} &= a_1 x_{t,1} + b_1 x_{t,2} + c_1 x_{t,3} + d_1 x_{t,4} + e_1 x_{t,5}, \quad \text{if } x_t \in A \\
&= a_2 x_{t,1} + b_2 x_{t,2} + c_2 x_{t,3} + d_2 x_{t,4} + e_2 x_{t,5}, \quad \text{if } x_t \in B \\
&= a_3 x_{t,1} + b_3 x_{t,2} + c_3 x_{t,3} + d_3 x_{t,4} + e_3 x_{t,5}, \quad \text{if } x_t \in C \\
&= a_4 x_{t,1} + b_4 x_{t,2} + c_4 x_{t,3} + d_4 x_{t,4} + e_4 x_{t,5}, \quad \text{if } x_t \in D
\end{aligned} \tag{4.11}$$

where $x_{t,i}$ represents the "*input observed driving signals described above; G_t is the observed pedal operation; a_i, b_i, c_i, d_i and e_i, $i = \{1,\dots,N\}$ are the ARX coefficients of each subspace (i.e., driving modes A, B, C, and D)*" [Ang11].

A better schematic overview of the PWARX modeling approach has been provided by [Nwa21]. Figure 4.5 shows a DBM where "*the mode segmentation is carried out automatically and the optimal number of modes is decided based on consistent variable selection. This car-following oriented model captures both the decision-making and motion-control facets of the driving behavior. The authors validated their proposed PWARX model through a comparison with ROS-CARLA-based car-following simulation and Gipp's driver model*" [Nwa21].
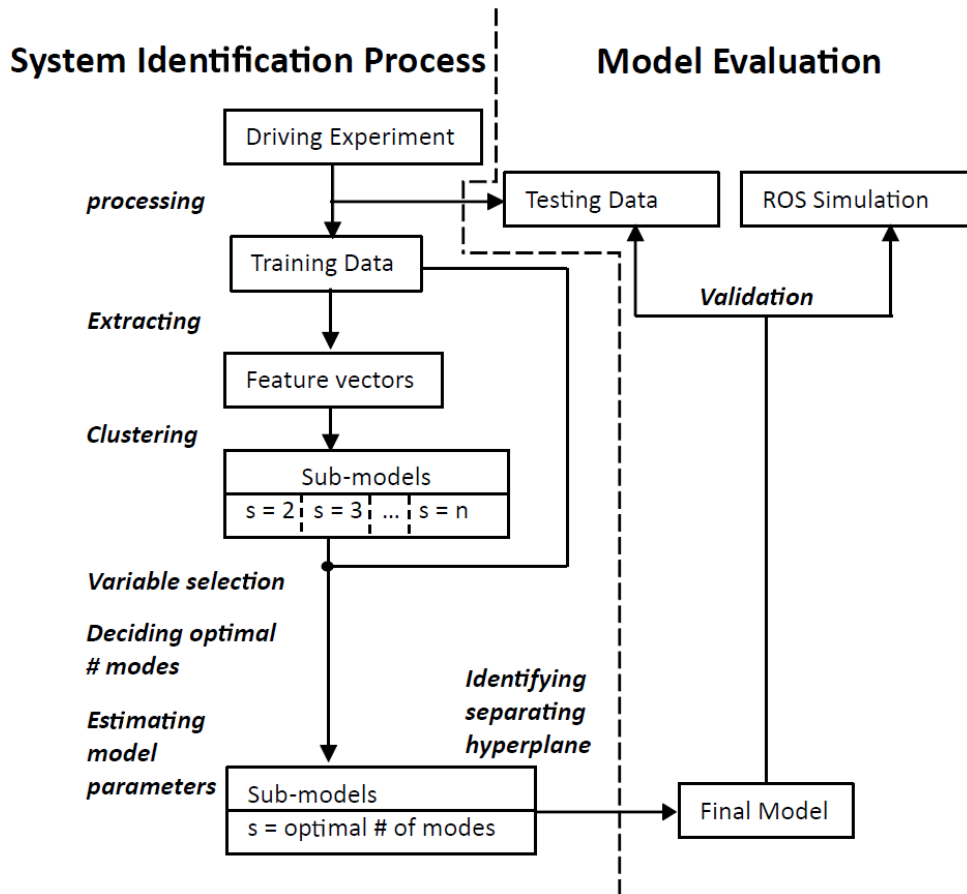
Figure 4.5. DBM framework based on the PWARX modeling technique [Nwa21].

4.3. Markovian Modeling of Road Traffic Lanes

"*Markov stochastic processes are used to describe the transition between several states of a system. These types of processes are frequently used for systems with random temporal development* [Bun14_2]" [**Pop19_2**].

4.3.1. Absorbing   Markov   Process   for   Traffic Modeling

"*For traffic modeling, we assume that network nodes are defined as states, according to the theory of MPA (absorbing Markov process). The transitions between two nodes from the studied road network have as a correspondent the event concept described by MPA. Further, the MPA representation for a road network with n nodes will be presented, using the following notations: g - generation, or origin, nodes and d - destination nodes, considering the approaches from* [Aka96] *and* [Tak05]*. Using (4.1) we calculate the remaining t nodes, which define the nodes used for the transitions, named traversal nodes*" [**Pop19_2**].

$$t = n - g - d \qquad (4.1)$$

"*The transition probability matrix that allows us to get an overview of vehicle movement in the road network is defined in (4.2)*" [**Pop19_2**].

$$P = \begin{bmatrix} I & O \\ R & Q \end{bmatrix} \qquad (4.2)$$

"*The significance of the components of the probability matrix will be further explained:*

- *I is a $(d \times d)$ unit matrix;*

- *O is a $((n-d) \times d)$ null matrix;*

- *R represents a $((g+t) \times g)$ matrix that contains the probability of attraction to a traversal node from a generation node or another traversal node;*

- *Q is a $((g+t) \times (g+t))$ matrix defining the transition probability between two nodes, excluding destination nodes*" [**Pop19_2**].

"*Assuming that there are no direct transitions between the generation and the destination nodes, the assignment of the R matrix can be done by defining a R_2 matrix with dimension $(g+t)$, as in (4.3)*" [**Pop19_2**].

$$R = \begin{bmatrix} 0 \\ R_2 \end{bmatrix} \qquad (4.3)$$

"*Equation (4.4) shows that the difference between the generation nodes and the traversal nodes, the Q matrix will be rewritten using a Q_1 matrix of dimension $(t \times g)$ and Q_2 matrix of dimension $(t \times t)$*" [**Pop19_2**].

$$Q = \begin{bmatrix} 0 & Q_1 \\ 0 & Q_2 \end{bmatrix} \qquad (4.4)$$

"*The probability that after n transitions a vehicle that started to move from the initial i-th node will stay at node j is given by the (i,j) element of matrix Q^n. The probabilities that a vehicle starting from the generation node passes through the other nodes are given by (4.5)*" [**Pop19_2**].

$$I + Q^1 + Q^2 + \ldots = \left[I - Q\right]^{-1} = \begin{bmatrix} I & Q_1 \cdot \left[I - Q_2\right]^{-1} \\ 0 & \left[I - Q_2\right]^{-1} \end{bmatrix} \qquad (4.5)$$

"*Using the above equations, the destination volumes u and traffic volumes on the road x can be calculated using the following relations:*

$$u = v \cdot \left[I - Q \right]^{-1} \cdot R \tag{4.6}$$

$$x = v \cdot Q_1 \cdot \left[I - Q_2 \right]^{-1} \tag{4.7}$$

where:

- $v = \left(v_1, v_2, \ldots, v_g, 0, \ldots, 0 \right)$ *is a* $(g + t)$ *vector containing the generation nodes;*

- $\left[I - Q \right]^{-1} \cdot R$ *defines the probability that a vehicle departing from each of* $(g + t)$ *nodes, attracts to* g *attraction nodes;*

- $Q_1 \cdot \left[I - Q_2 \right]^{-1}$ *contains the node-choice probabilities for each generation node"* [**Pop19_2**].

4.3.2. Bayesian Inference

"*Route choice can be considered a process in which probabilities provide a level of uncertainty. The main reason for this uncertainty comes from the driver decisions regarding his personal reasons, the lengths of the queues on different lanes, traffic injuries, etc. The necessity of knowing the probability that a route will be chosen conditioned by the last destination chosen node makes this a Bayesian specific problem. The current decision will be influenced by prior behavior in route choosing but will have the scope to find the optimal OD matrix that provides a cost and travel time reducing method"* [**Pop19_2**].

"*The classical approach from the theory of probabilities delivers the probability that an event is taking place, established at the confidence level achieved after running the experiment several times. Therefore, the probabilities associated with various events are based on previous knowledge"* [**Pop19_2**].

"*The Bayesian approach brings as a novelty the re-computation of probabilities obtained from previous knowledge taking into account the newest information. In this way, the probability of an event occurring can be estimated using the probabilities of some prior events that can influence the behavior of current event"* [**Pop19_2**].

"*A Bayesian inference-based system can be considered specific to artificial intelligence. The starting point of this procedure is the knowledge base, which contains the probabilities obtained by previous repetitions of the experiment. The system will be aware of all changes that occur during the experiment and will try to estimate its next own state"* [**Pop19_2**].

"*In Bayesian theory, the probabilities associated with the next state achieved on the prior available information are named posterior probabilities"* [**Pop19_2**].

"*Equation* (4.8) *is the representation of the Bayes rule. The probability of an event* x *is computed conditioned on the observed event* y. *Using data from previous experiments, a prior probability distribution is obtained for* $p(x)$. *The influence of the observed event or state* y *is represented through the conditional probability* $p(y \mid x)$, *also known as the likelihood function. The form* $p(x \mid y)$ *is*

called the posterior probability and allows us to evaluate the level of uncertainty in
x after the event y was observed [Bar12], [Bis06]" [**Pop19_2**].

$$p(x \mid y) = \frac{p(y \mid x) \cdot p(x)}{p(y)} \qquad (4.8)$$

The probability of the event y conditioned on the knowing event x can be
expressed using (4.9) [Bar12].

$$p(y \mid x) = \frac{p(y,x)}{p(x)} \qquad (4.9)$$

"*Assuming that x and y are independent events, then $p(y,x)$ can be*
defined as (4.10) [Aka96]" [**Pop19_2**].

$$p(y,x) = p(y) \cdot p(x) \qquad (4.10)$$

The expression in words of the Bayes theorem is defined by (4.11) [Bis06]:

$$posterior \propto likelihood \times prior \qquad (4.11)$$

4.3.3. OD Volumes Estimation Using Bayes Inference

"*In many traffic management systems, it is usually required to have a*
prediction of travel demand. This requirement, together with the need to have a
simulation of traffic flow in a road network, proves the aim of estimating OD
volumes" [**Pop19_2**].
  "*We should note that OD estimation plays an important role in the*
calibration of traffic models. OD volumes are estimated using data from previous
crossings of the network and will be compared with real-traffic data when these are
available from traffic sensors. Finally, these will play an essential role in setting the
timing of traffic signals" [**Pop19_2**].
  "*Given the road network represented by using the Markov chains in* Figure
4.6*, we want to calculate the probability of arriving at a node k, crossing other*
nodes and having i as the starting point node. We can see that it is also
represented a node starting from i that will not influence our route choice between
i to k. The reason why it was added is to ensure that the probabilities of
transitions to j or l will not be equal to 0.50. Considering that the conditional
probability to make a transition between nodes is computed as a forward conditional
probability, our proposal is to take into account also the probability of joining a
traversal node to predict a precise probability of arriving at node k. We assume
that every node corresponds to a lane from the road and the lane change behavior
will be studied" [**Pop19_2**].
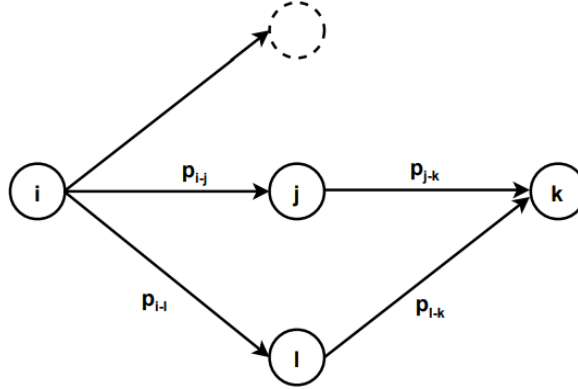
Figure 4.6. "*Forward conditional probability for a Markov traffic road model*" [**Pop19_2**].

    "*The new proposal to calculate the probability of joining the k -th node is to use the Bayes theorem instead of classical Markov specific formulas. In the next step, the probabilities from* (4.2) *will be updated according to the new values obtained*" [**Pop19_2**].

    "*To reach the node k , the vehicle shall pass through one traversal node, j or l . Based on the choice of one of these traversal nodes, we propose to calculate the maximum probability of reaching the node k using* (4.12)" [**Pop19_2**].

$$P(k) = \begin{cases} max\left(p_{j-k}, p_{l-k}\right), p_{i-j} = p_{i-l}; \\ p(k \mid j) = \dfrac{p(j \mid k) \cdot p(k)}{p(j)}, p_{i-j} > p_{i-l}; \\ p(k \mid l) = \dfrac{p(l \mid k) \cdot p(k)}{p(l)}, p_{i-j} < p_{i-l}. \end{cases} \tag{4.12}$$

    "*We can observe that the numerator of each fraction represents the probability of transition between i to j or l . In this case, we will make the notations according to* (4.13), *assuming that we use lowercase in these notations of probabilities because we refer to values from previous crossings of the road network*" [**Pop19_2**].

$$p_{j-k} = p(j \mid k) \cdot p(k)$$
$$p_{l-k} = p(l \mid k) \cdot p(k) \tag{4.13}$$

    "*The probabilities $p(j)$ and $p(l)$ are the same as the probabilities associated with the links that have connection to node j and l , because these values are taken from previous knowledge. In this case, the relations from* (4.14) *will be used*" [**Pop19_2**].

$$p(j) = p_{i-j}$$
$$p(l) = p_{i-l}$$

(4.14)

"Equation (4.15) *is the rewritten form of* (4.12) *using the assumptions of* (4.13) *and* (4.14). *It is important to note that the uppercase notation for link probabilities shows the newest value associated with that link. The value obtained will be used to predict the route choice and will replace the old value in the matrix from* (4.2)" [**Pop19_2**].

$$P(k) = \begin{cases} max\left(p_{j-k}, p_{l-k}\right), p_{i-j} = p_{i-l}; \\ P_{j-k} = \dfrac{p_{j-k}}{p_{i-j}}, p_{i-j} > p_{i-l}; \\ P_{l-k} = \dfrac{p_{l-k}}{p_{i-l}}, p_{i-j} < p_{i-l}. \end{cases}$$

(4.15)

"*An observation is needed for the case where the computation of* $P(k)$ *gives a result greater than 1. In this case, the probability will be changed according to* (4.16)*, where* $\{P(k)\}$ *is the fractional part of* $P(k)$" [**Pop19_2**].

$$P(k) = \left|1 - \{P(k)\}\right|$$

(4.16)

"*As we can observe, this* $P(k)$ *probability is the maximum probability that will be attached to a link entering node* k. *For our case, the probability for the remaining link,* $P_{RL}(k)$, *will be calculated using* (4.17)*, a relation based on probabilities theory*" [**Pop19_2**].

$$P_{RL}(k) = \left|\frac{(1 - P(k)) \cdot p_{RL}(k)}{1 - p(k)}\right|$$

(4.17)

"*A generalized expression of* (4.16)*, for the case of q nodes, with* $q \in \mathbb{N}$*, that are having a connection to node k is defined in* (4.18)" [**Pop19_2**].

$$P_{q-1}^{RL}(k) = \left|\frac{(1 - P(k)) \cdot p_{q-1}^{RL}(k)}{1 - p(k)}\right|$$

(4.18)

The use of genetic algorithms for the prediction of OD volumes has proved its efficiency. Starting from a study of the current situation regarding traffic prediction and a detailed study of generalities related to genetic algorithms, Pop et al. [**Pop18_3**] proposed a new approach of traffic modeling by using a specific chromosome structure for the modeling of OD routes. Each origin node has a chromosome that will be divided into four subchromosomes, corresponding to each

possible destination that can be reached from a four-way crossroad. "*Different routes to the same destination were modeled as parents of the same chromosome*" [**Pop18_3**]. Pop et al. [**Pop18_3**] also proposed a new fitness function used for a further evaluation based on roulette wheel selection. In addition, new algorithms have been proposed for crossover and mutation operators, specific to genetic algorithms.

OD volumes estimation can achieve good results by applying the minimax gaming strategy to model the driver behavior and anticipate his decisions [**Pop20_4**]. All destinations that are reachable from a specific origin node have been represented as a final layer in the minimax game tree. The intermediate layers contain various nodes according to possible lane changes in vehicle movement from the origin node to the destination node [**Pop20_4**].

4.4. Bayesian Reasoning for Lane Change Actions Estimation

"*A lane change action can be considered a process in which estimations can be performed while assuming a high level of uncertainty. This arises because of driver decisions that are difficult to predict or plan. The driver acts based on real-time traffic conditions to maximize his/her chances of obtaining a lower travel cost and reaching a planned destination on time. In addition, the driver lane change action is also influenced by other drivers through the politeness factor, as presented before (*see* Equations (3.3), (3.4), and (3.5) *from* **Section 3.3**)*" [**Pop19_1**], [**Pop20_3**].

"*After admitting the existence of a level of uncertainty, we can say that this lane change action is a Bayesian specific problem. Here, the main conditions for a successful lane change are: having a driver decision to initiate the action and the contribution of neighboring drivers to help this action happen. Other factors that have important roles are the routing alternatives associated with a lane at a vehicle entry point on the road network and the previously established destination*" [**Pop19_1**], [**Pop20_3**].

"*The proposed approach is to calculate the probabilistic estimator of a lane change action as an intersection of five Bayes probabilities, according to (4.19) and Figure 4.7. We can observe that the lane L_1 offers the possibility to go straight or leave the road network using a right exit, while the lane L_n facilitates the driver's decision to leave the road network using a left exit. $P\left(e_{FV_i}\right)$ denotes the probability of the FV which joined the traffic link using the entrance lane e_{L_i}, and $P\left(d_{FV_i}\right)$ the probability that FV will leave the link using the exit (destination) lane d_{L_i}. Probability $P\left(v_{FV_i}\right)$ shows the level of influence of the LV's velocity on the FV's lane change decision from lane L_i. The significance of the other probabilities is related to the target lane probabilities associated with respect to FV and LV*" [**Pop19_1**], [**Pop20_3**].

$$\hat{P}\left(L_j\right) = P\left(e_{FV_i} \mid L_i\right) \cdot P\left(d_{FV_i} \mid L_i\right) \cdot P\left(v_{FV_i} \mid L_i\right) \cdot P\left(d_{FV_j} \mid L_i\right) \cdot P\left(v_{FV_j} \mid L_i\right), j = \{i \pm 1\} \quad (4.19)$$
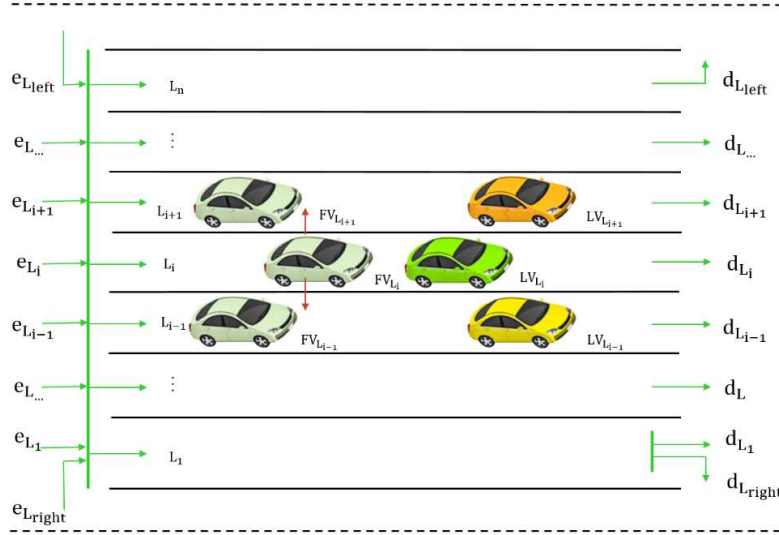
Figure 4.7. "*General traffic link configuration*" [**Pop20_3**].

"*Based on previous assumptions, p was defined as the total advantage of the two immediately affected neighboring vehicles. In this case, the politeness factor $p_{L_{i \to j}}$ can be defined as a product of the last two conditional probabilities from* Equation (4.19)" [**Pop19_1**], [**Pop20_3**]:

$$p_{L_{i \to j}} = P\left(d_{FV_j} \mid L_i\right) \cdot P\left(v_{FV_j} \mid L_i\right), j = \{i \pm 1\} \tag{4.20}$$

In this manner, Equation (4.19) becomes:

$$\hat{P}\left(L_j\right) = P\left(e_{FV_i} \mid L_i\right) \cdot P\left(d_{FV_i} \mid L_i\right) \cdot P\left(v_{FV_i} \mid L_i\right) \cdot p_{L_{i \to j}}, j = \{i \pm 1\} \tag{4.21}$$

"*By expanding* Equation (4.21) *according to the Bayes rule, we obtain*" [**Pop19_1**], [**Pop20_3**]:

$$\hat{P}\left(L_j\right) = \frac{P\left(L_i \mid e_{FV_i}\right) P\left(e_{FV_i}\right)}{P\left(L_i\right)} \cdot \frac{P\left(L_i \mid d_{FV_i}\right) P\left(d_{FV_i}\right)}{P\left(L_i\right)} \cdot \frac{P\left(L_i \mid v_{FV_i}\right) P\left(v_{FV_i}\right)}{P\left(L_i\right)} \cdot p_{L_{i \to j}}, j = \{i \pm 1\} \tag{4.22}$$

"*After estimating the probability of a lane change action based on the probabilities of previous road network crossings, it is necessary to introduce new notations, similar to the approach presented in* [**Pop19_2**]. *Lowercase notation will be used to represent the probabilities computed based on previous traffic data*" [**Pop19_1**], [**Pop20_3**]:

$$\begin{cases} p\left(e_{FV_i}\right) = P\left(L_i \mid e_{FV_i}\right) P\left(e_{FV_i}\right) \\ p\left(d_{FV_i}\right) = P\left(L_i \mid d_{FV_i}\right) P\left(d_{FV_i}\right) \\ p\left(v_{FV_i}\right) = P\left(L_i \mid v_{FV_i}\right) P\left(v_{FV_i}\right) \\ p\left(L_i\right) = P\left(L_i\right) P\left(L_i\right) P\left(L_i\right) \end{cases} \tag{4.23}$$

"*By replacing these notations in* Equation (4.22)*, we can obtain the final form of the estimated probability of a lane change action from lane i to j*" [**Pop19_1**], [**Pop20_3**]:

$$\hat{P}\left(L_j\right) = \frac{p\left(e_{FV_i}\right) \cdot p\left(d_{FV_i}\right) \cdot p\left(v_{FV_i}\right)}{p\left(L_i\right)} \cdot p_{L_{i \to j}}, \, j = \{i \pm 1\} \tag{4.24}$$

"*The proposed approach also consists of modifications to the lane change rules that were previously defined by* (3.3)*,* (3.4)*, and* (3.5) (**Section 3.3**) [Kes07]. *Furthermore, the new relations that define these rules are as follows*" [**Pop19_1**], [**Pop20_3**]:
- "*incentive criterion for symmetric lane change rules*" [**Pop19_1**], [**Pop20_3**]:

$$a_{driver} + \hat{P}\left(L_j\right) \cdot \left(a_{newfollower} + a_{oldfollower}\right) > \Delta a_{th}, \, j = \{i \pm 1\} \tag{4.25}$$

- "*incentive criterion for asymmetric lane change rules - lane change from left to right*" [**Pop19_1**], [**Pop20_3**]:

$$a^{eur}_{FV^*_{L_i}}\left(t + \tau\right) - a_{FV_{L_i}}\left(t\right) + \hat{P}\left(L_j\right) \cdot a_{oldfollower} > \Delta a_{th} - \Delta a_{bias}, \, j = \{i \pm 1\} \tag{4.26}$$

- "*incentive criterion for asymmetric lane change rules - lane change from right to left*" [**Pop19_1**], [**Pop20_3**]:

$$a_{FV^*_{L_i}}\left(t + \tau\right) - a^{eur}_{FV_{L_i}}\left(t\right) + \hat{P}\left(L_j\right) \cdot a_{newfollower} > \Delta a_{th} + \Delta a_{bias}, \, j = \{i \pm 1\} \tag{4.27}$$

4.5. Refinement Process of the Car-Following Model

Figure 4.8 illustrates the steps followed during the refinement process of the single-lane car-following model. This refinement aims to extend the car-following modeling approach to multiple-lane roads. For this reason, this thesis applies the Bayes theorem in the computation of lane choice probabilities. The main sources of influence of driver decision are:
- the entrance lane of the target vehicle (e_{FV});
- the destination lane of the target vehicle (d_{FV});

- the influence of LV behavior on the velocity changes of the FV (v_{FV}), represented as a coefficient in the interval $[0;1]$.
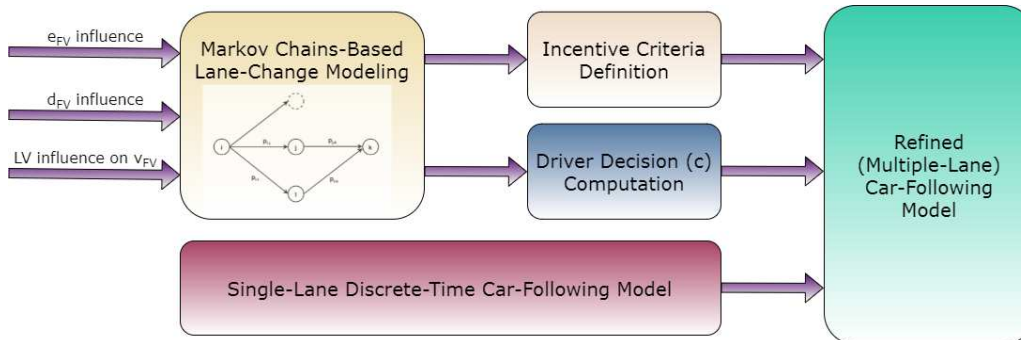
Figure 4.8. Refinement process of the single-lane car-following model.

The modeling of the lane change behavior uses the Markov chains to represent each lane as a node, and the transition between the modeled road network considers the probability calculated according to the previously defined factors of influence. Further, the calculated values for the lane change probabilities facilitate the update of the incentive criteria equations and the driver decision coefficient. The extension of the standard car-following to multiple-lane traffic environments consists of a permanently update of acceleration values considering the incentive criteria and driver decision.

4.5.1. State Space Representation of the Car-Following Concept

Based on previous assumptions in **Section 3.4** and "*on Multiple Input Multiple Output (MIMO) systems theory, a state-space representation of the car-following concept is needed*" [**Pop19_1**], [**Pop20_3**].

"*A good way to expand the research possibilities for car-following models and create a framework for new optimal control approaches for these models is to follow the next three steps:*
- *create a linear continuous system model without time-delay;*
- *add the time-delay factor to the model;*
- *create a discrete model to control the behavior of FV and LV*" [**Pop19_1**], [**Pop20_3**].

"*According to the listed steps, the obtaining of car-following models, as proposed in* [Kho10]*,* [Pan08]*, is further presented. Using* x_1 *and* x_3 *as notations for car velocities,* x_2 *and* x_4 *for running distances of the cars,* u_1 *and* u_2 *for the car accelerations, the linear continuous car-following model can be described by system equations from* Relation (4.28)" [**Pop19_1**], [**Pop20_2**], [**Pop20_3**].

$$\begin{cases} \begin{bmatrix} \dot{x}_1 \\ \dot{x}_2 \\ \dot{x}_3 \\ \dot{x}_4 \end{bmatrix} = \begin{bmatrix} 0 & 0 & 0 & 0 \\ 1 & 0 & 0 & 0 \\ 0 & 0 & 0 & 0 \\ 0 & 0 & 1 & 0 \end{bmatrix} \cdot \begin{bmatrix} x_1 \\ x_2 \\ x_3 \\ x_4 \end{bmatrix} + \begin{bmatrix} 1 & 0 \\ 0 & 0 \\ 0 & 1 \\ 0 & 0 \end{bmatrix} \cdot \begin{bmatrix} u_1 \\ u_2 \end{bmatrix} \\ \\ y = \begin{bmatrix} 0 & -1 & 0 & 1 \end{bmatrix} \cdot \begin{bmatrix} x_1 \\ x_2 \\ x_3 \\ x_4 \end{bmatrix} + S \end{cases} \qquad (4.28)$$

"*The standard safety distance* S *computation is done according to* Relation (4.29) *considering the vehicle average length* L" [**Pop20_2**], [**Pop20_3**]:

$$S = L \cdot \left(1 + \frac{x_3}{16.10} \right) \qquad (4.29)$$

"*To transform the previous equations into the classic form for MIMO state-space representation from* Relation (4.30)*, it is necessary to define* $\bar{x}_1 = x_3 - x_1$, $\bar{x}_2 = x_4 - x_2 = s$ (s *– is the dynamic distance between two cars) and* $\bar{y} = \bar{x}_2$ [Kho10]*,* [Pan08]*:*

$$\begin{cases} \dot{\bar{x}}(t) = A \cdot \bar{x}(t) + B \cdot u(t) \\ \bar{y}(t) = C \cdot \bar{x}(t) + S \end{cases} \qquad (4.30)$$

where the vectors and matrices are: $\bar{x} = \begin{bmatrix} \bar{x}_1 \\ \bar{x}_2 \end{bmatrix}$, $u = \begin{bmatrix} u_1 \\ u_2 \end{bmatrix}$, $A = \begin{bmatrix} 0 & 0 \\ 1 & 0 \end{bmatrix}$, $B = \begin{bmatrix} -1 & 1 \\ 0 & 0 \end{bmatrix}$,

$C = \begin{bmatrix} 0 & 0 \\ 0 & 1 \end{bmatrix}$. *In addition, we have* $\begin{bmatrix} A & B \end{bmatrix}$ *controllable and* $\begin{bmatrix} A & C \end{bmatrix}$ *observable; additionally the system eigenvalues are 0*" [**Pop19_1**], [**Pop20_2**], [**Pop20_3**].

"*To introduce the time-delay* τ, *we assume that* $u_1 = u_1(t)$ *and* $u_2 = u_2(t - \tau)$. *Introducing these notations in* Relation (4.30) *yields the linear continuous time-delay car-following model as follows* [Kho10]*,* [Pan08]" [**Pop19_1**], [**Pop20_3**]:

$$\begin{cases} \dot{\bar{x}}(t) = A \cdot \bar{x}(t) + B \cdot \begin{bmatrix} u_1(t) \\ u_2(t - \tau) \end{bmatrix} \\ \bar{y}(t) = C \cdot \bar{x}(t) + S \end{cases} \qquad (4.31)$$

"*Considering that* $\tau = \lambda \cdot T$, *where* T *is the sampling period,* Relation (4.32) *is defined as* [Kho10]*,* [Pan08]" [**Pop19_1**], [**Pop20_3**]:

$$u(t) = u(k \cdot T) = u(k), \ k \cdot T \le t < (k+1) \cdot T \tag{4.32}$$

"*If we rewrite* Equation (4.31) *according to* Equation (4.32)*, we obtain the following relation* [Kho10]*,* [Pan08]" [**Pop19_1**], [**Pop20_3**]:

$$\begin{cases} \dot{\bar{x}}(t) = e^{A \cdot (t-t_0)} \cdot \bar{x}(t_0) + \int_0^t e^{A \cdot (t-\eta)} \cdot B \cdot \begin{bmatrix} u_1(\eta) \\ u_2(\eta - \tau) \end{bmatrix} d\eta \\ \bar{y}(t) = C \cdot \bar{x}(t) + S \end{cases} \tag{4.33}$$

"*If we consider* $t_0 = k \cdot T$ *,* $t = (k+1) \cdot T$ *in the state equation and* $t = k \cdot T$ *in the output equation, we obtain the discrete car-following model, as in* Relation (4.34) [Kho10]*,* [Pan08]" [**Pop19_1**], [**Pop20_3**].

$$\begin{cases} \bar{x}[k+1] = e^{A \cdot T} \cdot \bar{x}[k] + \int_0^T e^{A \cdot \eta} \cdot B \cdot \begin{bmatrix} u_1[k] \\ u_2[k-\lambda] \end{bmatrix} d\eta \\ \bar{y}[k] = C \cdot \bar{x}[k] + S \end{cases} \tag{4.34}$$

4.5.2. Proposed Car-Following Model

Figure 4.9 shows the refined car-following model that includes the extension of the single-lane oriented "*car-following model to multiple lane roads. This model built based on the modeling theory presented in* **Section 4.5.1** *implements the proposal to estimate the probability of a lane change*" [**Pop19_1**], [**Pop20_3**] from **Section 4.4**.

"*Considering the likelihood of initiating a lane change maneuver by driver* c *to initiate a lane change maneuver, the probabilities computed based on previous data, using* (4.24)*, will offer the lane with the highest probability to be chosen by the driver from lane* L_i *. The driver decision* c *to perform a lane change maneuver is computed according to* (4.35) *and its meaning can be summarized as the probability of not choosing the lane* L_i *"* [**Pop19_1**], [**Pop20_3**]:

$$c = 1 - P(L_i) \tag{4.35}$$

"*A*cceleration and other parameters, such as velocity and running distance for the target vehicle, are updated according to the specific rules of lane change actions. If there is no driver decision for a lane change maneuver, the model behaves as a standard car-following model without incorporating the lane change rules into the vehicle behavior description*" [**Pop19_1**], [**Pop20_3**].
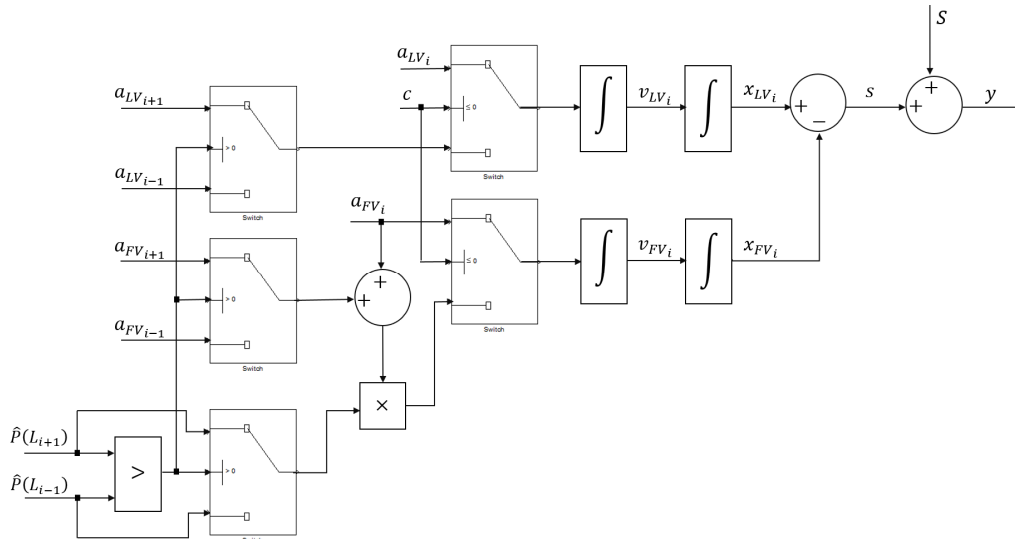
Figure 4.9. Refined car-following model [**Pop19_1**], [**Pop20_3**].

"*For simplicity, a procedure for lane change behavior estimations has been built considering incentive criteria for the symmetric lane change rule. The simulation results are available in* **Section 4.5.4**" [**Pop20_3**].

4.5.3. Experimental Setup

This section aims to describe the experimental setup used to analyse the behavior of the proposed refined car-following model. This section contains a description of the real traffic data and details of the simulation process.

Road Traffic Data

"*To show the practical application of the refined car-following model, this thesis presents a case study for a three-lane road from Timisoara, Romania.* Figure 4.10 *illustrates a real map of the studied section of road and its lane configuration*" [**Pop20_3**]. The data used for experimental analysis have been collected using inductive loop sensors and have been received based on a written request of Politehnica University of Timișoara in the name of the author of this thesis (Mădălin-Dorin Pop), from "*Timișoara City Hall - General Directorate of Roads, Bridges, Parking and Utility Networks - Traffic Monitoring Office, Timișoara, Romania*" [**Pop20_3**].

Figure 4.10. "*Case study – three lanes piece of road from Calea Sagului, Timisoara, Romania (Source of the map: OpenStreet Maps)*" [**Pop20_3**].

"*The simulation used the data from* Table 4.2 *as inputs. The table defines the velocities for the studied lanes and the probabilities of lane choice behavior. The number of vehicles considered in the probability and velocity computation consisted of raw data retrieved from inductive loops placed on the road network. The simulation applied a derivative for the velocities to obtain the acceleration values as a first step, and further application led to the implementation of the proposal described in this thesis based on the approach from* [**Pop19_1**]" [**Pop20_3**].

Table 4.2. "*Road traffic data[1]*" [**Pop20_3**].

Velocities (m/s)						Lane choice probabilities		
$LV_{L_{i-1}}$	$FV_{L_{i-1}}$	LV_{L_i}	FV_{L_i}	$LV_{L_{i+1}}$	$FV_{L_{i+1}}$	$\hat{P}(L_{i-1})$	$\hat{P}(L_i)$	$\hat{P}(L_{i+1})$
6.90	2.14	14.28	12.69	10.94	10.29	0.04	0.48	0.48
4.66	2.05	16.78	13.44	10.51	11.80	0.06	0.56	0.38
3.83	1.64	16.30	13.49	10.58	10.83	0.04	0.49	0.47
1.04	1.06	15.43	9.24	11.17	7.74	0.07	0.30	0.63
1.81	1.74	12.85	14.54	5.89	9.29	0.05	0.44	0.51
2.78	3.50	11.00	9.49	8.39	6.91	0.12	0.41	0.46
4.94	3.97	11.14	11.05	8.66	9.01	0.10	0.47	0.43
2.45	3.43	11.97	12.04	9.57	9.43	0.08	0.54	0.38
3.99	2.91	12.43	11.07	8.72	9.47	0.06	0.57	0.37
4.89	5.83	10.99	11.92	9.38	8.04	0.05	0.58	0.37

"[1]*Data source: Timişoara City Hall - General Directorate of Roads, Bridges, Parking and Utility Networks - Traffic Monitoring Office, Timişoara, Romania*" [**Pop20_3**].

Simulation Model

"*To perform the experiments for the multiple-lane car-following model, a simulation was done in Simulink, part of MATLAB R2020a (MathWorks, Natick, MA, USA)*" [**Pop20_3**]. For a better overview of the contributions brought by the refined car-following model, this thesis presents the case of a three-lane road where the implementation of the refined car-following subsystem has the inputs and outputs represented as in Figure 4.11. A detailed description of all variables used in this simulation is available in Table A1 from **Appendix A** of this thesis.
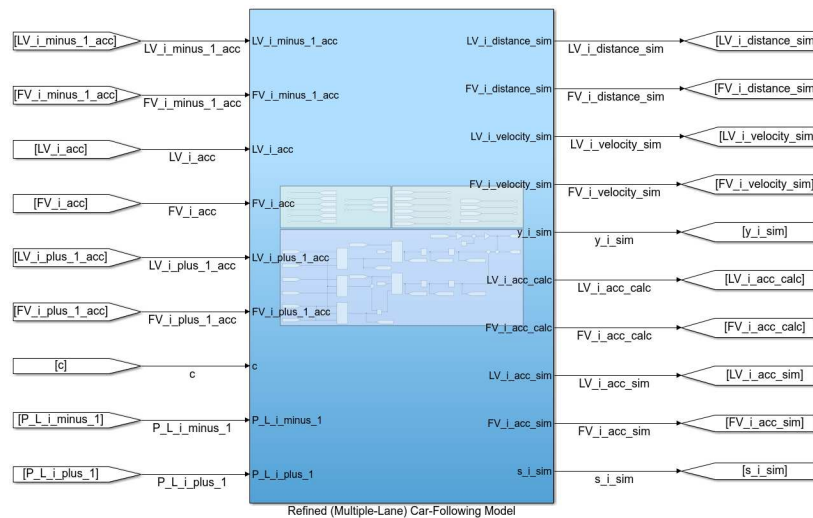
Figure 4.11. "*Refined car-following subsystem overview - implementation using Simulink (MATLAB R2020a)*" [**Pop20_3**].

"*The transformation of velocity into acceleration is covered by the input handler subsystem, shown in* Figure 4.12. *Here, a discrete-time derivative block was applied to the raw velocity data to transform them into acceleration data, ensuring the functionality of the blocks presented previously*" [**Pop20_3**].
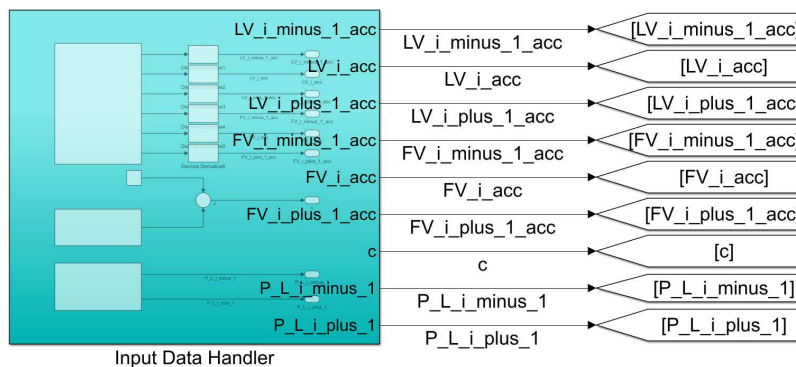
Figure 4.12. "*Input handler subsystem overview - implementation using Simulink (MATLAB R2020a)*" [**Pop20_3**].

"Figure 4.13 *depicts the implementation of the model for monitoring possible lane change maneuvers from lane* L_i *to* L_{i-1} *or* L_{i+1}. *The main outputs of this block are the LV and FV velocities and running distances. It is necessary to mention again that the standard safety distance* S *calculation was done according to* Equation (4.29) [Kho10] *and assuming that the vehicle average length* L *for passenger vehicles was* $L = 4.50\ m$" [**Pop20_3**].
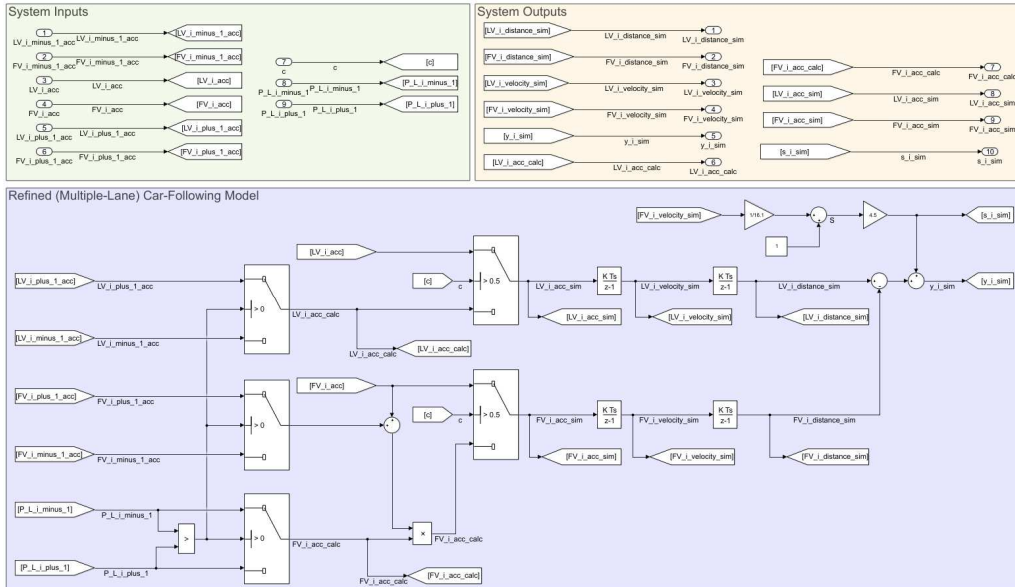
Figure 4.13. "*Refined car-following model - implementation using Simulink (MATLAB R2020a)*" [**Pop20_3**].

4.5.4. Results

"Figure 4.14 *shows the acceleration profiles and the internal update of the acceleration values for LV and FV after c is greater or lower than the threshold. The threshold value was set at 0.50 and showed a greater than 50% chance of changing lanes. In this case, the simulated values for LV and FV were set to the calculated values, taking* Equation (4.26) *into account. For a better understanding of these switches of simulated acceleration values incorporating lane change actions, the case of a lane change action from* L_i *to* L_{i-1} *at time 0.2 s can be considered. The LV from the lane* L_i *performs this action and starts to follow the movement behavior described by vehicles moving into the lane* L_{i-1}. *The FV from the lane* L_i *will also change its movement behavior due to the new LV after the initial LV changes lane. Another similar case, but with a lane change from* L_i *to* L_{i+1}, *is observable at time 6.3 s*" [**Pop20_3**].
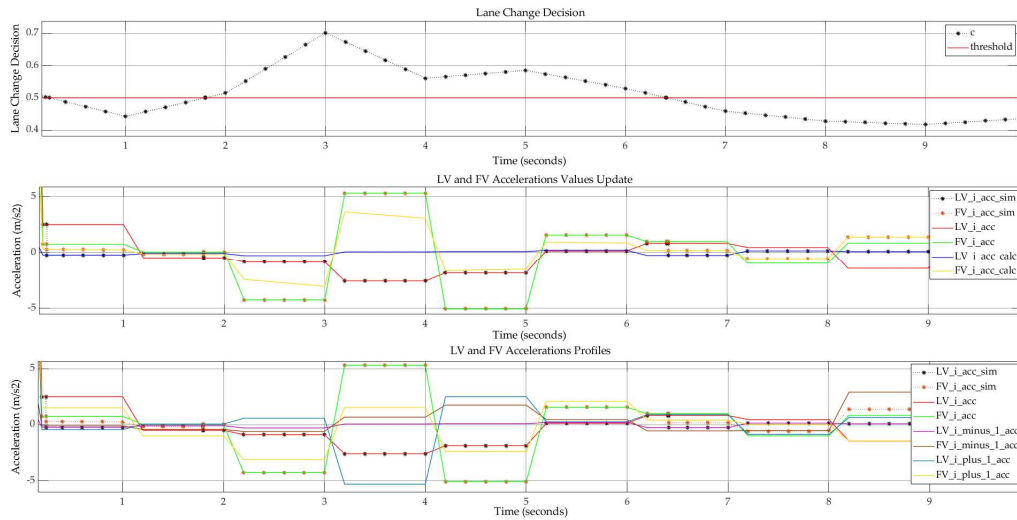
Figure 4.14. "*LV and FV from lane L_i –accelerations values update*" [**Pop20_3**].

"*Changing acceleration values also implies a change of velocity.* Figure 4.15 *shows an overview of the velocity values for all lanes, and incorporates a velocity change after a lane change maneuver. Here, the outputs of both the standard car-following model and the proposed approach can be seen*" [**Pop20_3**].
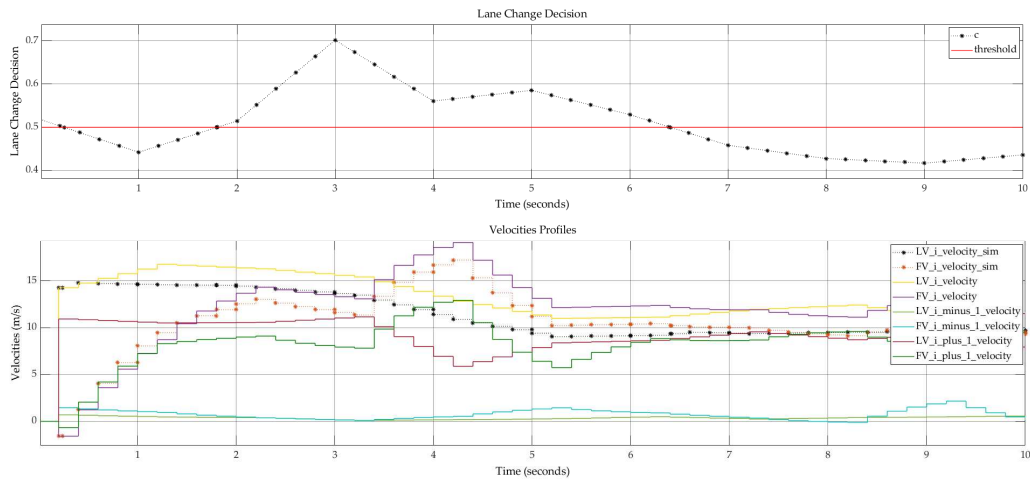
Figure 4.15. "*LV and FV–velocities profiles*" [**Pop20_3**].

"*The running distances profiles shown in* Figure 4.16 *create an overview of the simulated distances by covering the lane change action and offering the evolution of the values after the action has taken place. The vehicles continue their movement based on different trajectories after a lane change action. Here, the disadvantage of the proposed approach can be seen, i.e., the incorporation of lane change behavior in the current lane does not highlight the impact on adjacent traffic lanes*" [**Pop20_3**].
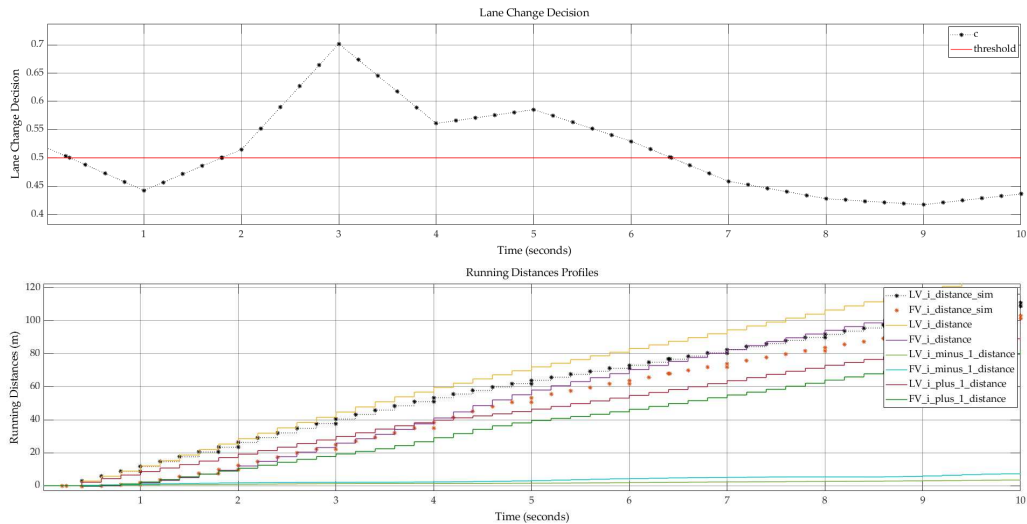
Figure 4.16. "*LV and FV–running distances profiles*" [**Pop20_3**].

4.6. Conclusions

This chapter presented a new approach to car-following modeling adapted to multiple-lane roads. The modeling process considered the modeling of traffic lanes as nodes of a Markov chain and the lane choice probabilities computation applies the Bayesian inference concept. The probabilities calculation considered the following factors of influence: the entrance lane of the target, the destination lane of the target vehicle, and the influence of the LV behavior on the velocity changes of the FV.

A simulation has been conducted for a three-lane road to analyse the results of the proposed method in comparison with the separate application of the standard car-following model for each of these traffic lanes. The results have shown good performance of the proposed approach but highlighted as a disadvantage the fact "*that the current model cannot provide a view of the initial lane road traffic evolution in parallel*" [**Pop20_3**].

The next chapters have to provide a fault analysis of the proposed refined car-following model and a new approach for the microscopic traffic model calibration that can also be adapted for the refined proposal.

5. FAULT DETECTION OF DISCRETE-TIME MICROSCOPIC TRAFFIC MODELS

5.1. Introduction

This chapter performs fault detection for the refined car-following model. The method chosen for fault detection consists of applying the method of parity equations. The purpose of this analysis is to identify the faults introduced by the computational approach. Therefore, the analysis starts from the assumption that the observed model already contains faults resulting from the extension of the standard car-following model by considering the influence introduced by vehicles moving on adjacent traffic lanes on the target vehicle from the current lane.

Before applying fault detection based on parity equations, this chapter presents the theoretical background of the fault detection process. After describing the models involved in this process, this thesis discusses step by step the methodological aspects of the computation of the residuals corresponding to the parity equations approach.

The next section adapts the presented methodology to the fault detection of refined car-following needs. Following this methodology, the identified residuals "*are the relative velocity residual and the dynamic running distance residual*" [**Pop20_3**]. The residuals calculation uses the discrete-time traffic model and considers the permanently updated acceleration values with respect to the incentive criteria defined in **Section 4.4**.

This chapter continues with the implementation of the fault detection process in Simulink (MATLAB R2020a). The corresponding subchapter provides a description of the models involved and the experimental results of the fault analysis consisting of the evolution of the residuals concerning the driver decision.

The last subchapter highlights the conclusions of this fault detection of the refined car-following model by mentioning both advantages and disadvantages of the proposed model.

5.2. Fault Detection using Parity Equations

A fault that occurs in a system describes an unacceptable deviation from the standard behavior of at least one characteristic and consists of a state within the system that leads to an abnormal behavior of that system [Ise11]. "*A system reaches the fault state after exceeding the threshold of the tolerance zone established for a fault value*" [**Pop20_3**].

"*To identify a fault in a monitored system, many fault detection methods can be used*" [**Pop20_3**]. When we refer to systems where fault detection implies multiple signals, a good method is the application of the process-model-based parity equations method [Ise11]. Figure 5.1 illustrates "*a general scheme for process-model-based fault detection*" [Ise11], customized for the car-following model. The output of the main interest consists of residuals. Their analysis leads to the identification of the fault source, time, location, etc. "*The generation of residuals*

requires three models: nominal, current (observed), and the faulty system [Pou94]. *The observed model is continuously compared with the nominal model and a faulty model. This faulty model is the result of a fault analysis of the implementation of the nominal model*" [**Pop20_3**].
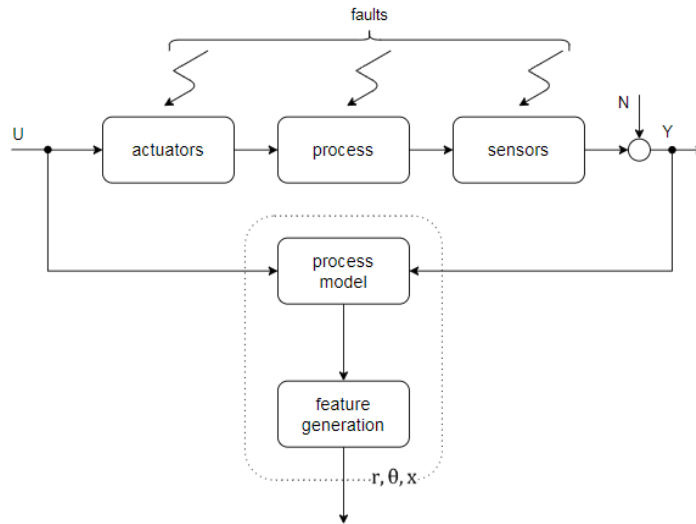
Figure 5.1. "*General scheme for process-model-based fault detection*" [Ise11] (fig.2.15).

The state-space model, considered without noise and additional faults, that will be used for residuals generation with parity equations in discrete-time is shown in Figure 5.2.
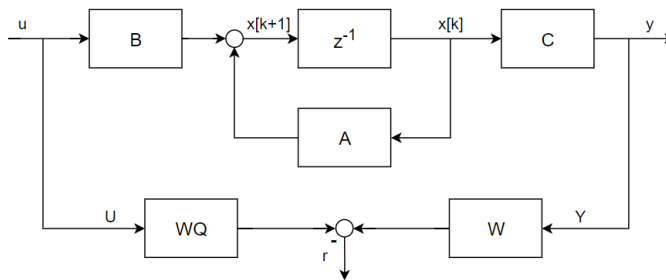
Figure 5.2. State-space model for the residual generation with parity equations in discrete-time [Ise06] (fig.10.5).

Translating in the equation the previous block diagram, the state-space model used to compute the residuals is defined as [Ise06], [Kra98]:

$$\begin{cases} x[k+1] = A \cdot x[k] + B \cdot u[k] \\ y[k] = C \cdot x[k] \end{cases}$$

(5.1)

The output at the next $k+1$ sampled time can be expressed as [Ise06]:

$$y\big[k+1\big] = C \cdot x\big[k+1\big] = C \cdot A \cdot x\big[k\big] + C \cdot B \cdot u\big[k\big] \tag{5.2}$$

The output will also be calculated for the sampled time $k+2$ [Ise06]:

$$\begin{aligned} y\big[k+2\big] &= C \cdot x\big[k+2\big] = C \cdot A \cdot x\big[k+1\big] + C \cdot B \cdot u\big[k+1\big] \\ &= C \cdot A^2 \cdot x\big[k\big] + C \cdot A \cdot B \cdot u\big[k\big] + C \cdot B \cdot u\big[k+1\big] \end{aligned} \tag{5.3}$$

in order to lead to a general relation that can define the computation for a q-th $(q \le m)$ sampled output [Ise06]:

$$y\big[k+q\big] = C \cdot x\big[k+2\big] = C \cdot A^q \cdot x\big[k\big] + C \cdot A^{q-1} \cdot B \cdot u\big[k\big] + \ldots + C \cdot B \cdot u\big[k+q-1\big] \tag{5.4}$$

Considering a time window of length $q+1$, the relation can be rewritten as [Ise06]:

$$Y\big[k+q\big] = M \cdot x\big[k\big] + Q \cdot U\big[k+q\big] \tag{5.5}$$

By shifting the previous equation by q backwards, we obtain [Ise06], [Kra98]:

$$Y\big[k\big] = M \cdot x\big[k-q\big] + Q \cdot U\big[k\big] \tag{5.6}$$

where the vectors $Y\big[k\big]$ and $U\big[k\big]$ have the following significance [Ise06], [Kra98]:

$$Y\big[k\big] = \begin{bmatrix} y\big[k-q\big] \\ y\big[k-q+1\big] \\ \vdots \\ y\big[k\big] \end{bmatrix}, \ U\big[k\big] = \begin{bmatrix} u\big[k-q\big] \\ u\big[k-q+1\big] \\ \vdots \\ u\big[k\big] \end{bmatrix} \tag{5.7}$$

and the matrices M and Q are calculated as [Ise06], [Kra98]:

$$M = \begin{bmatrix} C \\ C \cdot A \\ C \cdot A^2 \\ \vdots \\ C \cdot A^q \end{bmatrix}, \ Q = \begin{bmatrix} 0 & 0 & \cdots & 0 & 0 \\ C \cdot B & 0 & \cdots & 0 & 0 \\ C \cdot A \cdot B & C \cdot B & \cdots & 0 & 0 \\ \vdots & \vdots & \ddots & \vdots & \vdots \\ C \cdot A^{q-1} \cdot B & C \cdot A^{q-2} \cdot B & \cdots & C \cdot B & 0 \end{bmatrix} \tag{5.8}$$

"*As the state vector* $x\big[k-q\big]$ *is unknown, the* Relation (5.6) *is multiplied by a vector* w^T [Ise06]" [**Pop20_3**]:

$$w^T \cdot Y[k] = w^T \cdot M \cdot x[k-q] + w^T \cdot Q \cdot U[k] \tag{5.9}$$

By selecting the vector w^T of dimension $(1 \times (q+1) \cdot r)$, where r represents the number of outputs, such that

$$w^T \cdot M = 0 \tag{5.10}$$

the computational form for a residual vector is obtained [Ise06]:

$$r[k] = w^T \cdot Y[k] - w^T \cdot Q \cdot U[k] \tag{5.11}$$

The residual that represents the parity signal is the following described as [Ise06], [Kra98]:

$$r[k] = W \cdot \left[Y[k] - Q \cdot U[k] \right] \tag{5.12}$$

where the matrix W is chosen considering that the residual $r[k]$ is independent of the state of the system $x[k-q]$, thus [Ise06], [Kra98]:

$$W \cdot M = 0 \tag{5.13}$$

"*The system works correctly only if the residual is equal to zero, a non-zero residual may demonstrate a functional fault in the studied system* [Ise06], [Kra98]" [**Pop20_3**].

5.3. Fault Detection of the Refined Car-Following Model

The residual calculation uses the discrete car-following model described by Equation (4.34) from **Section 4.5.1**. Considering (5.4), the q-th $(q \le m)$ sampled output of the car-following model is [**Pop20_3**]:

$$y[k+q] = C \cdot e^{q \cdot A \cdot T} \cdot \begin{bmatrix} \bar{x}_1[k] \\ \bar{x}_2[k] \end{bmatrix} + C \cdot e^{(q-1) \cdot A \cdot T} \cdot \int_0^T e^{A \cdot \eta} \cdot B \cdot \begin{bmatrix} u_1[k] \\ u_2[k-\lambda] \end{bmatrix} d\eta + \ldots +$$
$$+ C \cdot \int_0^T e^{A \cdot \eta} \cdot B \cdot \begin{bmatrix} u_1[k+q-1] \\ u_2[k+q-1-\lambda] \end{bmatrix} d\eta \tag{5.14}$$

After applying a q backward shifting starting from the assumption of an existing time window of length $q+1$, the relation can be rewritten as [**Pop20_3**]:

$$Y[k] = M \cdot \begin{bmatrix} \bar{x}_1[k-q] \\ \bar{x}_2[k-q] \end{bmatrix} + Q \cdot U[k] \tag{5.15}$$

where the definition of the vectors from Equation (5.7) is adapted as follows [**Pop20_3**]:

$$Y[k] = \begin{bmatrix} \bar{x}_1[k-q] \\ \bar{x}_2[k-q] \\ \bar{x}_1[k-q+1] \\ \bar{x}_2[k-q+1] \\ \vdots \\ \bar{x}_1[k] \\ \bar{x}_2[k] \end{bmatrix}, \; U[k] = \begin{bmatrix} u_1[k-q] \\ u_2[k-q-\lambda] \\ u_1[k-q+1] \\ u_2[k-q-\lambda+1] \\ \vdots \\ u_1[k] \\ u_2[k-\lambda] \end{bmatrix} \tag{5.16}$$

and the redefinition of M and Q is described by Equations (5.17) and (5.18) [**Pop20_3**]:

$$M = \begin{bmatrix} C \\ C \cdot e^{A \cdot T} \\ C \cdot e^{2 \cdot A \cdot T} \\ \vdots \\ C \cdot e^{q \cdot A \cdot T} \end{bmatrix} \tag{5.17}$$

$$Q = \begin{bmatrix} 0 & 0 & \cdots & 0 & 0 \\ C \cdot \int_0^T e^{A \cdot \eta} \cdot B \, d\eta & 0 & \cdots & 0 & 0 \\ C \cdot e^{A \cdot T} \cdot \int_0^T e^{A \cdot \eta} \cdot B \, d\eta & C \cdot \int_0^T e^{A \cdot \eta} \cdot B \, d\eta & \cdots & 0 & 0 \\ \vdots & \vdots & \ddots & \vdots & \vdots \\ C \cdot e^{(q-1) \cdot A \cdot T} \cdot \int_0^T e^{A \cdot \eta} \cdot B \, d\eta & C \cdot e^{(q-2) \cdot A \cdot T} \cdot \int_0^T e^{A \cdot \eta} \cdot B \, d\eta & \cdots & C \cdot \int_0^T e^{A \cdot \eta} \cdot B \, d\eta & 0 \end{bmatrix} \tag{5.18}$$

"As the state vector $\begin{bmatrix} \bar{x}_1[k-q] \\ \bar{x}_2[k-q] \end{bmatrix}$ is unknown, the Equation (5.15) is multiplied by a vector w^T [Ise06]" [**Pop20_3**]:

$$w^T \cdot Y[k] = w^T \cdot M \cdot \begin{bmatrix} \bar{x}_1[k-q] \\ \bar{x}_2[k-q] \end{bmatrix} + w^T \cdot Q \cdot U[k] \tag{5.19}$$

The calculation of the residual $r[k]$ results from the replacement in Equation (5.12) of the new matrices defined by Relations (5.16) and (5.17), and (5.18) and taking into account that "*u_1 and u_2 are permanently updated considering the incentive criteria defined by* Equations (4.25)–(4.27) – **Section 4.4** *as the consequences of a possible lane change action according to* Equation (4.35) – **Section 4.5.2**" [**Pop20_3**].

5.4. Experimental Setup and Results Analysis

"*This section presents the results of the proposed multiple-lane car-following model in comparison with a separate, standard car-following model for each lane, as well as the fault detection results. Additionally, this section provides the implementation details and the input data used for the experiment. The purpose is to show that the proposed multiple-lane model is able to detect a lane change maneuver and can change the model parameters accordingly. For this reason, each figure also shows the driver's decision regarding a possible lane. The second part of this section presents the evolution of the residual values, which was based on an analysis of the impact of possible faults on the system inputs*" [**Pop20_3**].

5.4.1. Simulation Model

"*To perform fault detection based on parity equations for the multiple-lane car-following model, a simulation was done in Simulink, part of MATLAB R2020a (MathWorks, Natick, MA, USA). Usually, the fault detection considers three types of models: nominal, observed, and the model with a defect. This thesis assumed that the observed model had already incorporated faults as a result of the proposed computational approach. In this case, the implementation consisted of two main types of subsystems, as shown in* Figure 5.3*: three separate blocks for the standard implementation of a car-following model, consisting of the nominal model (orange); and the proposed model for multiple-lane car-following, consisting of the observed model (blue)*" [**Pop20_3**]. The inputs of these blocks are the acceleration values obtained as outputs of the input handler subsystem described in **Section 4.5.3**.
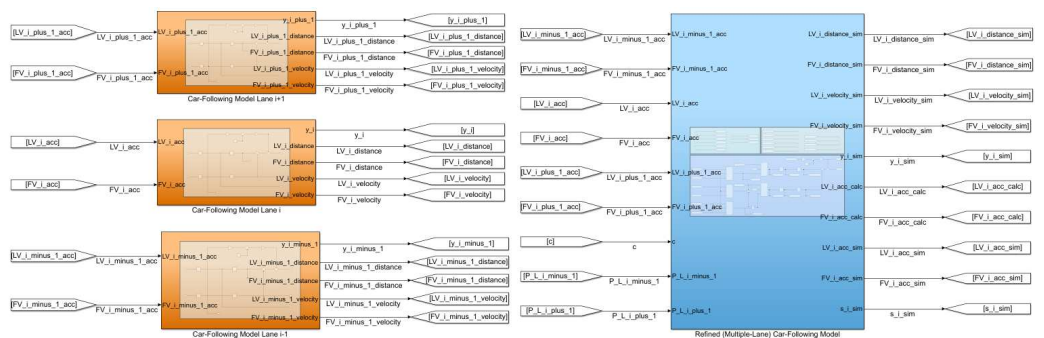

Figure 5.3. "*Main subsystems overview—implementation using Simulink (MATLAB R2020a)*" [**Pop20_3**].

"*The subsystem shown in* Figure 5.4 *covers the residual computation. The outputs are the relative_velocity_residual and dynamic_distance_residual, and consist of the differences between the values of* $\bar{x}_1$ *and* $\bar{x}_2$ *obtained from the adaptation of* Equation (5.12) *by using the nominal model and the observed model with faults introduced by the computation approach"* [**Pop20_3**].
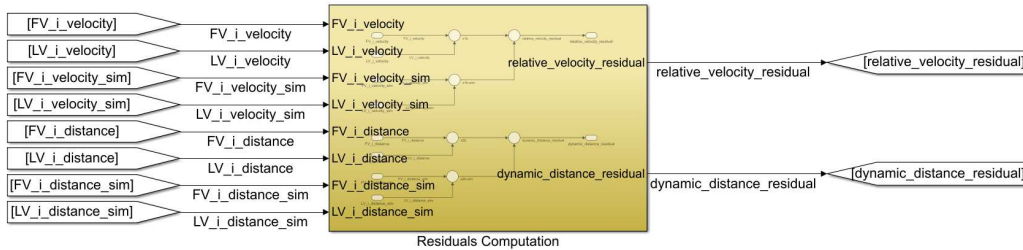
Figure 5.4. "*Residuals computation subsystem overview—implementation using Simulink (MATLAB R2020a)"* [**Pop20_3**].

"*To simplify the obtained results,* Table A1 *(from* **Appendix A***) describes the mapping between the models defined in this thesis and the signals used as simulations. Some of the internal states were passed as outputs from the subsystems for the creation of graphics. The table sets the parameter type based on the state-space representation concept"* [**Pop20_3**].

5.4.2. Experimental Results – Fault Analysis

"*The fault analysis created an overview of the evolution of two residuals, i.e., relative velocity and dynamic distance, based on the movement in lane* L_j . Figure 5.5 *shows the influence of the lane change actions on the velocity and distance computation using the multiple-lane car-following model. The proposed model introduces faults when the driver decision* c *has a low degree of uncertainty (i.e.,* c *is near the* 0.50 *threshold with* ± 0.10 *). In other cases, when the driver decision is not affected by this low level of uncertainty, the relative velocity residual tends to zero. The dynamic distance residual has a continuously increasing trend based on the same pattern, and its value remains relatively constant in the absence of a low level of uncertainty"* [**Pop20_3**].
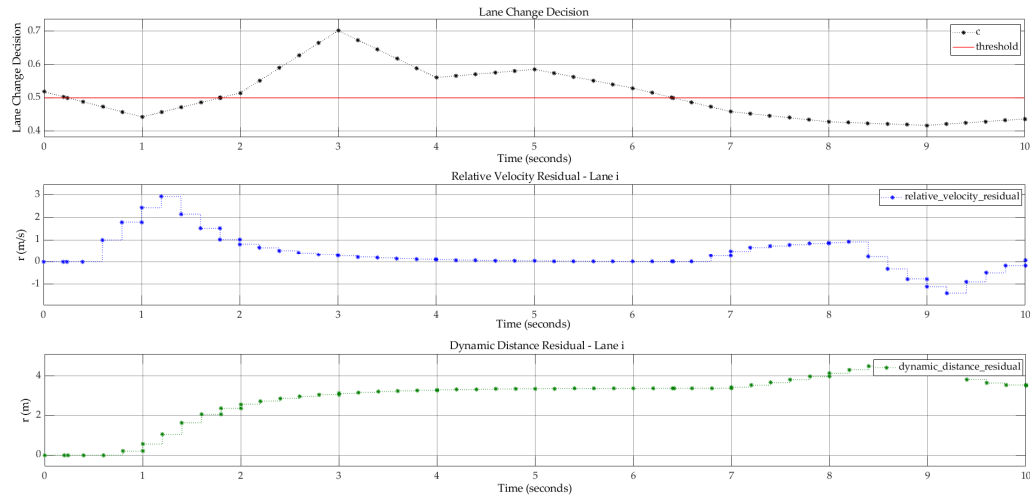
Figure 5.5. "*Fault detection – residuals overview*" [**Pop20_3**].

5.5. Conclusions

This chapter provided fault detection for the refined car-following model. The fault detection process considered the refined car-following model both as the observed model and as the model with defect to better highlight the possible defects introduced by the calculations that consider the influence of vehicles from adjacent traffic lanes. According to the chosen method represented by the parity equations, two residuals have been identified: the relative velocity residual and the dynamic running distance residual.

The fault detection process based on parity equations has been fully described and implemented in Simulink. The experimental results used real traffic data from the TMC responsible for Timişoara City. Analysis of the results of the evolution of the residuals showed that the uncertainty of the driver decision is the main source of fault in the refined car-following model.

The fault analysis showed that "*the main drawback of the proposed approach is that it currently only shows the behavior of the LV and FV from a specific lane in relation with other lanes after the insertion of a new vehicle into the current lane. For this reason, the model is not suitable for a real-time switch from one lane to another to ensure lane change behavior monitoring for each lane. Future work will focus on introducing an adaptive switch between road lanes to show the real-time updated traffic conditions for all lanes in parallel*" [**Pop20_3**].

6. CALIBRATION OF MICROSCOPIC TRAFFIC MODELS

6.1. Preliminaries

This chapter aims to bring improvements to the microscopic traffic modeling process through a new approach to online calibration of traffic parameters. It starts with a theoretical overview of the calibration concept that applies to microscopic traffic models.

Further, this chapter will describe the concepts of Kalman filtering and Takagi-Sugeno FIS. The proposed hybrid approach for online calibration of car-following models consists of a combination of these two concepts. The proposed calibration method proves its efficiency through a faster identification of the correct offsets to be applied to the model parameters compared to a simple Kalman filtering.

In addition to the outcome of the research of Pop et al. [**Pop20_2**], this chapter adapts this calibration method and applies it to the refined car-following model. The most challenging aspect is the adaptation of the initially proposed version for the continuous-time system to a discrete-time environment. This need arises from the discrete-time version proposed for the refined car-following model.

6.1.1. Calibration of Traffic Models – Theoretical Background

"Figure 6.1 *illustrates a description of road traffic systems at the microscopic level. The following three main components ensure the existence of a model closer to reality: microscopic traffic data, modeled microscopic traffic system, and model validation. The first component is responsible for collecting traffic data from the real world. The second component simulates the real system behavior and uses the estimated values for road traffic parameters as inputs to calculate the simulation output data. A comparison between the simulated data and the real microscopic traffic data consists of a validation step. The output of this component is a decision based on the similarity between the real and simulated model and consists of the calibration component input. The calibration step shall establish the offset values to be applied to the model inputs to reduce the difference compared to the real data. Calibration is performed until these offset values become equal to zero*" [**Pop20_2**].

"*The calibration process finds many issues in the case of microscopic traffic modeling. One of the common problems is the measurement of traffic characteristics like velocity, travel times, and the distance between vehicles because of the influence introduced by each vehicle behavior or travel conditions* [Bar10]*. The calibration data shall consider this uncertainty in driver decisions and need to adapt to it*" [**Pop20_2**].
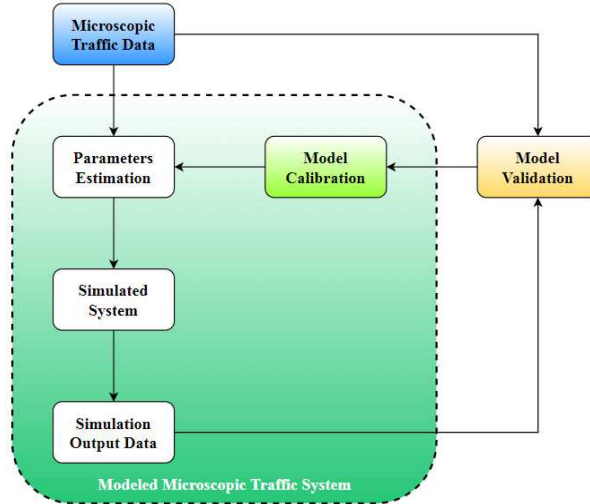
Figure 6.1. "*Microscopic traffic system*" [**Pop20_2**].

6.2. Hybrid Approach for Car-Following Models Calibration

6.2.1. Kalman Filter for Online Calibration

"*Online calibration is specific for systems that are using real-time data in order to adapt the model, by changing the system parameters to be close to the real system. This category of calibration includes the Kalman filter method* [Ema19], [Kal61], [Pun05_2]" [**Pop20_2**].

"*Kalman filters are popular in the calibration of state-space models characterizing a system in discrete-time, but also applies to continuous-time systems* [Pen99], *as in the current case. For microscopic road traffic, this method proved its efficiency even if the traffic conditions are nonstationary or stationary. This approach permits a real-time continuous update of studied parameters by updating them through the specific offsets. Further, the application of this method will be presented for car-following model calibration as stated by* [Pun05_2]" [**Pop20_2**].

"*The state equations for the calibration system of the car-following model according to Kalman filtering concept are shown in* (6.1), *where* $\gamma_i(t)$, $i = \{1,3,s\}$ *are the parameters that need calibration*" [**Pop20_2**].

$$\begin{cases} \dot{x}_1(t) = x_1(t) + \gamma_1(t) \\ \dot{x}_3(t) = x_3(t) + \gamma_3(t) \\ \dot{s}(t) = s(t) + \left[x_1(t) - x_3(t) \right] \cdot T + \gamma_s(t) \end{cases} \tag{6.1}$$

"*Considering that* $\zeta_i(t)$, $i = \{1,3,s\}$ *are the measurement errors for the real traffic parameters, the output equations of the calibration system are computed by using the* Relation (6.2)" [**Pop20_2**].

$$\begin{cases} \dot{x}_1^{obs}(t) = x_1(t) + \zeta_1(t) \\ \dot{x}_3^{obs}(t) = x_3(t) + \zeta_3(t) \\ \dot{s}^{obs}(t) = s(t) + \zeta_s(t) \end{cases} \tag{6.2}$$

"*Based on previous assumptions, the Kalman filter state-space representation can be obtained as follows:*"

$$\begin{cases} \dot{x}(t) = A_k \cdot x(t) + B_k \cdot u(t) + D_k \cdot \gamma(t) \\ y(t) = C_k \cdot x(t) + \zeta(t) \end{cases} \tag{6.3}$$

where the matrices specific for the continuous-time Kalman filter have the following values: $A_k = \begin{bmatrix} 1 & 0 & 0 \\ 0 & 1 & 0 \\ T & -T & 1 \end{bmatrix}$, $B_k = \begin{bmatrix} 0 \end{bmatrix}$, $C_k = \begin{bmatrix} 1 & 0 & 0 \\ 0 & 1 & 0 \\ 0 & 0 & 1 \end{bmatrix}$, *and* $D_k = \begin{bmatrix} 1 & 0 & 0 \\ 0 & 1 & 0 \\ 0 & 0 & 1 \end{bmatrix}$"

[**Pop20_2**].

"*The continuous-time Kalman filter estimates the values according to* (6.4)*:*"

$$\hat{x}(t) = \hat{x}_{pr}(t) + K_k \cdot \left[y(t) - C_k \cdot \hat{x}_{pr}(t) \right] \tag{6.4}$$

where $\hat{x}_{pr}(t)$ *is a prediction obtained based on the previous knowledge using the following relation:*

$$\dot{\hat{x}}_{pr}(t) = A_{k_{t-1}} \cdot \hat{x}_{pr}(t) + B_{k_{t-1}} \cdot \hat{x}_{pr}(t) \tag{6.5}$$

where $A_{k_{t-1}}$ *and* $B_{k_{t-1}}$ *represent the values of* A_k *and* B_k *at time* $t-1$" [**Pop20_2**].

"*The gain matrix* K_k *incorporates the compromise to adjust the estimated parameters by using real measured data but, at the same time, to avoid the propagation of measurement errors*" [**Pop20_2**]:

$$K_k = P_{pr_k} \cdot C_k^T \cdot \left[C_k \cdot P_{pr_k} \cdot C_k^T + R_k \right]^{-1} \tag{6.6}$$

"*The matrix* P_{pr_k} *is the covariance matrix that contains the estimation error and will be updated at each step by applying the following relation*:

$$P_{pr_{k+1}} = A_k \cdot P_{F_k} \cdot A_k^T + D_k \cdot Q_k \cdot D_k^T \tag{6.7}$$

where $P_{pr_{k+1}}$ *represents the value of* P_{pr_k} *at time* $t+1$ *and* P_{F_k} *is defined as*" [**Pop20_2**]:

$$P_{F_k} = \left[I - K_k \cdot C_k \right] \cdot P_{pr_k} \tag{6.8}$$

"*The Kalman filter covariance matrix of errors* R_k *is:*

$$R_k = \begin{bmatrix} \sigma_{x_1(t),x_1(t)} & 0 & \sigma_{x_1(t),s(t)} \\ 0 & \sigma_{x_3(t),x_3(t)} & \sigma_{x_3(t),s(t)} \\ \sigma_{s(t),x_1(t)} & \sigma_{s(t),x_3(t)} & \sigma_{s(t),s(t)} \end{bmatrix} \tag{6.9}$$

with the propagation of variances and covariances expressed as:

$$\sigma_{x_n s} = \sum_{i,j} \frac{\partial x_n}{\partial x_i} \cdot \frac{\partial s}{\partial x_j} \cdot \sigma_{x_{ij}} \tag{6.10}$$

for the functions of interests defined as: $x_n = (x_1, x_2, \cdots, x_i, \cdots)$ *and* $s = (x_1, x_2, \cdots, x_j, \cdots)$ *with the explanation that* $\sigma_{x_n s}$ *is the covariance of* x_n *and* s, *and the term* $\sigma_{x_{ij}}$ *represents the covariance of* x_i *and* x_j" [**Pop20_2**].

6.2.2. Fuzzy-Based Calibration

"*FIS usually solves problems related to the nonlinearity of systems or in the cases of systems that have time delays, but is also suitable to continuous-time systems* [Lam18]" [**Pop20_2**].

"*Microscopic traffic modeling is a complex problem because of the uncertainty in drivers' decisions for lane changes or for the acceleration/deceleration behavior. The driver behavior influences all corresponding dynamic traffic parameters, introducing, in some cases, a swap in role between LV and FV. These reasons make the microscopic traffic modeling problem suitable for implementation with FIS, especially for the calibration process where all mentioned uncertainties need filtering in order to establish the best offset values. The application of these values ensures the dynamical adaptation of the modeled system to the received real traffic conditions*" [**Pop20_2**].

"*In the following, the particularities of the FIS are shown, especially on the use of Takagi–Sugeno. A new calibration method will be issued based on this theoretical background in combination with the Kalman filtering concept previously presented. Compared to the simple use of Kalman filters, this hybrid approach tries to cover the learning of patterns in an offset setting*" [**Pop20_2**].

Takagi-Sugeno FIS

"*Probably the most known model to implement a FIS is to use the Takagi-Sugeno approach* [Bou15]*,* [Had11]*,* [Pet19]*,* [Tak85]*. Similar to other fuzzy methods, this model description uses the fuzzy specific IF-THEN rules. These input-output associations of the nonlinear modeled system characterize the dynamics of each fuzzy rule by creating a linear system model*" [**Pop20_2**].

"*A general Takagi-Sugeno FIS for continuous-time models can be described by the following fuzzy rules* [Abd15], [Bou15]*:*

$$IF \ z_1(t) \ is \ F_{i1} \ AND \ ... \ IF \ z_p(t) \ is \ F_{ip}$$

$$THEN \ \begin{cases} \dot{x}(t) = (A_i + \Delta A_i) \cdot x(t) + (B_i + \Delta B_i) \cdot u(t) \\ y(t) = (C_i + \Delta C_i) \cdot x(t) \end{cases} \quad (6.11)$$

where the notations have the following meaning:

- $z_j(t)$, $j = \{1, 2, \cdots, p\}$ *are the premise variables;*

- $F_{ij}(t)$, $i = \{1, 2, \cdots, r\}$, *and* $j = \{1, 2, \cdots, p\}$ *represent the fuzzy sets;*

- r *is the number of defined fuzzy rules;*

- $x(t) \in \mathbb{R}^n$ *is the state vector;*

- $u(t) \in \mathbb{R}^m$ *is the input vector;*

- $A_i \in \mathbb{R}^{n \times n}$ *is the state matrix;*

- $B_i \in \mathbb{R}^{n \times m}$ *is the input matrix;*

- $C_i \in \mathbb{R}^{q \times n}$ *is the output matrix where* q *is the number of outputs parameters;*

- ΔA_i, ΔB_i, *and* ΔC_i *are the matrices that incorporate the uncertainties*" [**Pop20_2**].
  "*The previous assumptions lead to the inferred model expression:*

$$\begin{cases} \dot{x}(t) = \sum_{i=1}^{r} h_i(z(t)) \cdot \left[(A_i + \Delta A_i) \cdot x(t) + (B_i + \Delta B_i) \cdot u(t) \right] \\ y(t) = \sum_{i=1}^{r} h_i(z(t)) \cdot (C_i + \Delta C_i) \cdot x(t) \end{cases} \quad (6.12)$$

where $h_i(z(t))$ *is the normalized grade of membership for each rule and is compliant with* (6.13)" [**Pop20_2**].

$$\begin{cases} \sum_{i=1}^{r} h_i(z(t)) = 1 \\ 0 < h_i(z(t)) < 1 \end{cases} \quad (6.13)$$

"*These equations represent the fundamentals for the implementation of an optimized calibration method for the special case of car-following models*" [**Pop20_2**].

6.2.3. Proposed Online Hybrid Calibration Method

"Figure 6.2 *shows the proposal for the calibration system internal structure. Moreover, its relations with the other external subsystems are also represented. As part of the modeled microscopic traffic system, the calibration model has the feature of providing the necessary data to adapt the internal model parameters based on the evaluation received as input from the system responsible for the model validation. Together with the validation result, two sets of parameters consisting of simulation values and microscopic traffic real data will be sent to the calibration subsystem*" [**Pop20_2**].
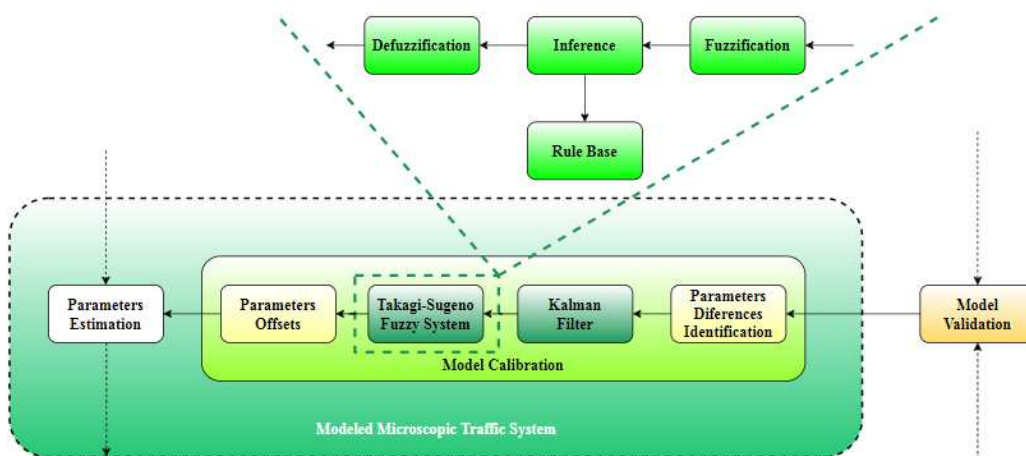

Figure 6.2. The proposed approach for microscopic traffic model calibration [**Pop20_2**].

"*The first internal subsystem of a calibration system is intended for identifying the differences between real and simulation data. These will be forwarded to the Kalman filter. The filtered values will be forwarded to the final decision step regarding the offset values consisting of a Takagi-Sugeno FIS. This last subsystem embeds the fuzzy specific components. The fuzzification ensures that the identified differences between the real and simulation parameters are converted to a fuzzy variable. Further, after the fuzzy rules have been defined, the output fuzzy variables will consider them in establishing the connections with the input fuzzy variables through an inference step. Defuzzification will convert the fuzzy variables to the corresponding types of analyzed parameters. These values consisting of offsets that shall be applied to the simulation parameters will also be saved by a subsystem that will build a knowledge base for the parameters offset*" [**Pop20_2**].

"*After the model parameters have been updated with the offsets provided by the calibration subsystem, the process will be resumed until the offsets tend to zero. As the values of the simulation are closer to the real ones, the chances of the model to be validated increase. When the offsets are equal to zero, the model is considered as validated*" [**Pop20_2**].

"*The inter-vehicle spacing offset for the next run of the simulation can be considered the same as the new estimated simulation error. From this point of view, the calibration module will be responsible for estimating the values that can reduce the difference between simulation values and the values retrieved from real traffic*

measurements. The new estimation error shall be computed as it is presented below and will be further applied directly by the subsystem that estimates the model parameters based on retrieved real traffic data, depending on corresponding conditioned parameters:

$$\begin{cases} \Delta s(t) = \Delta s_0(t) + \zeta_s(t) - \gamma_s(t), & \gamma_s(t) \neq \zeta_s(t) \\ \Delta s(t) = \Delta s_0(t) + \gamma_s(t) = \Delta s_0(t) + \zeta_s(t), & \gamma_s(t) = \zeta_s(t) \end{cases} \tag{6.14}$$

where $\Delta s_0(t)$ *is considered an initial offset that can be defined based on FV and LV behavior for velocity evolution, as can be seen in* (6.15)*. This correction step shall be applied to ensure that it maintains the standard safety distance* s *between LV and FV"* [**Pop20_2**]:

$$\Delta s_0(t) = \begin{cases} 0, & x_1(t) \geq x_3(t) \\ S, & x_1(t) < x_3(t) \end{cases} \tag{6.15}$$

"*The model calibration will be done for the linguistic variables defined in Table.6.1. The inputs and outputs are defined in a manner that simplifies the fuzzy rules writing process. More than that, the output is defined for each possible situation that can describe the car-following model behavior from the LV and velocity evolution perspectives. Additional information that is taken into account is related to the measurement and simulation errors of dynamic safety distance between LV and FV (the inter-vehicle spacing). The output consisting of the necessary offsets that shall be applied to the simulation values for LV and FV vehicles will be defined by equations that use the Kalman filter-specific data. These offsets* Δs *will be computed according to* (6.14)" [**Pop20_2**].

Table 6.1. "*Linguistic variables for Takagi-Sugeno Fuzzy Inference System (FIS) based on Kalman filtered values*" [**Pop20_2**].

Parameter Role	Variable Name	Variable	Definition
Input 1	LV velocity relative to FV velocity (*REL_SPEED*)	LOW	$x_1(t) < x_3(t)$
		EQUAL	$x_1(t) = x_3(t)$
		HIGH	$x_1(t) > x_3(t)$
Input 2	Simulated inter-vehicle spacing estimation error relative to measurement error (*REL_ERR*)	LOW	$\gamma_s(t) < \zeta_s(t)$
		EQUAL	$\gamma_s(t) = \zeta_s(t)$
		HIGH	$\gamma_s(t) > \zeta_s(t)$
Output	Inter-vehicle spacing offset Δs (*OFFSET*)	REDUCE	Equation (6.14)
		MAINTAIN	
		INCREASE	

"*Considering the introduced linguistic variables and the possible offset values defined by* (6.14)*, the fuzzy rules are according to* (6.16)" [**Pop20_2**].

IF REL_SPEED = LOW   AND REL _ ERR = LOW   THEN OFFSET = INCREASE
IF REL_SPEED = LOW   AND REL _ ERR = EQUAL THEN OFFSET = MAINTAIN
IF REL_SPEED = LOW   AND REL _ ERR = HIGH   THEN OFFSET = REDUCE
IF REL_SPEED = EQUAL AND REL _ ERR = LOW   THEN OFFSET = INCREASE
IF REL_SPEED = EQUAL AND REL _ ERR = EQUAL THEN OFFSET = MAINTAIN (6.16)
IF REL_SPEED = EQUAL AND REL _ ERR = HIGH   THEN OFFSET = REDUCE
IF REL_SPEED = HIGH   AND REL _ ERR = LOW   THEN OFFSET = INCREASE
IF REL_SPEED = HIGH   AND REL _ ERR = EQUAL THEN OFFSET = MAINTAIN
IF REL_SPEED = HIGH   AND REL _ ERR = HIGH   THEN OFFSET = REDUCE

"*The fuzzy matrix F_k that considers the fuzzy rules and* (6.15) *is shown below*" [**Pop20_2**].

$$F_k = \begin{bmatrix} S + \zeta_S(t) - \gamma_S(t) & S + \gamma_S(t) & S + \zeta_S(t) - \gamma_S(t) \\ \zeta_S(t) - \gamma_S(t) & \gamma_S(t) & \zeta_S(t) - \gamma_S(t) \\ \zeta_S(t) - \gamma_S(t) & \gamma_S(t) & \zeta_S(t) - \gamma_S(t) \end{bmatrix} \tag{6.17}$$

6.2.4. Simulation Model

"*Figure 6.3 shows the Simulink (MATLAB R2020a) implementation model. The implementation is a simplified car-following model that studies the impact of velocities in the FV strategy to adapt its running distance based on the FV moving behavior. In this case, the acceleration was not taken into account*" [**Pop20_2**].
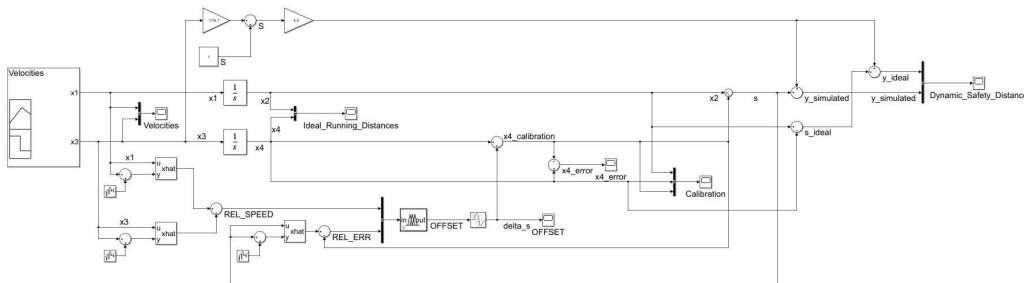
Figure 6.3. "*Simulation model – implementation using Simulink (MATLAB R2020a)*" [**Pop20_2**].

"*The computation of the standard safety distance S is done continuously considering equation* (4.29)*. This value is needed to ensure collision avoidance in the case of the increase in FV velocity. For this computation, an average vehicle length L = 4.50 m was used. The output of the modeled system also considers S in the dynamic safety distance profile*" [**Pop20_2**].

"*The inputs of the model and also the internal states can be affected by noise in the case of model implementation. To simulate this behavior a Band-Limited White Noise Simulink block was added to the simulation for the velocities and inter-vehicle spacing to see their impact on the running distances for the LV and FV, and the dynamic safety distance y . The applied noise consists of normally*

distributed random numbers with the following characteristics that are the default values for the mentioned Simulink block:

- *noise power: 0.10;*
- *sample time: 0.10;*
- *seed: 23341"* [**Pop20_2**].

"*An adaptive system based on Kalman filtering and Takagi-Sugeno FIS will ensure the removal of the introduced noises by the simulated model. The Fuzzy Controler Simulink block uses the Kalman filtered values as input for the relative speed between the FV and LV and also the simulated inter-vehicle spacing estimation error relative to measurement error. The implementation details of the Takagi-Sugeno FIS are available in the second part of the current section"* [**Pop20_2**].

"*Scope Simulink blocks were added in some points of interest for the following reasons:*

- *to monitor the input values;*
- *to obtain the running distances profile for the real behavior of the LV and FV;*
- *to capture the influences in the simulated running distances introduced by the simulated system;*
- *to correlate the calculated offset values for inter-vehicle spacing with the calibration process evolution;*
- *to create an overview of the calibration process impact on the system output"* [**Pop20_2**].

Simulation Input Data

"*To prove the proposed model validity, the simulation uses as input data, the data provided by Timișoara City Hall - General Directorate of Roads, Bridges, Parking and Utility Networks - Traffic Monitoring Office, Timișoara, Romania. Figure 6.4 shows, marked in red, the chosen piece of road between two crossroads: Liviu Rebreanu - Calea Șagului and Liviu Rebreanu – Gheorghe Ranetti. These crossroads have a high daily traffic flow and consists of a good input for analyzing the impact of the proposed approach. The data was collected by using inductive loops sensors that were placed on the studied road network to monitor the vehicle numbers and the velocities"* [**Pop20_2**].
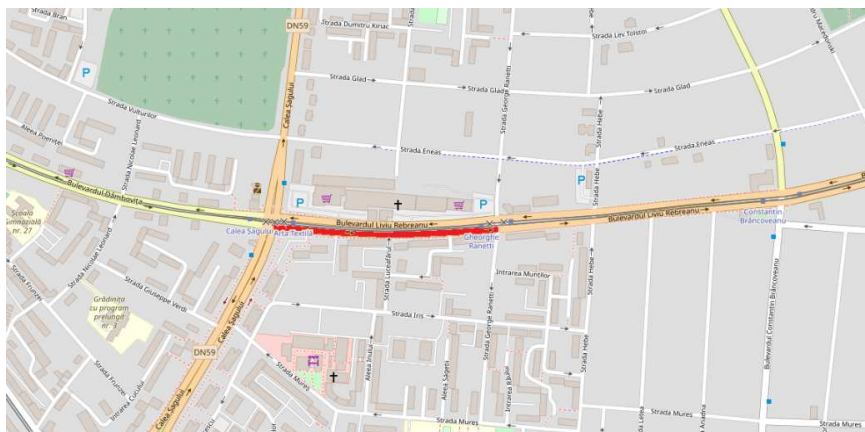

Figure 6.4. "*Real mapping of the studied piece of road (Source: OpenStreet Maps view)*"
[**Pop20_2**].

Takagi–Sugeno Model Implementation Details
        "*The implementation Takagi-Sugeno FIS using the Kalman filtered values as inputs, according to the assumptions previously mentioned, uses Fuzzy Logic Toolbox from MATLAB R2020a. Figure 6.5 shows the implemented calibration step as it looks in the chosen simulation tool*" [**Pop20_2**].
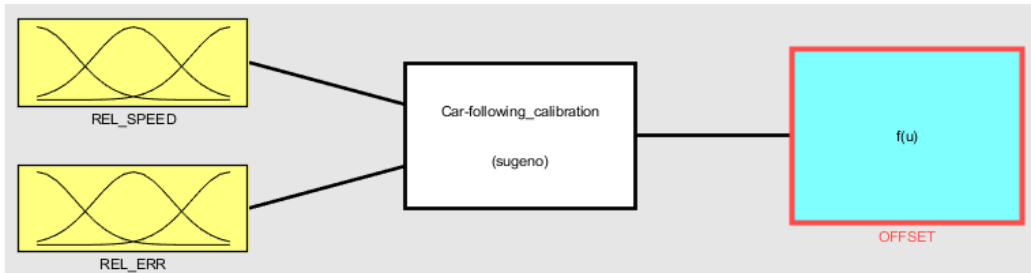
Figure 6.5. "*Takagi-Sugeno FIS calibration model implementation using Kalman-filtered values as input*" [**Pop20_2**].

        "*The established fuzzy rules presented in (6.16) were implemented for the car-following model calibration using the rule editor for Takagi-Sugeno FIS provided by the simulation tool, as it can be seen in Figure 6.6*" [**Pop20_2**].

Figure 6.6. "*Fuzzy rules implementation using rule editor*" [**Pop20_2**].

        "*A manner to analyze the simulation results specific to MATLAB R2020a is the usage of rule viewer. Each input of the calibration system and the output are shown in Figure 6.7. The output values of the car-following calibration system will*

be modified interactively based on chosen inputs. Membership functions were defined based on historical traffic data evolution" [**Pop20_2**].
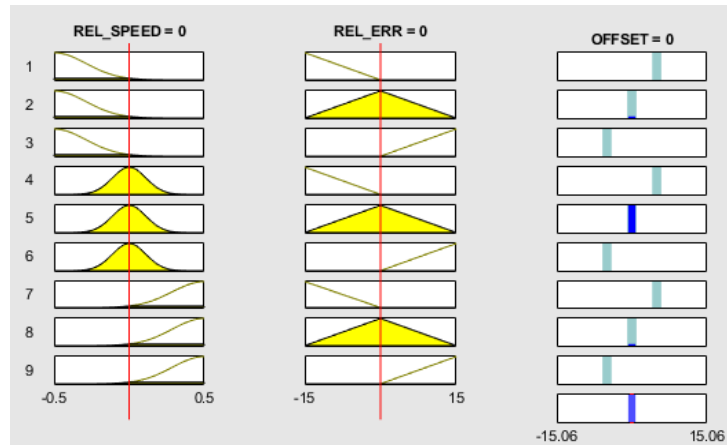
Figure 6.7. "*Rule viewer for Takagi-Sugeno FIS car-following calibration system*" [**Pop20_2**].

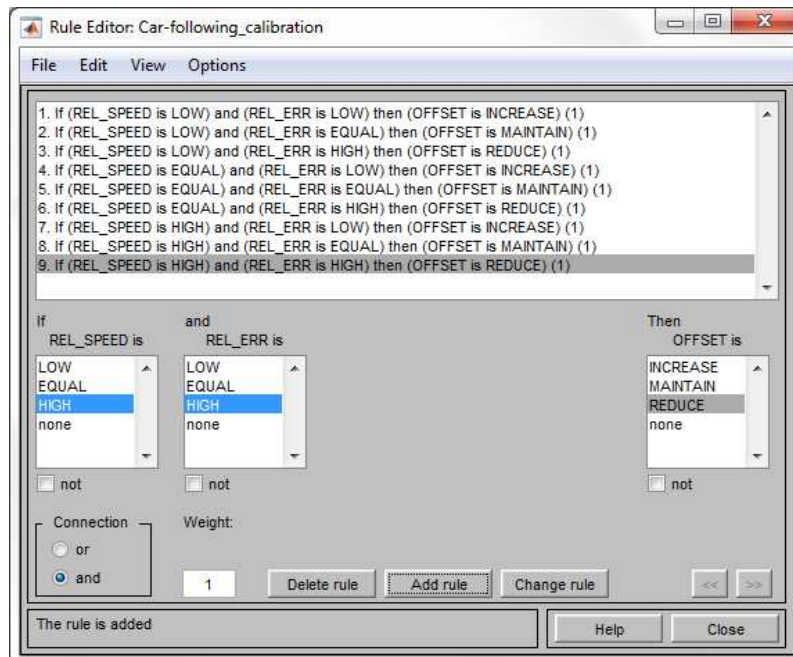"*Another option to analyze the results of fuzzy rules evaluation is through the surface viewer.* Figure 6.8 *illustrates the system performance for the relationship between the linguistic variables used as inputs or as output for the modeled microscopic traffic calibration system*" [**Pop20_2**].
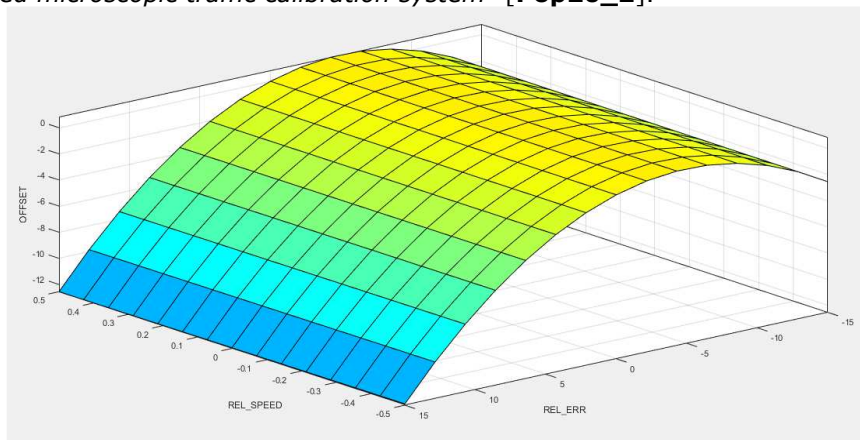
Figure 6.8. "*Surface viewer for Takagi-Sugeno FIS car-following calibration system*" [**Pop20_2**].

6.2.5. Simulation Results

"Figure 6.9 *shows the input data for the proposed traffic calibration method. Can be observed the evolution in time of the LV and FV velocities for the chosen piece of road between two crossroads*" [**Pop20_2**].
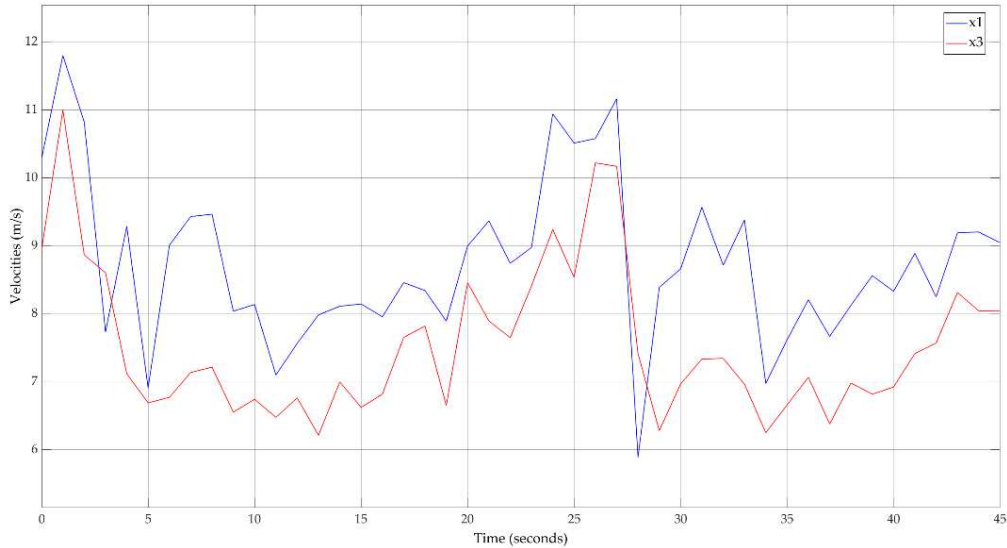
Figure 6.9. "*Input data - velocities for LV (x_1) and FV (x_3)*" [**Pop20_2**].

"*Based on the input values the ideal evolution was computed for the LV and FV running distances.* Figure 6.10 *shows this result after the application of the car-following approach for the real traffic data*" [**Pop20_2**].
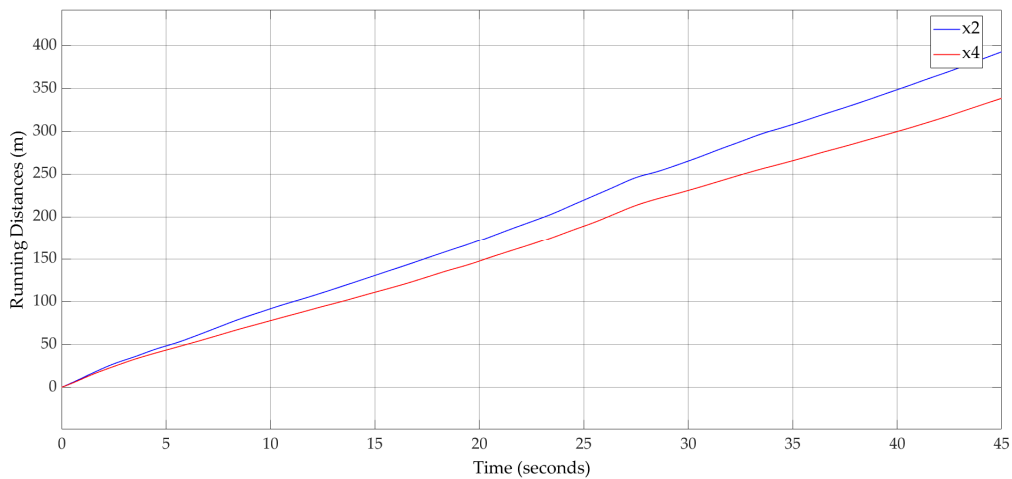
Figure 6.10. "*Running distances for LV (x_2) and FV (x_4) – ideal evolution*" [**Pop20_2**].

"*The result of the proposed hybrid approach for calibration of the car-following model in continuous-time is available in* Figure 6.11. *The modeled running distance of the FV that is affected by noise succeeds at reproducing the real behavior of the FV*" [**Pop20_2**].
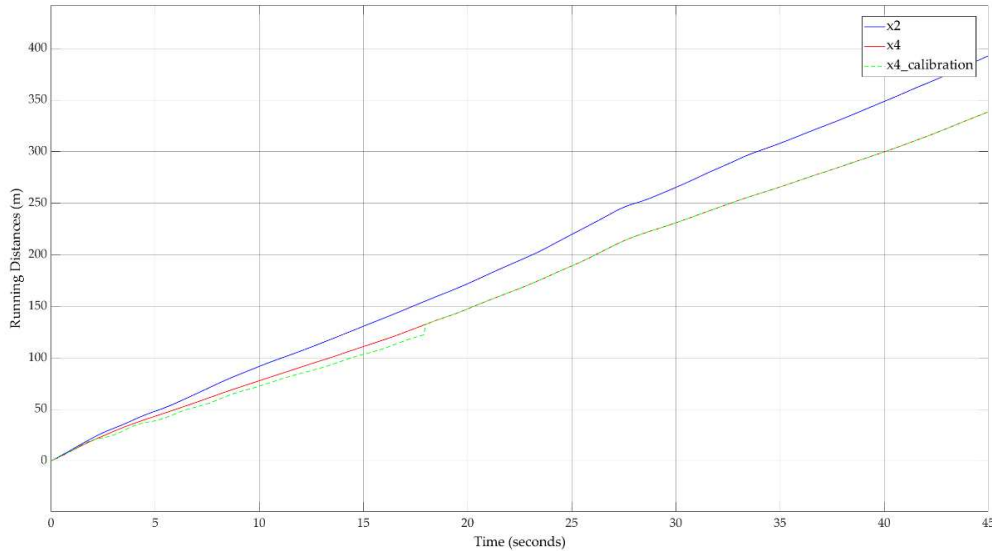
Figure 6.11. "*Running distances for LV (x_2) and FV (x_4) - calibration result for FV (x_4)*"
[**Pop20_2**].

"*A better way to see the utility of the proposed approach is to analyze the calculated offset values.* Figure 6.12 *illustrates the evolution of the calculated offset values for the inter-vehicle spacing applied to the FV. Before the system joins the calibrated state, both positive and negative offset values are applied. After approximately* $t = 18\,s$ *, the system succeeded at learning different patterns of velocities and simulated inter-vehicle spacing error patterns and could reproduce the real behavior. After that time, the system was calibrated and could continuously reproduce the real behavior*" [**Pop20_2**].
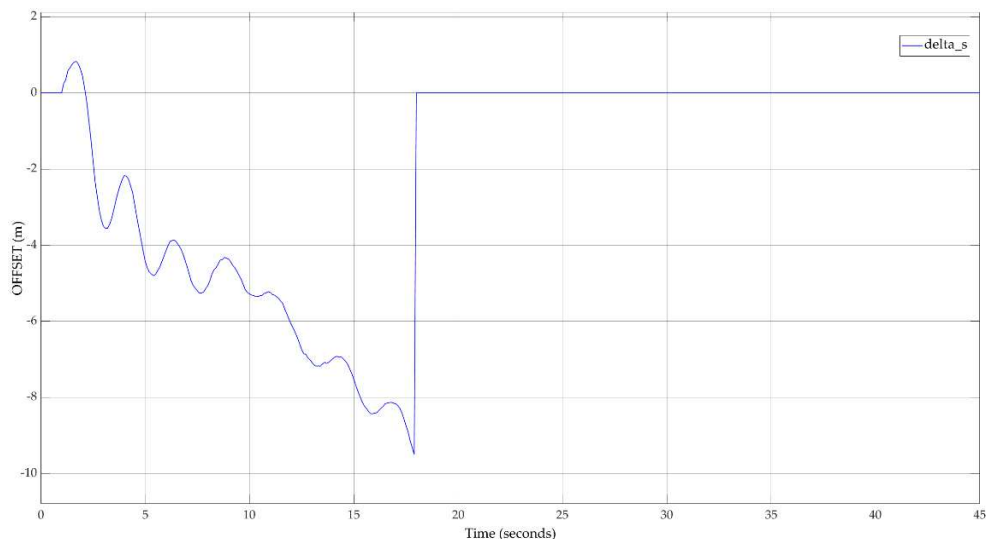
Figure 6.12. "*Inter-vehicle spacing offset applied to FV (x_4)*" [**Pop20_2**].

"*The calibration result can also be observed by analyzing the dynamic safety distance that includes the standard safety distance. Figure 6.13 depicts the overview of the calibration result for the system output. The safety level is ensured by the direct application of safety length on the output, and safety is guaranteed by the car-following model even in cases of vehicles with different lengths*" [**Pop20_2**].
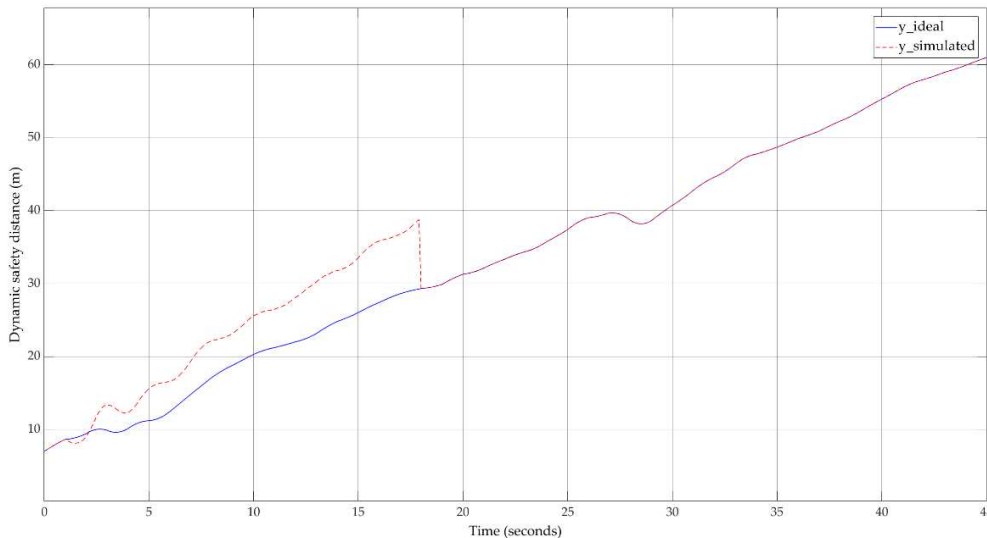
Figure 6.13. "*Dynamic safety distance – calibration overview*" [**Pop20_2**].

Discussion

"*To show the motivation of using the hybrid proposal of Kalman filtering with Takagi-Sugeno FIS instead of a solution based on Kalman filtering-only, a simulation is needed for this comparison. Figure 6.15 depicts the implementation using Simulink (MATLAB R2020a) for the mentioned reason. The simulation aims to analyze the behavior of FV for both cases of calibration methods. In addition to the simulation blocks from Figure 6.3, an extension introduces the computation of the FV running distance based on the Kalman filtering-only approach. In this case, the model uses only the filtered values to control the FV movement strategy. A big disadvantage, in this case, is the neglect of the FV relative velocity that can result in wrong offset values that will negatively influence the movement strategy. The calibration system shall ensure the capability for time-varying offset values application*" [**Pop20_2**].

"*The simulation results for this comparison (Figure 6.14) illustrate that both approaches succeeded in filtering the noises and provided similar-to-real-case trajectory evolution. The Kalman filtering-only approach cannot reproduce the real behavior through its neglect of inter-vehicle interaction from a relative velocity perspective. The hybrid approach takes advantage of this interaction between FV and LV and succeeds at identifying the time-varying appropriate offset value that reproduces the real behavior. This advantage can be visually observed from trajectory evolution where, after $t = 18\,s$, the system is calibrated using the hybrid approach. At the same time, the Kalman filter-only approach introduces a uniform increase in computation error that leads to a scaled running distance compared to*

real traffic conditions. From a computational complexity perspective, both approaches fit to real-time processing. The Takagi-Sugeno FIS does not introduce computational delays that can lead to a major increase in the real-time data processing timings" [**Pop20_2**].
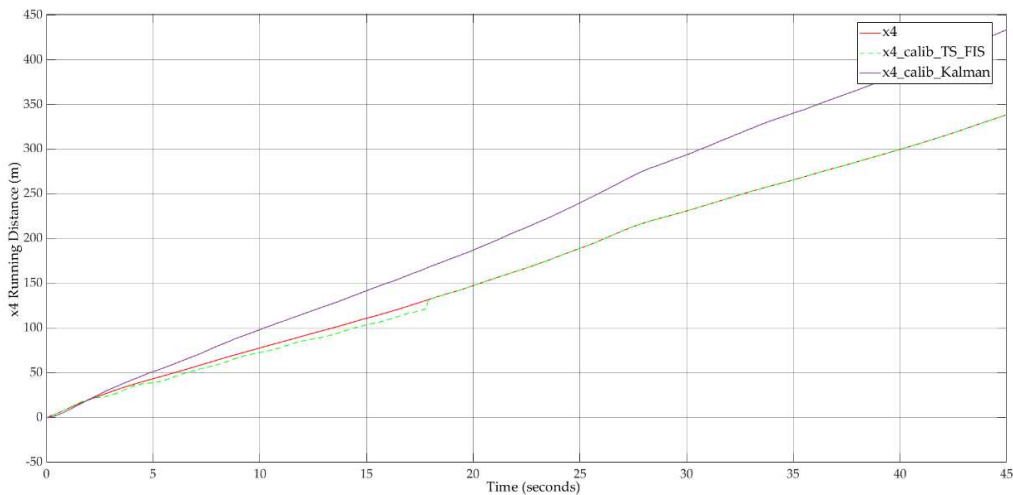
Figure 6.14. "*Running distance for FV (x_4) - comparison of calibration result for the Kalman filtering-only approach and the hybrid Kalman filtering and Takagi-Sugeno FIS approach*" [**Pop20_2**].
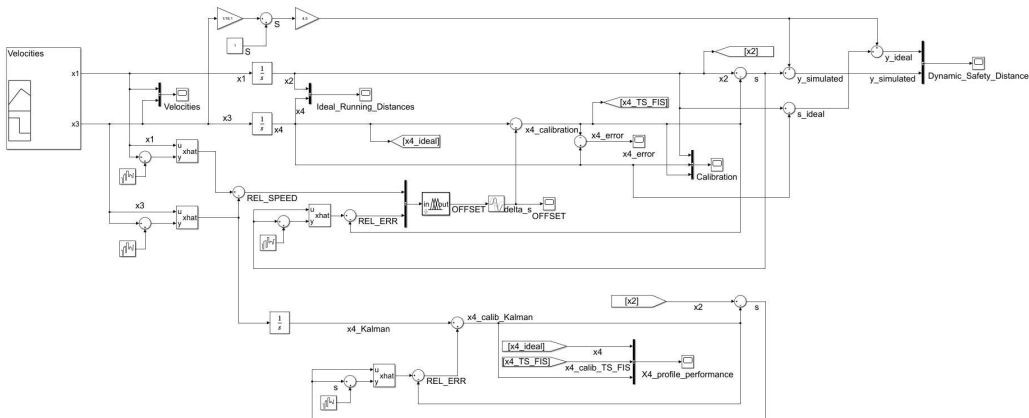
Figure 6.15. "*Simulation model to compare the Kalman filtering-only approach with the hybrid Kalman filtering and Takagi-Sugeno FIS approach – implementation using Simulink (MATLAB R2020a)*" [**Pop20_2**].

Besides the application of this proposed calibration method for standard car-following models, this thesis also verifies its performance in the case of the refined car-following model.

6.3. Calibration of the Refined Car-Following Model

6.3.1. Simulation Model

The application of the hybrid calibration method for the refined car-following model requires the extraction of the implementation of the computational logic to a standalone subsystem because in [**Pop20_2**] the simulation model also included the computational logic for the standard car-following model. Figure 6.16 illustrates a parallel view of the subsystems designed for the refined car-following model and the subsystem that contains the computational logic for calibration. The inputs for the calibration subsystem are the outputs of the refined model related to the target lane i. Designed initially for continuous-time, the adaptation to the discrete-time version of the refined car-following model proposed by this thesis involved the usage of an *ode45* solver for continuous states.
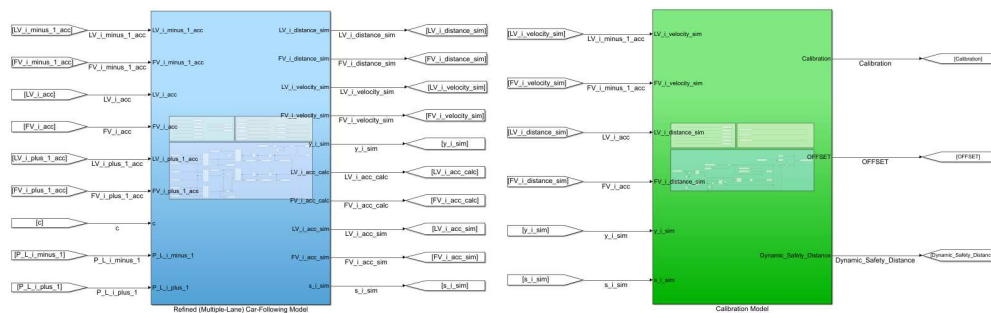
Figure 6.16. Refined car-following model and calibration model subsystems - implementation using Simulink (MATLAB R2021a).

Figure 6.17 illustrates a detailed overview of the calibration model after the extraction of the computational logic from the initial implementation for the standard car-following model (Figure 6.3). This facilitates the reusability of the proposed calibration method.
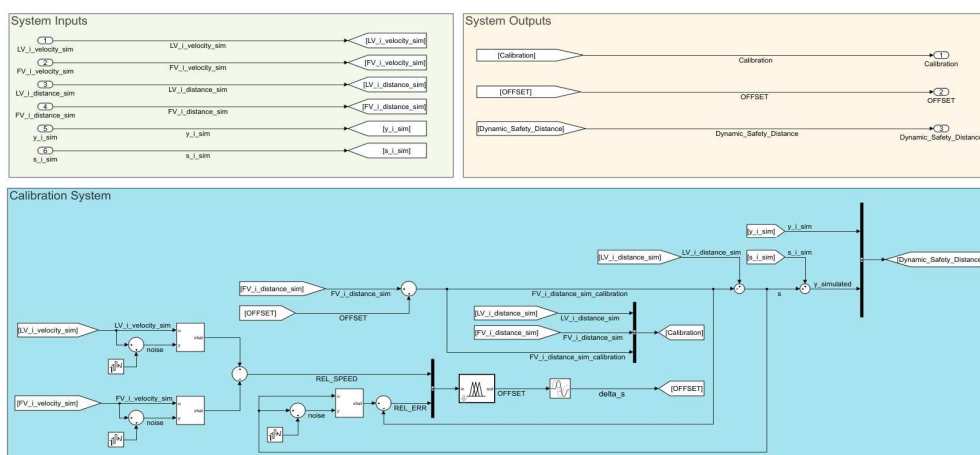
Figure 6.17. Calibration model – a detailed overview of the model implementation in Simulink (MATLAB R2021a).

6.3.2. Simulation Results

After running the simulation for the refined car-following model and using as input the data specified in Table 4.2 (**Section 4.5.3**), the offset that applies to the inter-vehicles spacing is changing according to Figure 6.18. Noise has been injected into the model according to the explanations given at the beginning of **Section 6.2.4**. The calibration method succeeds in "learning" different patterns of changes in the running distance value and after approximately $t = 5\ s$ the calibration process is completed and the refined car-following model is fully calibrated.
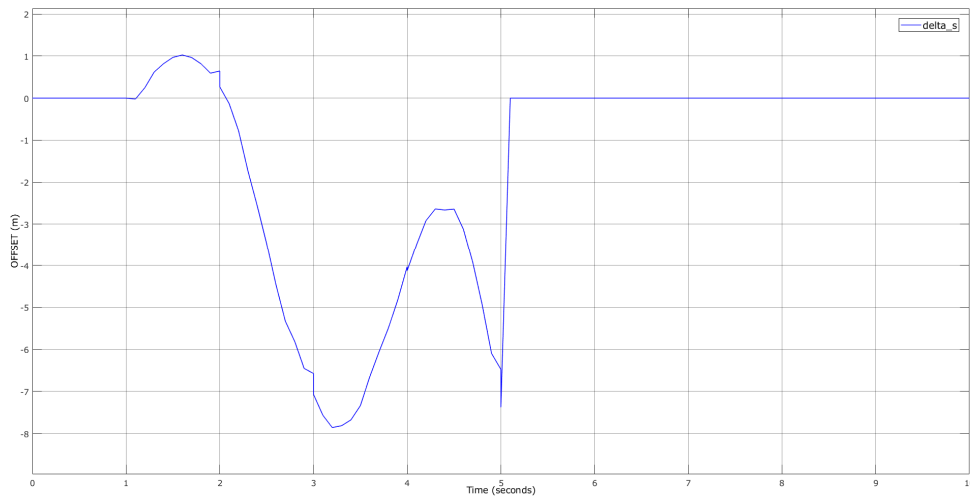
Figure 6.18. Inter-vehicle spacing offset applied to FV (*FV_i_distance_sim*).

Figure 6.19 shows a better overview of the efficiency of the proposed calibration model. This presents the running distance profiles for LV and FV and the calibrated running distance for the FV in the case of a noise presence.
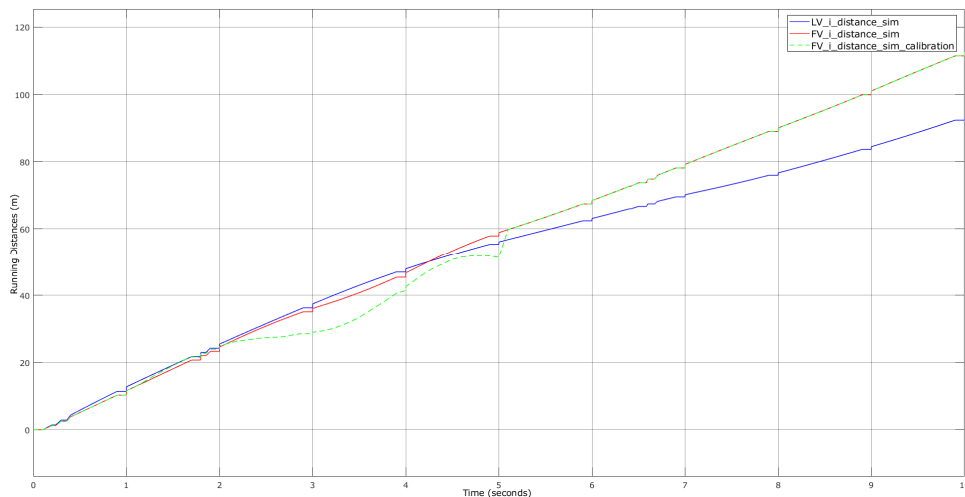
Figure 6.19. Calibration result for FV (*FV_i_distance_sim*).

6.4. Summary and Conclusions

This chapter proposed a new online calibration method for car-following models. This method combined Kalman filtering and Takagi-Sugeno FIS to eliminate the noises introduced by the modeling process.

"*The proposed method was validated by the simulation results obtained from the Simulink (MATLAB R2020a) implementation of the continuous-time car-following model together with the system responsible for the calibration process. The input data of this study consisted of real road traffic data from Timișoara, Romania. Takagi-Sugeno FIS proved again its utility in adaptive systems through the optimization of parameters offsets establishing process*" [**Pop20_2**]. Additionally, the proposed calibration method has been adapted for the refined car-following model needs and has also demonstrated satisfying results proved by a simulation done in Simulink (MATLAB R2021a). Moreover, the offsets determined through the calibration process can also reduce the impact of computational faults resulting from the fault analysis performed in the previous chapter.

"*A comparison between the Kalman filtering only approach and the hybrid Kalman filtering with Takagi-Sugeno FIS was conducted in Simulink (MATLAB R2020a). The comparison results show that the hybrid approach could provide a closer model to the real model. The big advantage of the hybrid approach was that it can provide the time-varying offset based on real-time road traffic parameters. Moreover, this proposal implies the specific interaction between FV and LV in the offset computation according to the microscopic traffic modeling theory*" [**Pop20_2**].

"*Further works can extend this approach at the mesoscopic traffic modeling level where the conditions for velocities evaluation can be assigned to vehicle groups instead of individual vehicles. A big challenge in that direction will be the safety distance assurance inside a group of vehicles because mesoscopic modeling does not offer enough granularity compared to microscopic traffic models*" [**Pop20_2**].

7. CONCLUSIONS, CONTRIBUTIONS AND FUTURE RESEARCH

7.1. Study Conclusions

This thesis addresses a current direction of research consisting of intelligent control and modeling of road traffic systems. The developments of new systemic approaches used the microscopic level of road traffic representation and addressed the uncertainties introduced by driver behavior in the modeling process. Moreover, this thesis reproduces the scientific contributions of the author that were achieved during the PhD research program and were published in journals or proceedings volumes of international conferences. At the end of each chapter, the author emphasizes the conclusions, advantages, and disadvantages of the proposed approaches.

The development of "*a new car-following model for multiple-lane roads was the main objective of this research*" [**Pop19_1**]. The proposed approach introduced the vehicle's behavior from the adjacent traffic lanes as a relevant parameter to better control the acceleration of the FV from the target traffic lane. An analysis of crossroads configuration methods followed by new approaches for the prediction of origin-destination traffic volumes and the traffic lanes modeling as a Markov process were the intermediate steps of the refinement of the standard car-following model. The refinement process predicts the lane change actions by employing the Bayesian reasoning concept and has as an outcome the update of the incentive criteria that control the FV acceleration.

This study also performs "*a fault detection and analysis based on parity equations of the refined car-following model to determine the faults introduced by the modeling process*" [**Pop20_3**]. The residuals evaluation showed that the refined model provides an accurate description of the behavior of the LV and FV from the target lane if a new vehicle from an adjacent lane joins the target lane. However, the fault analysis also illustrates the main disadvantage of the proposed multiple-lane car-following model consisting of the fact that "*the model is not suitable for a real-time switch from one lane to another to ensure lane change behavior monitoring for each lane*" [**Pop20_3**].

Moreover, this thesis develops a new solution for car-following models calibration. The proposed approach combines the usage of Kalman filtering with Takagi-Sugeno FIS and demonstrated improved results in compared to the simple usage of Kalman filtering. This method also proved good results for the application of the calibration process for the refined car-following model.

Besides the systemic contributions on the microscopic traffic modeling, this thesis presented an overview of the influence of crossroads configuration methods, inter-vehicle communications protocols, existing policies and regulations for smart city projects, and local administrations decisions regarding the implementation of smart solutions for mobility inside urban areas.

Furthermore, this study briefly presents the author's contributions and defines the possible directions of improvements and developments, having as input the original approaches discussed in this thesis.

7.2. Contributions

According to the objectives mentioned, the outcome of this thesis consists of the following original contributions by the author, divided into four main categories:

- a critical analysis of the concepts used in road traffic modeling at the microscopic level and the evaluation of possible factors of influence:
    - a critical analysis and synthesis of microscopic road traffic simulators;
    - a comparative overview of the car-following model and its derivatives;
    - a critical analysis and synthesis of the recent developments of car-following models designed to respond to CAVs and EVs needs;
    - a critical analysis and synthesis of the car-following calibration methods;
    - identification of the influence of road infrastructure, traffic policies and regulations, and smart mobility solutions in traffic congestion reduction;
    - identification of possible improvements in the modeling of road traffic at the microscopic level;
    - identification of possible improvements in the modeling car-following calibration methods;
- a systemic approach and modeling of road traffic at the microscopic level of representation:
    - modeling and implementation in AnyLogic Simulation Software of different crossroads configuration methods;
    - a comparative analysis of the traffic volumes and velocity profiles corresponding to all crossroad configuration methods;
    - a safety analysis of the single-lane roundabout management systems;
    - modeling and implementation of green-intervals schedulers using AnyLogic Simulation Software and Simulink (MATLAB R2020a);
    - development of new approaches of traffic lanes modeling as nodes in a Markov chain that corresponds to a road network;
    - development of new algorithms based on Bayesian reasoning, genetic algorithms and minimax gaming-specific strategy for driver behavior prediction and, implicitly OD volumes estimation;
    - development of new models for lane change to incorporate the uncertainty of driver behavior;
    - development and implementation of a refined car-following model that overcomes the disadvantage of single-lane orientation of the standard car-following models by considering the behavioral changes according to the lane change actions to adjacent traffic lanes;
    - conducting an experimental study on the proposed refined car-following model based on real road traffic dataset for a three-lane piece of road from Timisoara (Romania);
    - a comparative critical analysis of the results of the proposed refined car-following model with the separate application of the standard car-following model for each lane of a three-lane piece of road;

- a systemic fault detection and analysis of the faults introduced by the modeling process of the refined car-following model:
    - "*defining a fault detection methodology based on parity equations for multiple-lane car-following models*" [**Pop20_3**];
    - identification of relative velocity and dynamic running distance as the residuals of the refined car-following model;
    - development and implementation of the fault detection mechanisms in Simulink (MATLAB R2020a);
    - conducting an experimental fault detection study of the proposed refined car-following model using real road traffic dataset for a three-lane piece of road from Timisoara (Romania);
    - providing measurements and evaluation of the obtained residuals values;
    - a critical analysis of the advantages and disadvantages of the proposed refined car-following model as an outcome of the evaluation of the residuals;
- a systemic approach and modeling of the calibration process of car-following models:
    - development and implementation of a new calibration model for car-following models as a hybrid solution that combines Kalman filtering with Takagi-Sugeno FIS;
    - identification of the possible changes in the proposed calibration model to adapt it to the needs of the proposed refined car-following model;
    - conducting an experimental study on the proposed calibration model based on a real road traffic dataset from Timisoara (Romania) for both standard and refined car-following models;
    - a comparative critical analysis of the proposed calibration model in terms of accuracy and performance.

7.3. Recommendations for Future Research

Further research can propose solutions that provide real-time control for all vehicles moving on multiple traffic lanes, allowing the permanent update of the FVs accelerations for all traffic lanes of a road network, not only for a traffic lane as proposed in this thesis. This extension will show a full overview of the acceleration control possibilities and better model the behavioral interactions between vehicles moving on different traffic lanes.

New systemic approaches for microscopic road traffic control can apply genetic algorithms, fuzzy-based algorithms and neural networks concepts to provide safe solutions for traffic congestion reduction. The mentioned concepts can also be used to improve the calibration methods for microscopic traffic models.

Moreover, a deep study is necessary to identify the behavioral patterns that describe the relationship between crossroads configuration methods and driver behavior.

LIST OF PUBLICATIONS

A. Scientific papers published in Web of Science-WoS (ISI) indexed journals

1. **M.-D. Pop**, O. Proștean, T.-M. David, and G. Proștean, "Hybrid Solution Combining Kalman Filtering with Takagi–Sugeno Fuzzy Inference System for Online Car-Following Model Calibration," *Sensors*, vol. 20, no. 19, p. 5539, **Oct. 2020**, doi: 10.3390/s20195539, indexată în **Clarivate Analytics Web of Science**, **cuartila Q1, factor de impact = 3.576** - conform 2020 Journal Citation Reports (JCR) publicat de Clarivate Analytics în 2021. (*WOS:000586442700001*)

2. **M.-D. Pop**, O. Proștean, and G. Proștean, "Fault Detection Based on Parity Equations in Multiple Lane Road Car-Following Models Using Bayesian Lane Change Estimation", *Journal of Sensor and Actuator Networks*, vol. 9, no. 4, p. 52, **Dec. 2020**, doi: 10.3390/jsan9040052. (*WOS:000601811500001*)

B. Scientific papers published in volumes of scientific manifestations (Proceedings) indexed Web of Science-WoS (ISI) Proceedings

1. **M.-D. Pop,** "Traffic Lights Management Using Optimization Tool", *Procedia - Social and Behavioral Sciences*, vol. 238, pp. 323–330, **2018**, *Proceedings of the 14th International Symposium in Management SIM 2017*, doi: 10.1016/j.sbspro.2018.04.008. (*ISI WoS indexing process ongoing; previous conference 2015 ISI WoS indexed*)

2. **M.-D. Pop** and O. Proștean, "A Comparison Between Smart City Approaches in Road Traffic Management", *Procedia - Social and Behavioral Sciences*, vol. 238, pp. 29–36, **2018**, *Proceedings of the 14th International Symposium in Management SIM 2017*, doi: 10.1016/j.sbspro.2018.03.004. (*ISI WoS indexing process ongoing; previous conference 2015 ISI WoS indexed*)

3. **M.-D. Pop**, O. Prostean, and G. Prostean, "Prediction of Route Choosing Behavior Based on Genetic Algorithm Approach", in *2018 IEEE 22nd International Conference on Intelligent Engineering Systems (INES)*, Las Palmas de Gran Canaria, **Jun. 2018**, pp. 193–198, doi: 10.1109/INES.2018.8523917. (*WOS:000517754600036*)

4. **M.-D. Pop**, O. Prostean, and G. Prostean, "Analysis of Policies and Regulations for a Sustainable Smart Mobility System", in *2018 Proceedings of the 32nd International Business Information Management Association Conference, IBIMA 2018 - Vision 2020: Sustainable Economic Development and Application of Innovation Management from Regional expansion to Global Growth*, Seville, Spain, **Nov. 2018**, pp. 875–883. (*WOS:000508553201033*)

5. **M.-D. Pop** and O. Prostean, "Bayesian Reasoning for OD Volumes Estimation in Absorbing Markov Traffic Process Modeling", in *2019 4th MEC International Conference on Big Data and Smart City (ICBDSC)*, Muscat, Oman, **Jan. 2019**, pp. 1–6, doi: 10.1109/ICBDSC.2019.8645611. (*WOS:000469429600002*)

6. **M. D. Pop** and O. Proştean, "Identification of significant metrics and indicators for smart mobility*", IOP Conf. Ser.: Mater. Sci. Eng., vol. 477, p. 012017*, **Feb. 2019**, doi: 10.1088/1757-899X/477/1/012017. (*WOS:000461184100017*)

7. **M.-D. Pop**, O. Proştean, and G. Proştean, "Multiple Lane Road Car-Following Model using Bayesian Reasoning for Lane Change Behavior Estimation: A Smart Approach for Smart Mobility", in *Proceedings of the 3rd International Conference on Future Networks and Distributed Systems - ICFNDS '19*, Paris, France, **Jul. 2019**, pp. 1–8, doi: 10.1145/3341325.3341996. (*ISI WoS indexing process ongoing; previous conference 2018 ISI WoS indexed*)

8. **M.-D. Pop,** J. Pandey, and V. Ramasamy, "Future Networks 2030: Challenges in Intelligent Transportation Systems," in *2020 8th International Conference on Reliability, Infocom Technologies and Optimization (Trends and Future Directions) (ICRITO)*, Noida, India, **Jun. 2020**, pp. 898–902, doi: 10.1109/ICRITO48877.2020.9197951. (*ISI WoS indexing process ongoing; previous conference 2018 ISI WoS indexed*)

9. **M.-D. Pop,** "Decision Making in Road Traffic Coordination Methods: A Travel Time Reduction Perspective", in *2020 International Conference Engineering Technologies and Computer Science (EnT)*, Moscow, Russia, **Jun. 2020**, pp. 42–46, doi: 10.1109/EnT48576.2020.00014. (*ISI WoS indexing process ongoing; previous conference 2019 ISI WoS indexed*)

10. **M.-D. Pop**, O. Proştean, and G. Proştean, "Minimax Strategy for Lane Choice Prediction in Markovian Traffic Modeling", in *2020 5th International Conference on Logistics Operations Management (GOL)*, **Oct. 2020**, pp. 1–6, doi: 10.1109/GOL49479.2020.9314764. (WOS:00068072250001)

11. **M.-D. Pop**, C. C. Niculescu, O. Proştean, and G. Proştean, "Safety Aspects of Single-Lane Roundabout Management Systems in Connected Vehicles Environments," in *Proceedings of the 37th International Business Information Management Association Conference, IBIMA 2021 - Innovation Management and Information Technology Impact on Global Economy in the Era of Pandemic*, Cordoba, Spain, **May 2021**, pp. 10451-10457. (*ISI WoS indexing process ongoing; previous conference 2020 ISI WoS indexed*)

C. Scientific papers published in the volumes of scientific manifestations (Proceedings) indexed BDI

1. **M.-D. Pop**, "Real-Time Adaptive Traffic Signals Using Rate-Monotonic Scheduling", *ITM Web Conf.*, vol. 29, 3002, pp. 1–7, **2019**, Timisoara, Romania, doi: 10.1051/itmconf/20192903002. (*Crossref*)

APPENDIX A

Table A1. "*Mapping between model parameters and simulation defined signals*" [**Pop20_3**].

"*Parameter Type[1]*	*Model Parameter*	*Simulation Defined Signal*	*Significance*
Inputs	u_1 *for* L_{i-1}	*LV_i_minus_1_acc*	*acceleration of LV from lane* L_{i-1}
	u_1 *for* L_i	*LV_i_acc*	*acceleration of LV from lane* L_i
	u_1 *for* L_{i+1}	*LV_i_plus_1_acc*	*acceleration of LV from lane* L_{i+1}
	u_2 *for* L_{i-1}	*FV_i_minus_1_acc*	*acceleration of FV from lane* L_{i-1}
	u_2 *for* L_i	*FV_i_acc*	*acceleration of FV from lane* L_i
	u_2 *for* L_{i+1}	*FV_i_plus_1_acc*	*acceleration of FV from lane* L_{i+1}
	c	c	*driver decision to initiate a lane change maneuver*
	$\hat{P}(L_{i-1})$	*P_L_i_minus_1*	*probability of lane change from* L_i *to* L_{i-1} *according to (4.24)*
	$\hat{P}(L_{i+1})$	*P_L_i_plus_1*	*probability of lane change from* L_i *to* L_{i+1} *according to (4.24)*
Internal calculated values for multiple-lane car-following model	u_1 *for* L_j, $j=\{i-1,i+1\}$	*LV_i_acc_calc*	*calculated acceleration of new LV after lane change maneuver to* L_j, $j=\{i-1,i+1\}$
	u_2 *for* L_j, $j=\{i-1,i+1\}$	*FV_i_acc_calc*	*calculated acceleration of new FV after lane change maneuver to* L_j, $j=\{i-1,i+1\}$ *considering equation (4.25)*
	S	S	*standard safety distance calculated according to (4.29)*

Table A1. Cont.

Parameter Type [1]	Model Parameter	Simulation Defined Signal	Significance
Internal system states for standard car-following model	x_1 for L_{i-1}	LV_i_minus_1_velocity	velocity of LV from lane L_{i-1}
	x_1 for L_i	LV_i_velocity	velocity of LV from lane L_i
	x_1 for L_{i+1}	LV_i_plus_1_velocity	velocity of LV from lane L_{i+1}
	x_3 for L_{i-1}	FV_i_minus_1_velocity	velocity of FV from lane L_{i-1}
	x_3 for L_i	FV_i_velocity	velocity of FV from lane L_i
	x_3 for L_{i+1}	FV_i_plus_1_velocity	velocity of FV from lane L_{i+1}
	x_2 for L_{i-1}	LV_i_minus_1_distance	running distance of LV from lane L_{i-1}
	x_2 for L_i	LV_i_distance	running distance of LV from lane L_i
	x_2 for L_{i+1}	LV_i_plus_1_distance	running distance of LV from lane L_{i+1}
	x_4 for L_{i-1}	FV_i_minus_1_distance	running distance of FV from lane L_{i-1}
	x_4 for L_i	FV_i_distance	running distance of FV from lane L_i
	x_4 for L_{i+1}	FV_i_plus_1_distance	running distance of FV from lane L_{i+1}
Outputs for standard car-following model	y for L_{i-1}	y_i_minus_1	dynamic distance between LV and FV from L_{i-1} considering S
	y for L_i	y_i	dynamic distance between LV and FV from L_i considering S
	y for L_{i+1}	y_i_plus_1	dynamic distance between LV and FV from L_{i+1} considering S

Table A1. Cont.

Parameter Type [1]	Model Parameter	Simulation Defined Signal	Significance
Internal system states for multiple-lane car-following model	simulated u_1 for L_i	LV_i_acc_sim	simulated acceleration of LV (considers a possible lane change maneuver)
	simulated u_2 for L_i	FV_i_acc_sim	simulated acceleration of FV (considers a possible lane change maneuver)
	simulated x_1 for L_i	LV_i_velocity_sim	simulated velocity of LV (considers a possible lane change maneuver)
	simulated x_3 for L_i	FV_i_velocity_sim	simulated velocity of FV (considers a possible lane change maneuver)
	simulated x_2 for L_i	LV_i_distance_sim	simulated running distance of LV (considers a possible lane change maneuver)
	simulated x_4 for L_i	FV_i_distance_sim	simulated running distance of FV (considers a possible lane change maneuver)
Output for multiple-lane car-following model	simulated y for L_i	y_i_sim	simulated dynamic distance between LV and FV from L_i considering S
Output from residuals computation subsystem	r for $\bar{x}_1$ from L_i	relative_velocity_r esidual	residual of relative velocity between LV and FV from L_i
	r for $\bar{x}_2$ from L_i	dynamic_distance _residual	residual of dynamic distance between LV and FV from L_i without considering S

[1] *Some of the internal states or internal calculated values can be used as outputs in the Simulink (MATLAB R2020a) blocks implementation"* [**Pop20_3**].

REFERENCES

[Abd15] R. Abdelkrim, H. Gassara, M. Chaabane, and A. El Hajjaji, "Stability approaches for Takagi-Sugeno systems," in *2015 IEEE International Conference on Fuzzy Systems (FUZZ-IEEE)*, Istanbul, Turkey, Aug. 2015, pp. 1–6. doi: 10.1109/FUZZ-IEEE.2015.7338051.

[Abu16] N. AbuAli and H. Abou-zeid, "Driver Behavior Modeling: Developments and Future Directions," *International Journal of Vehicular Technology*, vol. 2016, pp. 1–12, Dec. 2016, doi: 10.1155/2016/6952791.

[Aco15] A. F. Acosta, J. E. Espinosa, and J. Espinosa, "TraCI4Matlab: Enabling the Integration of the SUMO Road Traffic Simulator and Matlab® Through a Software Re-engineering Process," in *Modeling Mobility with Open Data*, M. Behrisch and M. Weber, Eds. Cham: Springer International Publishing, 2015, pp. 155–170. doi: 10.1007/978-3-319-15024-6_9.

[Aka96] T. Akamatsu, "Cyclic flows, Markov process and stochastic traffic assignment," *Transportation Research Part B: Methodological*, vol. 30, no. 5, pp. 369–386, Oct. 1996, doi: 10.1016/0191-2615(96)00003-3.

[Aki07] T. Akita, S. Inagaki, T. Suzuki, S. Hayakawa, and N. Tsuchida, "Analysis of Vehicle Following Behavior of Human Driver Based on Hybrid Dynamical System Model," in *2007 IEEE International Conference on Control Applications*, Oct. 2007, pp. 1233–1238. doi: 10.1109/CCA.2007.4389404.

[Alj14] A. Aljaafreh and N. Al Oudat, "Optimized Timing Parameters for Real-Time Adaptive Traffic Signal Controller," in *2014 UKSim-AMSS 16th International Conference on Computer Modelling and Simulation*, Cambridge, Mar. 2014, pp. 244–247. doi: 10.1109/UKSim.2014.84.

[Ang11] P. Angkititrakul, C. Miyajima, and K. Takeda, "Modeling and adaptation of stochastic driver-behavior model with application to car following," in *2011 IEEE Intelligent Vehicles Symposium (IV)*, Jun. 2011, pp. 814–819. doi: 10.1109/IVS.2011.5940464.

[Ban95] M. Bando, K. Hasebe, A. Nakayama, A. Shibata, and Y. Sugiyama, "Dynamical model of traffic congestion and numerical simulation," *Phys. Rev. E*, vol. 51, no. 2, pp. 1035–1042, Feb. 1995, doi: 10.1103/PhysRevE.51.1035.

[Ban98] M. Bando, K. Hasebe, K. Nakanishi, and A. Nakayama, "Analysis of optimal velocity model with explicit delay," *Phys. Rev. E*, vol. 58, no. 5, pp. 5429–5435, Nov. 1998, doi: 10.1103/PhysRevE.58.5429.

[Bar10] J. Barceló, "Models, Traffic Models, Simulation, and Traffic Simulation," in *Fundamentals of Traffic Simulation*, vol. 145, J. Barceló, Ed. New York, NY: Springer New York, 2010, pp. 1–62. doi: 10.1007/978-1-4419-6142-6_1.

[Bar12] D. Barber, *Bayesian Reasoning and Machine Learning*, Cambridge University Press: Cambridge, 2012, ISBN 9780511804779, pp. 7-11. Accessed: Dec. 01, 2021. [Online]. Available: http://web4.cs.ucl.ac.uk/staff/D.Barber/textbook/200620.pdf.

[Bek03] E. Bekiaris, A. Amditis, and M. Panou, "DRIVABILITY: a new concept for modelling driving performance," *Cognition, Technology & Work*, vol. 5, no. 2, pp. 152–161, Jun. 2003, doi: 10.1007/s10111-003-0119-x.

[Ber00] W. Bernhard and P. Portmann, "Traffic simulation of roundabouts in Switzerland," in *2000 Winter Simulation Conference Proceedings (Cat. No.00CH37165)*, Orlando, FL, USA, 2000, vol. 2, pp. 1148–1153. doi: 10.1109/WSC.2000.899078.

[Bis06] C. M. Bishop, *Pattern recognition and machine learning*. New York: Springer, 2006, ISBN 9780387310732, pp. 21-24.

[Boe98] E.R. Boer and M. Hoedemaeker, "Modeling driver behavior with different degrees of automation: A hierarchical decision framework of interacting mental models," in *Proceedings of the 17th European annual conference on human decision making and manual control*, Dec. 1998, pp. 63-72.

[Bor19] R. Borsche and A. Meurer, "Microscopic and macroscopic models for coupled car traffic and pedestrian flow," *Journal of Computational and Applied Mathematics*, vol. 348, pp. 356–382, Mar. 2019, doi: 10.1016/j.cam.2018.08.037.

[Bou15] A. Bouyahya, Y. Manai, and J. Haggege, "New Lyapunov function for Takagi-Sugeno discrete time uncertain systems," in *2015 7th International Conference on Modelling, Identification and Control (ICMIC)*, Sousse, Dec. 2015, pp. 1–5. doi: 10.1109/ICMIC.2015.7409347.

[Bre84] L. Breiman, J. Friedman, R. Olshen, and C. Stone, *Classification and regression trees*, Boca Raton, FL: CRC Press, 1984.

[Bun14_1] H.-J. Bungartz, S. Zimmer, M. Buchholz, and D. Pflüger, "Microscopic Simulation of Road Traffic," in *Modeling and Simulation*, Berlin, Heidelberg: Springer Berlin Heidelberg, 2014, pp. 171–201. doi: 10.1007/978-3-642-39524-6_8.

[Bun14_2] H.-J. Bungartz, S. Zimmer, M. Buchholz, and D. Pflüger, "Stochastic Traffic Simulation," in *Modeling and Simulation*, Berlin, Heidelberg: Springer Berlin Heidelberg, 2014, pp. 203–238. doi: 10.1007/978-3-642-39524-6_9.

[Cao20] X. Cao, J. Wang, and C. Chen, "A Modified Car-following Model Considering Traffic Density and Acceleration of Leading Vehicle," *Applied Sciences*, vol. 10, no. 4, p. 1268, Feb. 2020, doi: 10.3390/app10041268.

[Cha58] R. E. Chandler, R. Herman, and E. W. Montroll, "Traffic Dynamics: Studies in Car Following," *Operations Research*, vol. 6, no. 2, pp. 165–184, Apr. 1958, doi: 10.1287/opre.6.2.165.

[Che16] D. Chen, S. Ahn, S. Bang, and D. Noyce, "Car-Following and Lane-Changing Behavior Involving Heavy Vehicles:," *Transportation Research Record*, vol. 2561, no. 1, pp. 89–97, Jan. 2016, doi: 10.3141/2561-11.

[Che20] L. Chettri and R. Bera, "A Comprehensive Survey on Internet of Things (IoT) Toward 5G Wireless Systems," *IEEE Internet Things J.*, vol. 7, no. 1, pp. 16–32, Jan. 2020, doi: 10.1109/JIOT.2019.2948888.

[Che21] J. Chen, D. Sun, Y. Li, M. Zhao, W. Liu, and S. Jin, "Human–machine cooperative scheme for car-following control of the connected and automated vehicles," *Physica A: Statistical Mechanics and its Applications*, vol. 573, p. 125949, Jul. 2021, doi: 10.1016/j.physa.2021.125949.

[Col21] C. Colombaroni, G. Fusco, and N. Isaenko, "Modeling Car Following with Feed-Forward and Long-Short Term Memory Neural Networks," *Transportation Research Procedia*, vol. 52, pp. 195–202, 2021, doi: 10.1016/j.trpro.2021.01.022.

[Daa15] W. Daamen, C. Buisson, and S. P. Hoogendoorn, Eds., *Traffic simulation and data: validation methods and applications*. Boca Raton: CRC Press,Taylor & Francis Group, 2015, pp. 1-4, ISBN 978-1-4822-2870-0.

[Dar06] J. Darch, B. Milner, and S. Vaseghi, "MAP prediction of formant frequencies and voicing class from MFCC vectors in noise," *Speech Communication*, vol. 48, no. 11, pp. 1556–1572, Nov. 2006, doi: 10.1016/j.specom.2006.06.001.

[Ech21] J. Echeto, M. G. Romana, and M. Santos, "Swarm Modelling Considering Autonomous Vehicles for Traffic Jam Assist Simulation," in *15th International Conference on Soft Computing Models in Industrial and Environmental Applications (SOCO 2020)*, vol. 1268, Á. Herrero, C. Cambra, D. Urda, J. Sedano, H. Quintián, and E. Corchado, Eds. Cham: Springer International Publishing, 2021, pp. 429–438. doi: 10.1007/978-3-030-57802-2_41.

[Edi61] L. C. Edie, "Car-Following and Steady-State Theory for Noncongested Traffic," *Operations Research*, vol. 9, no. 1, pp. 66–76, Feb. 1961, doi: 10.1287/opre.9.1.66.

[Ema19] A. Emami, M. Sarvi, and S. Asadi Bagloee, "Using Kalman filter algorithm for short-term traffic flow prediction in a connected vehicle environment," *J. Mod. Transport.*, vol. 27, no. 3, pp. 222–232, Sep. 2019, doi: 10.1007/s40534-019-0193-2.

[Fan20] X. Fang, T. Tettamanti, and A. C. Piazzi, "Online Calibration of Microscopic Road Traffic Simulator," in *2020 IEEE 18th World Symposium on Applied Machine Intelligence and Informatics (SAMI)*, Herlany, Slovakia, Jan. 2020, pp. 275–280. doi: 10.1109/SAMI48414.2020.9108744.

[Fer18] A. Ferrara, S. Sacone, and S. Siri, "Microscopic and Mesoscopic Traffic Models," in *Freeway Traffic Modelling and Control*, A. Ferrara, S. Sacone, and S. Siri, Eds. Cham: Springer International Publishing, 2018, pp. 113–143. doi: 10.1007/978-3-319-75961-6_5.

[Fu19] Z. Fu, J. Yu, and M. Sarwat, "Building a Large-Scale Microscopic Road Network Traffic Simulator in Apache Spark," in *2019 20th IEEE International Conference on Mobile Data Management (MDM)*, Hong Kong, Hong Kong, Jun. 2019, pp. 320–328. doi: 10.1109/MDM.2019.00-42.

[Gaz59] D. C. Gazis, R. Herman, and R. B. Potts, "Car-Following Theory of Steady-State Traffic Flow," *Operations Research*, vol. 7, no. 4, pp. 499–505, Aug. 1959, doi: 10.1287/opre.7.4.499

[Gaz61] D. C. Gazis, R. Herman, and R. W. Rothery, "Nonlinear Follow-the-Leader Models of Traffic Flow," *Operations Research*, vol. 9, no. 4, pp. 545–567, Aug. 1961, doi: 10.1287/opre.9.4.545.

[Ge08] H. X. Ge, R. J. Cheng, and Z. P. Li, "Two velocity difference model for a car following theory," *Physica A: Statistical Mechanics and its Applications*, vol. 387, no. 21, pp. 5239–5245, Sep. 2008, doi: 10.1016/j.physa.2008.02.081.

[Ger75] D. L. Gerlough and M. J. Huber, *Traffic flow theory: a monograph*. Washington: Transportation Research Board, National Research Council, 1975.

[Gka21] V. Gkania and L. Dimitriou, "Linking the microscopic traffic flow mechanics with the macroscopic phenomena by exploiting class-type traffic information retrieved from online traffic maps," *Transportation Research Procedia*, vol. 52, pp. 645–652, 2021, doi: 10.1016/j.trpro.2021.01.077.

[Gip81] P. G. Gipps, "A behavioural car-following model for computer simulation," *Transportation Research Part B: Methodological*, vol. 15, no. 2, pp. 105–111, Apr. 1981, doi: 10.1016/0191-2615(81)90037-0.

[Gor20] P. Gora, C. Katrakazas, A. Drabicki, F. Islam, and P. Ostaszewski, "Microscopic traffic simulation models for connected and automated vehicles (CAVs) – state-of-the-art," *Procedia Computer Science*, vol. 170, pp. 474–481, 2020, doi: 10.1016/j.procs.2020.03.091.

[Gou20] A. Gounni, N. Rais, and M. A. Idrissi, "A new car-following model considering the effect of complex driving behaviour," in *2020 5th International Conference on Logistics Operations Management (GOL)*, Rabat, Morocco, Oct. 2020, pp. 1–5. doi: 10.1109/GOL49479.2020.9314739.

[Gri16] Grigoryev, I.: AnyLogic 7 in three days: a quick course in simulation modeling, 2016, pp. 3.

[Had11] M. L. Hadjili and K. Kara, "Modelling and control using Takagi-Sugeno fuzzy models," in *2011 Saudi International Electronics, Communications and Photonics Conference (SIECPC)*, Apr. 2011, pp. 1–6. doi: 10.1109/SIECPC.2011.5876946.

[Ham12] S. Hamdar, "Driver Behavior Modeling," in *Handbook of Intelligent Vehicles*, A. Eskandarian, Ed. London: Springer, 2012, pp. 537–558. doi: 10.1007/978-0-85729-085-4_20.

[Has21] M. Hasan, D. Perez, Y. Shen, and H. Yang, "Distributed Microscopic Traffic Simulation with Human-in-the-Loop Enabled by Virtual Reality Technologies," *Advances in Engineering Software*, vol. 154, p. 102985, Apr. 2021, doi: 10.1016/j.advengsoft.2021.102985.

[Hel98] D. Helbing and B. Tilch, "Generalized force model of traffic dynamics," *Phys. Rev. E*, vol. 58, no. 1, pp. 133–138, Jul. 1998, doi: 10.1103/PhysRevE.58.133.

[Ise06] R. Isermann, "Fault detection with parity equations," in *Fault-Diagnosis Systems*, Berlin, Heidelberg: Springer Berlin Heidelberg, 2006, pp. 197–229. doi: 10.1007/3-540-30368-5_10.

[Ise11] R. Isermann, "Supervision, fault-detection and diagnosis methods – a short introduction," in *Fault-Diagnosis Applications*, Berlin, Heidelberg: Springer Berlin Heidelberg, 2011, pp. 11–45. doi: 10.1007/978-3-642-12767-0_2.

[Jia01] R. Jiang, Q. Wu, and Z. Zhu, "Full velocity difference model for a car-following theory," *Phys. Rev. E*, vol. 64, no. 1, p. 017101, Jun. 2001, doi: 10.1103/PhysRevE.64.017101.

[Jia20_1] S. Jiao, S. Zhang, B. Zhou, Z. Zhang, and L. Xue, "An Extended Car-Following Model Considering the Drivers' Characteristics under a V2V Communication Environment," *Sustainability*, vol. 12, no. 4, p. 1552, Feb. 2020, doi: 10.3390/su12041552.

[Jia20_2] B. Jia, D. Yang, X. Zhang, Y. Wu, and Q. Guo, "Car-following model considering the lane-changing prevention effect and its stability analysis," *Eur. Phys. J. B*, vol. 93, no. 8, p. 153, Aug. 2020, doi: 10.1140/epjb/e2020-10028-3.

[Kal61] R. E. Kalman and R. S. Bucy, "New Results in Linear Filtering and Prediction Theory," *Journal of Basic Engineering*, vol. 83, no. 1, pp. 95–108, Mar. 1961, doi: 10.1115/1.3658902.

[Ker21] B. S. Kerner and S. L. Klenov, "Methodology of Microscopic Traffic Prediction for Automated Driving," in *2021 Systems of Signals Generating and Processing in the Field of on Board Communications*, Moscow, Russia, Mar. 2021, pp. 1–4. doi: 10.1109/IEEECONF51389.2021.9416038.

[Kes07] A. Kesting, M. Treiber, and D. Helbing, "General Lane-Changing Model MOBIL for Car-Following Models," *Transportation Research Record*, vol. 1999, no. 1, pp. 86–94, Jan. 2007, doi: 10.3141/1999-10.

[Kho10] A. Khodayari, R. Kazemi, A. Ghaffari, and N. Manavizadeh, "Modeling and intelligent control design of car following behavior in real traffic flow," in *2010 IEEE Conference on Cybernetics and Intelligent Systems*, Jun. 2010, pp. 261–266. doi: 10.1109/ICCIS.2010.5518546.

[Kik92] S. Kikuchi and P. Chakroborty, "CAR-FOLLOWING MODEL BASED ON FUZZY INFERENCE SYSTEM," *Transportation Research Record*, no. 1365, 1992, Accessed: Oct. 29, 2021. [Online]. Available: https://trid.trb.org/view/371408

[Kra97] S. Krauss, P. Wagner, and C. Gawron, "Metastable states in a microscopic model of traffic flow," *Phys. Rev. E*, vol. 55, no. 5, pp. 5597–5602, May 1997, doi: 10.1103/PhysRevE.55.5597.

[Kra98] F. Kratz, W. Nuninger, and S. Ploix, "Fault detection for time-delay systems: a parity space approach," in *Proceedings of the 1998 American Control Conference. ACC (IEEE Cat. No.98CH36207)*, Philadelphia, PA, USA, 1998, pp. 2009–2011 vol.4. doi: 10.1109/ACC.1998.702978.

[Kug00] N. Kuge, T. Yamamura, O. Shimoyama, and A. Liu, "A Driver Behavior Recognition Method Based on a Driver Model Framework," Mar. 2000, pp. 2000-01–0349. doi: 10.4271/2000-01-0349.

[Lam18] H. K. Lam, "A review on stability analysis of continuous-time fuzzy-model-based control systems: From membership-function-independent to membership-function-dependent analysis," *Engineering Applications of Artificial Intelligence*, vol. 67, pp. 390–408, Jan. 2018, doi: 10.1016/j.engappai.2017.09.007.

[Li12] Y. Li and D. Sun, "Microscopic car-following model for the traffic flow: the state of the art," *J. Control Theory Appl.*, vol. 10, no. 2, pp. 133–143, May 2012, doi: 10.1007/s11768-012-9221-z.

[Li18] W. Li, T. Chen, J. Guo, and J. Wang, "Adaptive Car-Following Control of Intelligent Electric Vehicles," in *2018 IEEE 4th International Conference on Control*

Science and Systems Engineering (ICCSSE), Wuhan, China, Aug. 2018, pp. 86–89. doi: 10.1109/CCSSE.2018.8724753.

[Li19_1] Y. Li, Z. Liang, H. Zhu, and X. Tang, "Electric Vehicle Dynamics-Based Car-Following Model and Stability Analysis," in *2019 Chinese Control Conference (CCC)*, Guangzhou, China, Jul. 2019, pp. 6692–6696. doi: 10.23919/ChiCC.2019.8866395.

[Li19_2] G. Li and W. Zhu, "The Car-Following Model Based on Fuzzy Inference Controller," *IOP Conf. Ser.: Mater. Sci. Eng.*, vol. 646, p. 012007, Oct. 2019, doi: 10.1088/1757-899X/646/1/012007.

[Lu17] Y. Lu, Y. Cui, Q. Yang, and M. Zhang, "Car-following Model Based on Genetic Algorithm Optimized BP Neural Network," *dtetr*, no. ictim, Feb. 2017, doi: 10.12783/dtetr/ictim2016/5540.

[Mas16] P. Masek *et al.*, "A Harmonized Perspective on Transportation Management in Smart Cities: The Novel IoT-Driven Environment for Road Traffic Modeling," *Sensors*, vol. 16, no. 11, p. 1872, Nov. 2016, doi: 10.3390/s16111872.

[Mat14] T. V. Mathew, "Car following models," *Transportation Systems Engineering*, Chapter 14, 2014, pp. 1-8. Accessed: Dec. 01, 2021. [Online]. Available: https://nptel.ac.in/content/storage2/courses/105101008/downloads/cete_14.pdf.

[Mic85] J. A. Michon, "A Critical View of Driver Behavior Models: What Do We Know, What Should We Do?," in *Human Behavior and Traffic Safety*, L. Evans and R. C. Schwing, Eds. Boston, MA: Springer US, 1985, pp. 485–524. doi: 10.1007/978-1-4613-2173-6_19.

[Mis12] G. Misuraca, D. Broster, and C. Centeno, "Digital Europe 2030: Designing scenarios for ICT in future governance and policy making," *Government Information Quarterly*, vol. 29, pp. S121–S131, Jan. 2012, doi: 10.1016/j.giq.2011.08.006.

[Mog17] M. P. A. Moghadam, P. Pahlavani, and B. Bigdeli, "A New Car-Following Model Based on the Epsilon-Support Vector Regression Method using the Parameters Tuning and Data Scaling Techniques," *Int J Civ Eng*, vol. 15, no. 8, pp. 1159–1172, Dec. 2017, doi: 10.1007/s40999-017-0209-4.

[Nag01] K. Nagel and M. Rickert, "Parallel implementation of the TRANSIMS micro-simulation," *Parallel Computing*, vol. 27, no. 12, pp. 1611–1639, Nov. 2001, doi: 10.1016/S0167-8191(01)00106-5.

[Nis07] Y. Nishiwaki, C. Miyajima, N. Kitaoka, K. Itou, and K. Takeda, "Generation of Pedal Operation Patterns of Individual Drivers in Car-Following for Personalized Cruise Control," in *2007 IEEE Intelligent Vehicles Symposium*, Jun. 2007, pp. 823–827. doi: 10.1109/IVS.2007.4290218.

[Nwa21] J. C. Nwadiuto, H. Okuda, and T. Suzuki, "Driving Behavior Modeling Based on Consistent Variable Selection in a PWARX Model," *Applied Sciences*, vol. 11, no. 11, p. 4938, May 2021, doi: 10.3390/app11114938.

[Oku10] H. Okuda, Okuda Hybrid-System Package, 2010.

[Oss05] S. Ossen and S. P. Hoogendoorn, "Car-Following Behavior Analysis from Microscopic Trajectory Data," *Transportation Research Record*, vol. 1934, no. 1, pp. 13–21, Jan. 2005, doi: 10.1177/0361198105193400102.

[Pan05] S. Panwai and H. Dia, "Development and evaluation of a reactive agent-based car following model," *INTELLIGENT VEHICLES AND ROAD INFRASTRUCTURE CONFERENCE, 2005, MELBOURNE, VICTORIA, AUSTRALIA*, 2005.

[Pan08] D. Pan and Y. Zheng, "Optimal control and discrete time-delay model of car following," in *2008 7th World Congress on Intelligent Control and Automation*, Jun. 2008, pp. 5657–5661. doi: 10.1109/WCICA.2008.4593852.

[Par14] G. Park, S. Lee, S. Jin, and S. Kwak, "Integrated modeling and analysis of dynamics for electric vehicle powertrains," *Expert Systems with Applications*, vol. 41, no. 5, pp. 2595–2607, Apr. 2014, doi: 10.1016/j.eswa.2013.10.007.

[Pen99] Peng Shi, El.-K. Boukas, and R. K. Agarwal, "Kalman filtering for continuous-time uncertain systems with Markovian jumping parameters," *IEEE Trans. Automat. Contr.*, vol. 44, no. 8, pp. 1592–1597, Aug. 1999, doi: 10.1109/9.780431.

[Pet19] E. rico Petritoli, F. Leccese, and M. Cagnetti, "Takagi-Sugeno Discrete Fuzzy Modeling: an IoT Controlled ABS for UAV," in *2019 II Workshop on Metrology for Industry 4.0 and IoT (MetroInd4.0&IoT)*, Naples, Italy, Jun. 2019, pp. 191–195. doi: 10.1109/METROI4.2019.8792915.

[Pip53] L. A. Pipes, "An Operational Analysis of Traffic Dynamics," *Journal of Applied Physics*, vol. 24, no. 3, pp. 274–281, Mar. 1953, doi: 10.1063/1.1721265.

[**Pop17**] **M.-D. Pop**, "Simularea sistemelor inteligente de trafic rutier utilizând AnyLogic", Teză de disertaţie, Timisoara, 2017.

[**Pop18_1**] **M.-D. Pop**, "Traffic Lights Management Using Optimization Tool," *Procedia - Social and Behavioral Sciences*, vol. 238, pp. 323–330, 2018, doi: 10.1016/j.sbspro.2018.04.008.

[**Pop18_2**] **M.-D. Pop** and O. Proștean, "A Comparison Between Smart City Approaches in Road Traffic Management," *Procedia - Social and Behavioral Sciences*, vol. 238, pp. 29–36, 2018, doi: 10.1016/j.sbspro.2018.03.004.

[**Pop18_3**] **M.-D. Pop**, O. Prostean, and G. Prostean, "Prediction of Route Choosing Behavior Based on Genetic Algorithm Approach," in *2018 IEEE 22nd International Conference on Intelligent Engineering Systems (INES)*, Las Palmas de Gran Canaria, Jun. 2018, pp. 000193–000198. doi: 10.1109/INES.2018.8523917.

[**Pop18_4**] **M.-D. Pop**, O. Prostean, and G. Prostean, "Analysis of Policies and Regulations for a Sustainable Smart Mobility System," in *2018 Proceedings of the 32nd International Business Information Management Association Conference, IBIMA 2018 - Vision 2020: Sustainable Economic Development and Application of Innovation Management from Regional expansion to Global Growth*, Seville, Spain, Nov. 2018, pp. 875–883.

[**Pop19_1**] **M.-D. Pop**, O. Proştean, and G. Proştean, "Multiple Lane Road Car-Following Model using Bayesian Reasoning for Lane Change Behavior Estimation: A Smart Approach for Smart Mobility," in *Proceedings of the 3rd International Conference on Future Networks and Distributed Systems*, Paris France, Jul. 2019, pp. 1–8. doi: 10.1145/3341325.3341996.

[**Pop19_2**] **M.-D. Pop** and O. Proştean, "Bayesian Reasoning for OD Volumes Estimation in Absorbing Markov Traffic Process Modeling," in *2019 4th MEC*

International Conference on Big Data and Smart City (ICBDSC), Muscat, Oman, Jan. 2019, pp. 1–6. doi: 10.1109/ICBDSC.2019.8645611.

[**Pop19_3**] **M. D. Pop** and O. Proștean, "Identification of significant metrics and indicators for smart mobility," *IOP Conf. Ser.: Mater. Sci. Eng.*, vol. 477, p. 012017, Feb. 2019, doi: 10.1088/1757-899X/477/1/012017.

[**Pop19_4**] **M.-D. Pop**, "Real-Time Adaptive Traffic Signals Using Rate-Monotonic Scheduling," *ITM Web Conf.*, vol. 29, p. 03002, 2019, doi: 10.1051/itmconf/20192903002.

[**Pop20_1**] **M.-D. Pop**, "Decision Making in Road Traffic Coordination Methods: A Travel Time Reduction Perspective," in *2020 International Conference Engineering Technologies and Computer Science (EnT)*, Moscow, Russia, Jun. 2020, pp. 42–46. doi: 10.1109/EnT48576.2020.00014.

[**Pop20_2**] **M.-D. Pop**, O. Proștean, T.-M. David, and G. Proștean, "Hybrid Solution Combining Kalman Filtering with Takagi–Sugeno Fuzzy Inference System for Online Car-Following Model Calibration," *Sensors*, vol. 20, no. 19, p. 5539, Sep. 2020, doi: 10.3390/s20195539.

[**Pop20_3**] **M.-D. Pop**, O. Proștean, and G. Proștean, "Fault Detection Based on Parity Equations in Multiple Lane Road Car-Following Models Using Bayesian Lane Change Estimation," *JSAN*, vol. 9, no. 4, p. 52, Nov. 2020, doi: 10.3390/jsan9040052.

[**Pop20_4**] **M.-D. Pop**, O. Prostean, and G. Prostean, "Minimax Strategy for Lane Choice Prediction in Markovian Traffic Modeling," in *2020 5th International Conference on Logistics Operations Management (GOL)*, Rabat, Morocco, Oct. 2020, pp. 1–6. doi: 10.1109/GOL49479.2020.9314764.

[**Pop20_5**] **M.-D. Pop**, J. Pandey, and V. Ramasamy, "Future Networks 2030: Challenges in Intelligent Transportation Systems," in *2020 8th International Conference on Reliability, Infocom Technologies and Optimization (Trends and Future Directions) (ICRITO)*, Noida, India, Jun. 2020, pp. 898–902. doi: 10.1109/ICRITO48877.2020.9197951.

[**Pop21**] **M.-D. Pop**, C. C. Niculescu, O. Proștean, and G. Proștean, "Safety Aspects of Single-Lane Roundabout Management Systems in Connected Vehicles Environments," in *Proceedings of the 37th International Business Information Management Association Conference, IBIMA 2021 - Innovation Management and Information Technology Impact on Global Economy in the Era of Pandemic*, Cordoba, Spain, May 2021, pp. 10451-10457.

[Pou94] A. D. Pouliezos and G. S. Stavrakakis, "Analytical Redundancy Methods," in *Real Time Fault Monitoring of Industrial Processes*, Dordrecht: Springer Netherlands, 1994, pp. 93–178. doi: 10.1007/978-94-015-8300-8_2.

[Pou17] M. Pourabdollah, E. Bjarkvik, F. Furer, B. Lindenberg, and K. Burgdorf, "Calibration and evaluation of car following models using real-world driving data," in *2017 IEEE 20th International Conference on Intelligent Transportation Systems (ITSC)*, Yokohama, Oct. 2017, pp. 1–6. doi: 10.1109/ITSC.2017.8317836.

[Pun05] V. Punzo and F. Simonelli, "Analysis and Comparison of Microscopic Traffic Flow Models with Real Traffic Microscopic Data," *Transportation Research Record*, vol. 1934, no. 1, pp. 53–63, Jan. 2005, doi: 10.1177/0361198105193400106.

[Pun05_2] V. Punzo, D. J. Formisano, and V. Torrieri, "Nonstationary Kalman Filter for Estimation of Accurate and Consistent Car-Following Data," *Transportation Research Record*, vol. 1934, no. 1, pp. 2–12, Jan. 2005, doi: 10.1177/0361198105193400101.

[Pun21] V. Punzo, Z. Zheng, and M. Montanino, "About calibration of car-following dynamics of automated and human-driven vehicles: Methodology, guidelines and codes," *Transportation Research Part C: Emerging Technologies*, vol. 128, p. 103165, Jul. 2021, doi: 10.1016/j.trc.2021.103165.

[Pur18] S. Puri, R. S. Rai, and K. Saxena, "Barricades in Network Transformation from 4G to 5G in India," in *2018 7th International Conference on Reliability, Infocom Technologies and Optimization (Trends and Future Directions) (ICRITO)*, Aug. 2018, pp. 695–702. doi: 10.1109/ICRITO.2018.8748303.

[Raj04] B. Raj, M. L. Seltzer, and R. M. Stern, "Reconstruction of missing features for robust speech recognition," *Speech Communication*, vol. 43, no. 4, pp. 275–296, Sep. 2004, doi: 10.1016/j.specom.2004.03.007.

[Rot01] R.W. Rothery, "Car following models. In Traffic Flow Theory: A State-of-the-Art," Gartner, N., Messer, C.J., Rathi, A.K., Eds., Committee on Traffic Flow Theory and Characteristics (AHB45), Turner-Fairbank Highway Research Center: McLean, VA, USA, 2001, pp. 4-1–4-42.

[Sal13] G. Sallai, "Chapters of Future Internet research," in *2013 IEEE 4th International Conference on Cognitive Infocommunications (CogInfoCom)*, Dec. 2013, pp. 161–166. doi: 10.1109/CogInfoCom.2013.6719233.

[Sch16] T. Schwickart, H. Voos, J.-R. Hadji-Minaglou, and M. Darouach, "A Fast Model-Predictive Speed Controller for Minimised Charge Consumption of Electric Vehicles: Energy-Saving Model-Predictive Cruise Control System for Electric Vehicles," *Asian Journal of Control*, vol. 18, no. 1, pp. 133–149, Jan. 2016, doi: 10.1002/asjc.1251.

[Son14] J. Song, Y. Wu, Z. Xu, and X. Lin, "Research on car-following model based on SUMO," in *The 7th IEEE/International Conference on Advanced Infocomm Technology*, Fuzhou, China, Nov. 2014, pp. 47–55. doi: 10.1109/ICAIT.2014.7019528.

[Son18] D. Song, R. Tharmarasa, G. Zhou, M. C. Florea, N. Duclos-Hindie, and T. Kirubarajan, "Multi-Vehicle Tracking Using Microscopic Traffic Models," *IEEE Trans. Intell. Transport. Syst.*, vol. 20, no. 1, pp. 149–161, Jan. 2019, doi: 10.1109/TITS.2018.2804894.

[Tak05] J. Takayama and S. Nakayama, "Absorbing Markov Process OD Estimation and a Transportation Network Simulation Model," in *Simulation Approaches in Transportation Analysis*, vol. 31, R. Kitamura and M. Kuwahara, Eds. New York: Springer-Verlag, 2005, pp. 167–182. doi: 10.1007/0-387-24109-4_6.

[Tak85] T. Takagi and M. Sugeno, "Fuzzy identification of systems and its applications to modeling and control," *IEEE Trans. Syst., Man, Cybern.*, vol. SMC-15, no. 1, pp. 116–132, Jan. 1985, doi: 10.1109/TSMC.1985.6313399.

[Tia21] J. Tian, C. Zhu, D. Chen, R. Jiang, G. Wang, and Z. Gao, "Car following behavioral stochasticity analysis and modeling: Perspective from wave travel

time," *Transportation Research Part B: Methodological*, vol. 143, pp. 160–176, Jan. 2021, doi: 10.1016/j.trb.2020.11.008.

[Tre13_1] M. Treiber and A. Kesting, "Introduction," in *Traffic Flow Dynamics*, Berlin, Heidelberg: Springer Berlin Heidelberg, 2013, pp. 1–4. doi: 10.1007/978-3-642-32460-4_1.

[Tre13_2] M. Treiber and A. Kesting, "Car-Following Models Based on Driving Strategies," in *Traffic Flow Dynamics*, Berlin, Heidelberg: Springer Berlin Heidelberg, 2013, pp. 181–204. doi: 10.1007/978-3-642-32460-4_11.

[Tse19] L. Tseng and L. Wong, "Towards a Sustainable Ecosystem of Intelligent Transportation Systems," in *2019 IEEE International Conference on Pervasive Computing and Communications Workshops (PerCom Workshops)*, Mar. 2019, pp. 403–406. doi: 10.1109/PERCOMW.2019.8730669.

[Wan21] J. Wang, Z. Zhang, F. Liu, and G. Lu, "Investigating heterogeneous car-following behaviors of different vehicle types, traffic densities and road types," *Transportation Research Interdisciplinary Perspectives*, vol. 9, p. 100315, Mar. 2021, doi: 10.1016/j.trip.2021.100315.

[Wat07] T. Wada, S. Doi, K. Imai, N. Tsuru, K. Isaji, and H. Kaneko, "Analysis of Drivers' Behaviors in Car Following Based on Performance Index for Approach and Alienation," Apr. 2007, pp. 2007-01–0440. doi: 10.4271/2007-01-0440.

[Wie92] R. Wiedemann, U. Reiter, "Microscopic Traffic Simulation: The Simulation System MISSION, Background and Actual State," Project ICARUS (V1052) Final Report, CEC: Brussels, Belgium, 1992, Vol. 2, pp. 1–53.

[Wu19] P. Wu, F. Gao, and K. Li, "A Vehicle Type Dependent Car-following Model Based on Naturalistic Driving Study," *Electronics*, vol. 8, no. 4, p. 453, Apr. 2019, doi: 10.3390/electronics8040453.

[Xu20] T. Xu and J. Laval, "Driver Reactions to Uphill Grades: Inference from a Stochastic Car-Following Model," *Transportation Research Record*, vol. 2674, no. 11, pp. 343–351, Nov. 2020, doi: 10.1177/0361198120945597.

[Yan19] D. Yang, L. Zhu, Y. Liu, D. Wu, and B. Ran, "A Novel Car-Following Control Model Combining Machine Learning and Kinematics Models for Automated Vehicles," *IEEE Trans. Intell. Transport. Syst.*, vol. 20, no. 6, pp. 1991–2000, Jun. 2019, doi: 10.1109/TITS.2018.2854827.

[Yin15] B. Yin, M. Dridi, and A. El Moudni, "Adaptive Traffic Signal Control for Multi-intersection Based on Microscopic Model," in *2015 IEEE 27th International Conference on Tools with Artificial Intelligence (ICTAI)*, Vietri sul Mare, Italy, Nov. 2015, pp. 49–55. doi: 10.1109/ICTAI.2015.21.

[Yu20] J. Yu, Z. Fu, and M. Sarwat, "Dissecting GeoSparkSim: a scalable microscopic road network traffic simulator in Apache Spark," *Distrib Parallel Databases*, vol. 38, no. 4, pp. 963–994, Dec. 2020, doi: 10.1007/s10619-020-07306-x.

[Yu21] B. Yu, H. Zhou, L. Wang, Z. Wang, and S. Cui, "An extended two-lane car-following model considering the influence of heterogeneous speed information on drivers with different characteristics under honk environment," *Physica A: Statistical*

Mechanics and its Applications, vol. 578, p. 126022, Sep. 2021, doi: 10.1016/j.physa.2021.126022.

[Zak15] A. B. Zaky, W. Gomaa, and M. A. Khamis, "Car Following Markov Regime Classification and Calibration," in *2015 IEEE 14th International Conference on Machine Learning and Applications (ICMLA)*, Miami, FL, USA, Dec. 2015, pp. 1013–1018. doi: 10.1109/ICMLA.2015.126.

[Zha20] S. Zhang and X. Zhuan, "Research on Tracking Improvement for Electric Vehicle during a Car-following Process," in *2020 Chinese Control And Decision Conference (CCDC)*, Hefei, China, Aug. 2020, pp. 3261–3266. doi: 10.1109/CCDC49329.2020.9164836.

[Zhu17] F. Zhu and S. V. Ukkusuri, "An Optimal Estimation Approach for the Calibration of the Car-Following Behavior of Connected Vehicles in a Mixed Traffic Environment," *IEEE Trans. Intell. Transport. Syst.*, vol. 18, no. 2, pp. 282–291, Feb. 2017, doi: 10.1109/TITS.2016.2568759.

[Zhu19] H. Zhu, X. Yang, Y. Wang, and N. Zhang, "Simulating Car-following Behavior for Heteregeneous Drivers: the Need for Driver Specific Model Parameters," in *2019 5th International Conference on Transportation Information and Safety (ICTIS)*, Liverpool, United Kingdom, Jul. 2019, pp. 712–717. doi: 10.1109/ICTIS.2019.8883707.

[***_1] Online resource: 6. egueli/TraCI4J GitHub, n.d. Accessed: Dec. 01, 2021. [Online]. Available: https://github.com/egueli/TraCI4J.

[***_2] Online resource: Road traffic library. Accessed: Dec. 01, 2021. [Online]. Available: https://help.anylogic.com/index.jsp.